Stony Brook University

Post-entry Determinants of Poliovirus

Tissue and Host Tropism and Its Impact on Neurovirulence

A Dissertation Presented

By

Nusrat Jahan

to

The Graduate School

in Partial Fulfillment of the Requirements

for the Degree of

Doctor of Philosophy

in

Molecular and Cellular Biology

(Immunology and Pathology)

Stony Brook University

December 2009

Stony Brook University

The Graduate School

Nusrat Jahan

We, the dissertation committee for the above candidate for the Doctor of Philosophy degree, hereby recommend acceptance of this dissertation.

Eckard Wimmer – Dissertation Advisor
Distinguished Professor
Department of Molecular Genetics and Microbiology

Nancy Reich – Chairperson of Dissertation Committee
Professor
Department of Molecular Genetics and Microbiology

Patrick Hearing
Professor
Department of Molecular Genetics and Microbiology

Michael Hayman
Professor
Department of Molecular Genetics and Microbiology

Paul Freimuth
Biochemist
Biology Department, Brookhaven National Laboratory

This dissertation is accepted by the Graduate School

Lawrence Martin

Dean of the Graduate School

Abstract of the Dissertation

Post-entry Determinants of Poliovirus

Tissue and Host Tropism and Its Impact on Neurovirulence

By

Nusrat Jahan

Doctor of Philosophy

in

Molecular and Cellular Biology

(Immunology and Pathology)

Stony Brook University

2009

Using two different approaches, light was shed on the role of post-entry determinants in the PV tissue-host tropism.

In the first approach, a chimeric virus PV1(RIPO) that presents the exchange of the PV IRES with the IRES of human rhinovirus type 2 (HRV2), was used to study the potential contribution of the IRES element toward the cell tropism. I performed experiments to study the mechanism by which this variant expresses its remarkably attenuated phenotype in poliovirus-sensitive CD155 transgenic (tg) mice. In addition to previously observed growth restriction in human neuronal cells, PV1(RIPO) also exhibits a strong species-specific replication defect at physiological temperature in cells of murine origin. The block

in replication was enhanced at 39.5^{o}C but, remarkably, it is absent at 33^{o}C. PV1(RIPO) revertants, overcoming the block in either mouse cells or human neuronal cells, were derived by serial passage under restrictive conditions. Virus adaptation in mouse cells, but not in human neuronal cells, resulted in increased mouse neurovirulence *in vivo*. A translation defect associated with the HRV2 IRES was observed in mouse cells that correlated with the attenuation phenotypes of PV1(RIPO) in different mouse cells and in CD155-tg mice. Interestingly, this translation defect and the related growth defect of PV1(RIPO) could be rescued by expressing human IRES *trans*-activating factors in mouse cells.

The second approach was designed to study the PV tropism in a cell line known as MDCK$^{CD155\alpha}$, which is a first known example of CD155 expressing mammalian cell line that cannot be infected by wild type PV. My results indicate that once the virus is inside the cell, the IRES-driven translation of viral RNA is fully functional but the cells either fail to support or actively prevent the viral RNA replication resulting in nonproductive infection. Most perplexingly, despite the lack of replication and the absence of any progeny virus, the MDCK$^{CD155\alpha}$ cells exposed to PV die within hours.

This work demonstrates that poliovirus tissue and host tropism is also governed at a stage after the entry of the viral RNA in the cells either at the translational level or at the replication level of viral RNA.

Dedication

I dedicate this dissertation to my family

Table of Contents

List of Figures

List of Tables

ACKNOWLEDGEMENTS

I would like to thank Dr. Eckard Wimmer, my advisor, for providing me the opportunity to do my study and research in his laboratory. I am deeply indebted for his support, constructive criticism, friendship and guidance during this period. He has contributed a lot to my development as a scientist.

I would like to acknowledge Dr. Nancy Reich, Dr. Michael Hayman, Dr. Patrick Hearing, and Dr. Paul Freimuth for being on my thesis committee and for their thoughtful comments and criticism.

I am thankful to all of my present and past lab members for their help and friendship during my stay in the lab. It was a pleasure to work with them. I am especially indebted to Dr. Aniko Paul and Dr. Steffen Mueller. Dr. Paul has provided her enthusiasm, judgment, personal help, and guidance in the preparation of this dissertation. Dr. Mueller has helped enormously in the progress of the work presented here. He has provided constant input, critical judgement, advice, and enthusiasm at every level of this research. I am thankful to Dr. Shaukat Ali Khan and Dr. Robert Coleman for helping me with mice work.

I feel a deep sense of gratitude to my loving mother and my late father both of whom believed in the pursuit of academic excellence. I owe to my parents and my brothers for their unconditional love and support they gave to me.

Finally, I would like to express my appreciation to my husband, Aftabul Haque for his love and support and our precious daughter, Arshia Haque who is the joy of our lives.

Chapter I. Introduction

Background

The virus family of *Picornaviridae* includes several notable members of important human and animal pathogens, which cause a wide variety of illnesses. At present, there are eight genera in the *Picornaviridae* family: *Enterovirus, Cardiovirus, Aphtovirus, Hepatovirus, Parechovirus, Kobuvirus, Erbovirus* and *Teschovirus* (Stanway *et al.,* 2002). It should be noted that recently the genus *Rhinovirus* was incorporated into the *Enterovirus* genus (www.picornaviridae.com). Perhaps, the most well known of the *Picornaviridae* family is Poliovirus (PV) which is the prototype member of the genus *Enterovirus*.

PV is a small plus-strand RNA virus that was discovered 100 years ago (Landsteiner and Popper, 1909). PV causes a unique neurologic disease, called poliomyelitis, which causes the destruction of motor neurons resulting in paralysis or death. Despite the facts that PV has caused horrifying epidemics during the first half of the last century and that it is one of the most thoroughly investigated viruses of all times, our knowledge of the factors determining PV pathogenesis and tissue and host tropism are poorly understood. In order to fully understand the molecular mechanisms of PV pathogenicity, the events of virus-host interaction following PV entry must be clarified in detail. One way of tackling this problem is to study the determinants responsible for the inability of PV to replicate in certain tissues or hosts or under certain conditions, commonly referred to as tissue or host restrictions. These restrictions are the complement to a virus' tropism, i.e. the cells, tissues, and hosts that normally do get infected.

My thesis was focused on the identification of the post entry determinants of PV pathogenesis. Specifically, I wanted to answer the question of what factors might modify PV tissue tropism and host restriction after the virus particle has successfully bound the receptor and entered a cell. This was achieved by using two different model systems. The first model system was used to study the IRES dependent tissue tropism of an attenuated chimeric PV. In the second model system an attempt was made to identify the determinants of defective replication of PV in a canine epithelial cell line, MDCK (Madin-Darby Canine Kidney) cells.

Structure of the PV genome

(a) Genome organization. The PV genome (7441 nucleotide long) that is of plus-strand polarity, contains a long 5'-nontranslated region (NTR), a single open reading frame, and a short 3' NTR, with a poly A tail (Kitamura *et al.,* 1981; Wimmer *et al.,* 1993) (Fig. 1). Although the PV genome functions as mRNA it lacks, in contrast to most eukaryotic mRNAs, the 5'cap structure (Lee *et al.,* 1977). Instead a small viral protein, VPg, is covalently linked at the 5' end of the genome (Lee *et al.,* 1977; Flanegan *et al.,* 1977). The 5'NTR is composed of two functional RNA structure elements: the cloverleaf (nt 1 to 89) and the Internal Ribosome Entry Site (IRES) (nt 123 to 620) (Wimmer *et al.,* 1993). The main function of the cloverleaf is related to RNA replication (Andino *et al.,* 1990; Parsley *et al.,* 1997), while the IRES directs the cap-independent translation of the PV polyprotein (Jang *et al.,* 1988; Pelletier and Sonenberg, 1988; Trono *et al.,* 1988). The two highly structured elements are separated by a 35 nucleotide

long, single-stranded spacer sequence that was previously thought to lack any function in viral proliferation (Fig. 1). Two recent studies suggested the importance of (i) a conserved nucleotide in this spacer sequence for replication of PV in the CD155tg mice and in human cells of neuronal origin (De Jesus *et al.,* 2005) and (ii) conserved C-clusters absolutely necessary for genome replication (Toyoda, *et al.,* 2007a).

(b) PV IRES. The IRES elements of enteroviruses, cardio- and aphthoviruses, and hepatitis A virus have been classified as type I, type II, and type III IRESes, respectively based on the primary sequence as determinants of structures (Wimmer *et al.,* 1993) (Fig. 2A-C). According to this classification, the PV IRES element is designated as type I IRES. In spite of barely 50% nucleotide sequence homology between IRES types I, II and III, all three IRES types fold roughly into domains dominated by a large central domain (Fig. 2). In addition, representatives of type I and type II IRESes carry tetra loops (GNRA or GNAA; N, any nucleotide; R, purine) in the loops of their domains (Fig. 2A, B) that are required for IRES function. Unexpectedly the IRES of Porcine teschovirus-1 (PTV-1) is more related to the IRES of hepatitis C virus (HCV) in structure and function than to the type I–III IRESes discussed above (Fig. 2E) (Pisarev *et al.,* 2004). A recent report by Reuter *et al.,* (2009) shows the putative IRES element (nt 496--568) of Porcine kobuvirus (Fig. 2D) bears a 74% sequence similarity to that of Porcine teschovirus (Fig. 2E). Therefore, the HCV-like IRES elements of

picornaviruses which include IRESes of Porcine kobuvirus and Porcine teschovirus are designated as type IV IRESes.

Although the nt sequences and apparent higher order structures of the four picornavirus IRES types vary widely, the overall function of IRES elements – internal initiation of translation – is the same, regardless of the poorly understood underlying mechanisms by which this is accomplished. Surprisingly exchange of different IRES elements between different picornaviruses yield viable viruses. Many IRES chimeras were analyzed using PV as the backbone and exchanging the PV IRES with other type I IRESes such as coxsackie virus B3 (CVB3) (Semler *et al.,* 1986; Johnson *et al.,* 1988), human rhinovirus type 2 (HRV2) and human rhinovirus type 2 (HRV14) (Gromeier *et al.,* 1996), with type II IRESes such as encephalomyocarditis virus (EMCV) (Alexander *et al.,* 1994), and even with the IRES of hepatitis C virus (HCV) (Lu *et al.,* 1996), a virus belonging to a different family. These chimeric viruses replicated with wt kinetics in HeLa cells at 37^{o} C. When assayed under different conditions, however, they may express interesting phenotypes, for example tissue-specific phenotypes. For example: PV carrying the HRV2 IRES ["PV(RIPO)"] is highly attenuated in cells of neuronal origin but grows with wt kinetics in HeLa cells (Gromeier *et al.,* 1996; 2002).

Two conclusions can be drawn based on the studies using the chimeric viruses: (i) the IRESes of PV, HRV, CVB3, EMCV, or HCV do not carry essential signals necessary for PV genome replication, and (ii) IRES is defined solely by its function not by its specific structure.

Poliovirus replication

(a) An overview of the PV life cycle. Figure 3 illustrates the cellular life cycle of PV. PV infects a cell by binding to the cell surface receptor CD155. The virion is transported into the cell and uncoated which is followed by release of viral RNA into the cytoplasm. In the cytoplasm, the genome linked protein VPg is cleaved by a cellular enzyme after which the RNA is translated into a polyprotein. The polyprotein is subsequently processed into numerous functional proteins by virally encoded proteinases ($2A^{pro}$ and $3C^{pro}$). Next a replication complex is formed where the plus stranded genome RNA is transcribed into a minus-strand intermediate by the viral RNA polymerase and associated viral and cellular proteins. Minus-strand RNA in turn serves as template for the synthesis of plus-strand RNAs. Newly synthesized plus-stranded RNA has the choice of re-entering genome replication or serving as mRNA in translation or associating with procapsids to form mature virions that are released from the dying cell.

(b) Receptor binding and uncoating. There are several early events taking place in PV life cycle before the viral RNA is translated and replicated. These include binding of the virion to the cellular receptor CD155, followed by alteration of the capsid which releases the viral RNA into the cytoplasm (Fig. 3). At physiological temperature the binding of the virion to CD155 molecules triggers a conformational transition and the formation of altered particles. The altered virion sediments at 135S (versus 160S for native virion) and is no longer able to attach to susceptible cells (Hogle *et al.,* 1990). The conformational transition is the

result of the externalization of capsid protein VP4 and the N-terminal extension of VP1. These externalized proteins enable the particle to be inserted into the cell membrane which facilitates the cell entry (Hogle, 2002). The 135S particles are then internalized by an endocytic mechanism that is dependent tyrosine kinase and actin but independent of clathrin, caveolin, flotillin, and microtubule (Brandenburg *et al.,* 2007). Immediately after the internalization, the viral genome is released from endocytic compartment that are located within 100–200 nm of the plasma membrane.

(c) IRES-mediated initiation of translation of polyprotein. In eukaryotes translation of mRNA is initiated by a cap- and 5' end-dependent mechanism. PV RNA has a small polypeptide, VPg, covalently linked to its 5' end in contrast to the 5'-cap structure typical for most eukaryotic mRNAs (Nomoto *et al.,* 1977) (Fig. 1). After release in the cytoplasm, VPg is removed by an unknown cellular phosphodiesterase, leaving pUpU as the 5'-terminal structure of viral RNA (Wimmer, 1982). Following removal of VPg, the genome serves as a messenger RNA and is translated into a single precursor polyprotein through cap-independent translation of the ORF mediated by the IRES element (Fig. 4). A highly conserved motif (YnXmAUG) composed of an oligo pyrimidines tract (Yn), followed by a second tract of an unspecified sequence of 15-20 nucleotides (Xm), and an AUG is present in PV IRES (Jang *et al.,* 1990a, 1990b). As this motif is upstream of the initiating codon, the AUG codon present in this motif is cryptic. Genetic analyses involving elimination of Yn or shortening or enlarging

Xm, etc., that disrupted the integrity of the motif, have resulted in severe deficiencies in translation of PV RNA (Pestova *et al.,* 1991; Pilipenko *et al.,* 1992; Gmyl *et al.,* 1993). This indicates that the integrity of this motif is essential for IRES function. It has been speculated that during translation initiation the small ribosomal subunits use the YnXmAUG motif as the “landing pad” but there is no direct evidence for this hypothesis.

It is thought that the cellular proteins recognize the secondary and tertiary structural motifs in the IRES which in turn facilitate internal binding of ribosomal subunits (Sonenberg, 1990). Several cellular RNA binding proteins have been shown to bind multiple sites within the 5'-NTR of PV RNA. These proteins are not members of the canonical translation proteins and are known as the IRES *trans*-activating factors (ITAFs). These ITAFs are believed to function as RNA chaperones to recruit the ribosomal subunits and the initiation factors to the viral RNA (Sonenberg, 1991). As described earlier, many features of the IRES elements in different picornaviruses appear to be quite different and, thus, are suspected to play a role in determining host range or tissue tropism (Jang and Wimmer, 1990a). The various IRES elements may require different sets of factors for an efficient internal initiation of translation in different cells (Jang and Wimmer, 1990a).

(d) Proteolytic processing of polyprotein. The PV polyprotein is co-translationally processed into all the structural and non-structural proteins by three PV-encoded proteinases, $2A^{pro}$, $3C^{pro}$ and/or $3CD^{pro}$, in a cascade of slow

and quick proteolytic cleavage events (Fig. 1) (reviewed in (Paul, 2002)). The PV polyprotein is principally divided into three major precursors, designated P1, P2 and P3. The P1 region encodes the structural proteins, which form the viral capsid (VP4,VP2,VP3 and VP1). The three non-structural proteins 2A, 2B, and 2C are encoded by P2 precursor whereas the rest of the proteins 3A, 3B, 3C, and $3D^{pol}$ are encoded by the P3 precursor. As shown in the polyprotein processing maps for PV in Fig. 1, an initial cleavage event catalyzed in *cis* by $2A^{pro}$, between P1 and P2, releases P1 precursor. P1 precursor is further cleaved into the capsid proteins VP1, VP3, and the precursor VP0 by $3CD^{pro}$. In a secondary cleavage event catalyzed by $3C^{pro}$/$3CD^{pro}$, the P2 region is separated from P3 region, followed by production of the free 2A, and the relatively stable precursor 2BC (reviewed in (Paul, 2002)). $3C^{pro}$ and $3CD^{pro}$ are in charge of remaining secondary cleavage events to release the rest of the non-structural proteins, 3AB, 2B, 2C, 3A, 3B (VPg), $3C^{pro}$, $3D^{pol}$. The final cleavage, that of precursor VP0, yields the capsid proteins VP4 and VP2, which is known as maturation cleavage as it occurs during assembly of the virus particle. It is not catalyzed by a proteinase; its mechanism is unknown.

(d) RNA replication. Replication of PV RNA takes place in an endoplasmic reticulum membrane-associated replication complex. The general scheme of PV RNA replication is believed to include the following steps:

(+) strand RNA → (-) strand RNA synthesis → RF → (+) RNA synthesis → RI → (+) strand RNA, where RF stands for replicative form (double-stranded

RNA), and RI stands for replicative intermediate (partially double and partially single-stranded (Wimmer, Hellen, and Cao, 1993).

Mutational and genetic studies have shown that all of the non-structural proteins are involved in some step of the genome replication (reviewed in (Paul, 2002)). The viral-encoded RNA-dependent RNA polymerase, $3D^{pol}$ catalyzes the generation of both positive- and negative-strand viral RNA synthesis.

(e) Virion assembly and release of mature virions. An increasing fraction of the positive-strand RNAs in the replication complex is packaged into the icosahedral empty particle composed of capsid proteins. New progeny virions are stabilized by the final maturation cleavage of VP0 into VP4 and VP2 and the mature virions are released from the host cell. PV replication cycle is rapid which needs 6-8 hours from adsorption to cell lysis (reviewed in (Wimmer *et al.,* 1987)).

PV receptor

All three serotypes of PV use the same cellular receptor which is referred to as CD155, also known as Pvr (for the designation of CD155, see Freistadt *et al.,* 1997). It is a highly glycosylated 80 kDa single-pass transmembrane protein belonging to the Ig superfamily (Mendelsohn *et al,* 1989; Koike *et al.,* 1990; Bernhardt *et al.,* 1994; Bibb *et al.,* 1994a; Wimmer *et al.,* 1994). Alternative splicing of the *CD155* primary transcript gives rise to 4 isoforms. Of the four splice variants, CD155α and CD155δ are membrane bound, have a short cytoplasmic domain and serve as PV receptors. The significance of the two secreted versions, CD155β and γ, that arise from alternative splicing of the

transmembrane encoding exon 6, is not clear (Baury *et al.,* 2003; Koike *et al.,* 1990). The membrane-bound forms of CD155 serve as cellular adhesion molecules, that mediate cell to matrix adhesion by binding to vitronectin (Lange *et al.,* 2001) and cell to cell adhesion by interaction with Nectin-3 (Mueller *et al.,* 2003). The isolation and characterization of the PV receptor CD155 (Mendelsohn *et al.,* 1989; Koike *et al.,* 1990; Wimmer *et al.,* 1994) has made it possible to construct CD155tg mice, expressing CD155 under control of human *CD155* promoter (Ren *et al.,* 1990; Koike *et al.,* 1991). These transgenic animals, when injected with PV, show symptoms of paralysis similar to those of human poliomyelitis (Ren *et al.,* 1990; Koike *et al.,* 1991).

Neurovirulence and its attenuation as a parameter of PV pathogenesis

(a) PV neurovirulence versus attenuation. Neurovirulence in general refers to the potential for PV propagation in neuronal cells which can be viewed as an intracellular parameter determining the pathogenesis of poliomyelitis. Neurovirulence is influenced significantly by the choice of PV strains, the animal host employed (e.g. monkeys, chimpanzees, and mice) and the different routes of inoculation used (e.g. intracerebral, intraspinal, intraperitoneal, intramuscular, intravenous, and oral) (Racaniello, 1988). Therefore, neurovirulence for primates is a function, not only of the virus, but of the varying susceptibilities of different tissues and hosts. The intestine is the main site of PV replication and the disease occurs when the virus escapes its normal intestinal replication site and infects the central nervous system (CNS). Thus, a neurovirulent strain of PV may have to

possess certain other properties in addition to high neurotropism, such as a high capacity for multiplication in extraneural tissues other than the alimentary tract, which may be required for invading the CNS.

The early introduction of the live attenuated vaccine strains of PV (oral polio vaccines, OPV) aided the studies of genetic basis of PV neurovirulence and pathogenesis (Sabin *et al.,* 1973). The attenuated vaccine strains were either obtained from naturally occurring attenuated isolates or by passage of the virus in a different animal host or in various cultured cells. For instance, the Sabin type 2 strain and type 3 strain originated from an environmental isolate and a clinical case, respectively. In contrast, the type I strain originated from the Mahoney strain passaged through cultures of monkey testes (Li *et al.,* 1953). The candidate viruses were next produced by controlled passage of viruses in animals and cultured cells and were tested in primates for attenuation and stability on passage (reviewed in (Sabin and Boulger, 1973)). Owing to its mode of administration and the nature of the protective immune response, OPV has been overwhelmingly used in mass vaccinations globally. However, intrinsic properties of the OPV have become highly problematic. This relates to the possibility (i) of vaccine induced poliomyelitis in healthy recipients, (ii) of a vaccine induced PV carrier state in vaccine recipients with primary immune deficiency (MacLennan *et al.,* 2004), (iii) of generating highly neurovirulent OPV-derived PV strains circulating in poorly immunized populations, thereby causing outbreaks of poliomyelitis.

For the reasons discussed above, there were several attempts to produce alternative safer live vaccines than the Sabin strains. The first such attempts were based on the Sabin strains themselves (Kohra *et al.,* 1988) where the structural proteins of type 1 Sabin strain were replaced with those of either type 2 or type 3. This was based on the observations that some of the attenuating mutations in type 1 lie outside the structural proteins (Omata *et al.,* 1986). The attenuation phenotypes of the Sabin strains have been shown to be, at least partially, contributed by mutations in the IRES (Evans *et al.,* 1985; Westrop *et al.,* 1989; Kawamura *et al.,* 1989; Pollard *et al.,* 1989; Macadam *et al.,* 1991). These observations led to a second approach of making improved attenuated strains which involved the exchange of PV IRES with its counterpart from human rhinovirus type 2 (HRV2) (Gromeier *et al.,* 1996). The resulting chimera, named PV1(RIPO) was highly attenuated in CD155tg mice (Gromeier *et al.,* 1996) and in non-human primates (Gromeier *et al.,* 1999). The next approach to construct a neuro-attenuated variant of PV were based on an interesting observation regarding a genetic element, called *cre* (cis acting replication element), which maps to the open reading frame of the PV protein 2C. Inactivation of *cre* by point mutations are lethal but viral replication can be rescued if a second, intact *cre* is inserted into the genome somewhere else, for example into the sequence between the clover leaf and the IRES (Yin *et al.,* 2003). This virus referred to as mono-*cre* PV, was highly attenuated in CD155tg mice and no genetic variants with increased neurovirulence have been isolated from this variant (Toyoda *et al.,*

2007b). A more recent approach was undertaken where an attenuated virus with codon pair deoptimized capsid coding region was constructed (Coleman *et al.,* 2008). Two unique features of such a virus were (i) the amino acid sequence of the capsid remains unchanged to preserve the antigenic determinants of the capsid and (ii) 100-fold reduced specific infectivity, reducing the probability of causing an unwanted infection by100-fold.

(b) Determinants of attenuation. The complete genomic sequence of the attenuated Sabin vaccine strains and their neurovirulent parents (Nomoto *et al.,* 1982; Toyoda *et al.,* 1984) and the availability of infectious cDNA PV clones (Racaniello and Baltimore, 1981a, 1981b) has opened the way for crucial studies to determine the molecular and functional basis of attenuation (Reviewed in (Minor *et al.,* 2002)). These studies have revealed that the substitutions in the 5′-NTR (A480G in Sabin 1, G481A in Sabin 2, and C472U in Sabin 3) are the major attenuating mutations of the respective Sabin strains (Kawamura *et al.,* 1989; Westrop *et al.,* 1989; Macadam *et al.,* 1991). These mutations, mapping to a confined region of stem-loop domain V within the IRES, are considered to destabilize the base-paired RNA secondary structure (Skinner *et al.,*1989; Christodoulou *et al.,* 1990; Macadam *et al.,* 1992). The localization of these attenuating mutations in the IRES has been shown to affect the efficiency of IRES function i.e., a deficiency in translation (Svitkin *et al.,* 1985; 1988; 1990). This view was further supported by the finding that the attenuated form of the IRES of Sabin strains restricts growth in cells of neuronal origin associated with

lower efficiencies of translation in these cells (Agol *et al.,* 1989; La Monica *et al.,* 1989; Haller *et al.,* 1996). Definitive proof supporting the role of these mutations in the IRES in attenuation came from studies with an IRES recombinant, PV1(RIPO), construction and attenuation phenotypes of which has been described in previous section (Gromeier *et al.,* 1996; 1999). It is important to mention that neuroattenuation of this IRES chimera in CD155tg mice (Gromeier *et al.,* 1996) and in non-human primates (Gromeier *et al.,* 1999) is solely based on the IRES sequence.

In addition to the principal mutations in the IRES, all three Sabin strains possess mutations in the coding region for the structural proteins (Omata *et al.,* 1986; Ren *et al.,* 1992; Westrop *et al.,* 1989). These mutations are believed to interfere with the binding of the virus to CD155 (Bouchard *et al.,* 1995) or the assembly of the virion (Macadam *et al.,* 1991). These also confer to the vaccine a temperature sensitive (*ts*) phenotype that does not always co-varies with attenuation in the host (Omata *et al.,* 1986; Bouchard *et al.,* 1995). Not only in the structural proteins a number of point mutations were discovered in the viral RNA polymerase $3D^{pol}$ of Sabin type 1 (Nomoto *et al.,* 1982). The contribution of the Y73H (nt 6203) mutation in $3D^{pol}$, along with one or more of the other ten 3' terminal mutations to the *ts* phenotype of the type 1 Sabin strain is well established (Bouchard *et al.,* 1995; Tardy-Panit *et al.,* 1993). However, the presence of the Y73H 6203 nt $3D^{pol}$ mutation by itself is not sufficient for the *ts* phenotype in tissue culture (Paul *et al.,* 2000; Tardy-Panit *et al.,* 1993; Bouchard

et al., 1995). Conflicting results were observed from the studies establishing a link between neuroattenuation and *ts* phenotype (Omata *et al.,* 1986; Bouchard *et al.,* 1995; Tardy-Panit *et al.,* 1993). Type 2 and type 3 Sabin strains do not contain any mutation in their $3D^{pol}$. Therefore, a major role of these mutations in $3D^{pol}$ in attenuation of type 1 Sabin strain is a matter of debate.

It is apparent from the above discussion that multitude of unrelated determinants affects the complex process of PV pathogenesis on various levels in the host. Because of the multifactorial nature of the genetic basis of neurovirulence there has been little success in finding single determinants of the attenuation phenotype of PV neurovirulence. This composite nature of the neurovirulent phenotype and its attenuation involving the complex interaction of multiple determinants resulted in a flurry of conflicting reports (Gromeier *et al.,* 2002).

Tissue and host tropism as a parameter of PV pathogenesis

(a) PV tissue and host tropism. Tropism is defined as the affinity of a particular virus for specific types of host tissues or a population of host cells. This cell and tissue tropism results in distinct disease patterns and pathogenesis for different viruses in their respective hosts. Opposing neurovirulence as an intracellular parameter of pathogenesis, tropism could be viewed both as an extracellular and an intracellular parameter determining the pathogenesis of poliomyelitis. In spite of the presence of virus in many organs in the primate host during the viremic phase, PV infection is characterized by a restricted tissue

tropism (Bodian, 1955; Sabin, 1956). For many years it was believed that PV tropism was determined by the cellular receptor CD155. Later on it was found that CD155 is required for susceptibility to PV infection, but tropism is determined at a later stage of infection. Intracellular restriction can include any viral event in which host factors are involved.

Humans are the only known natural hosts of PV. Chimpanzees and old world monkeys can be experimentally infected (Khan *et al.,* 2008). Other animal species are not susceptible to most PV strains. However, there is variation in the susceptibility of the neurons of the primates to PV infection (Sabin, 1954). PV type 1 (Mahoney) produces paralysis when cynomolgus monkeys are inoculated intracerebrally with tissue culture infective doses (TCID) of 1 to 10, whereas intracerebral inoculation of 10^6 to 10^8 TCID viruses are unable to induce paralysis in chimpanzees (Sabin *et al.,* 1954). PV type 2 (Lansing) is highly neurotropic in monkeys by intracerebral inoculation, but does not infect the alimentary tract of monkeys, presumably due to the scarcity of CD155 expression in the monkey gut (Iwasaki *et al.,* 2002). Interestingly, PV type 2 infects great apes, such as chimpanzees, by the oral route (Sabin, 1956).

Most PV strains, such as the PV type 1 cause paralysis in primates but not in non-primates (La Monica *et al.,* 1986). However, researchers observed that strains of PV, including PV type 2, a variant of PV type 1, and a variant of PV type 3 (Leon), can be adapted in mice and other animal hosts (Armstrong, 1939; Li and Schaeffer, 1953). A host-range determinant of PV type 2 was later shown

to map to a stretch of amino acids (95-104) of capsid protein VP1 (Martin *et al.,* 1988; Murray *et al.,* 1988). Meanwhile, generation of mouse models for poliomyelitis (Koike *et al.,* 1991; Ren *et al.,* 1990) allowed easier comparison of neuropathogenicity of PV infection in wild-type mice and in CD155tg mice. When inoculated with PV, CD155tg mice developed neurological symptoms identical to primate poliomyelitis both clinically and histopathologically (Gromeier *et al.,* 1996; Koike *et al.,* 1991; Ren *et al.,* 1990). In sharp contrast, wild-type mice inoculated intracerebrally with PV type 2 developed neurological symptoms atypical for paralytic poliomyelitis with different clinical and histopathological features (Gromeier *et al.,* 1995). However, in contrast to the human disease, PV could not infect CD155tg mice by the oral route.

(b) Determinants of PV tissue-host tropism. The basis for the restricted host range of PV, which in turn is influencing its pathogenesis in animals, is not completely understood. The tissue tropism and pathogenesis of PV is possibly determined by a combination of several factors exerting their action on different steps of the PV life cycle in the host cells. The receptor for the PV, CD155 expression is required for the capture and entry of the virus into the cells. Therefore replication sites for PV are primarily determined by the presence of the receptor. In addition to the expression, the expression level of CD155 may add another level of restriction to the tropism of PV. Cells expressing CD155 at high levels may be favored for PV infection. In contrast to the extracellular restriction exerted by the cellular receptor, recently there have been several reports of

intracellular determinants, present in the cells that play a major role in tissue and host tropism of PV (Whitton *et al.,* 2005; Nathanson *et al.,* 2008). Available evidence strongly suggest that efficient replication of PV may be dependent on several post-entry factors which could be either viral or cellular. The following section discusses the experimental evidence to support the contribution of a multitude of factors toward the PV tissue-host tropism:

i) CD155-dependent tissue tropism: From the above discussion it is now clear that the host range of PV is restricted to humans and non-human primates. Humans are the only natural hosts of the virus although non-human primates can be experimentally infected. The primary determinant of this host restriction is the cellular receptor, CD155 (also known as Pvr) (Mendelsohn *et al.,* 1989; Koike *et al.,* 1990). So far, CD155, which is expressed only in humans and primates, is the only cell surface protein known to serve as the PV receptor. Introduction of human genomic DNA containing the PV receptor gene or of cloned human PV receptor cDNA into non-permissive cells (mouse L cells) is sufficient for productive PV infection (Mendelsohn *et al.,* 1989). The isolation and characterization of the PV receptor CD155 made possible the construction of CD155tg mice (Koike *et al.,* 1991; Ren *et al.,* 1990). As mentioned earlier, these transgenic animals, when injected with PV, show symptoms of paralysis similar to those of human poliomyelitis. Although CD155 mRNA could be detected in various human tissues, many of those tissues are not necessarily sites of PV replication (Mendelsohn *et al.,* 1989; Freistadt *et al.,* 1990). Epithelial cells in the

Bowman's capsule, podocytes in the glomerulus, and some of the tubular epithelial cells in the medulla of the kidneys of CD155tg mice showed high level expression of human CD155 mRNA, although the cells of these tissues were not susceptible to PV *in vivo* (Ren and Racaniello, 1992). Therefore, PV tissue tropism requires other factors in addition to the expression of CD155. Complicating the interpretation of receptor-mediated tropism, is the fact that expression of CD155 in a particular tissue does not necessarily mean, that the receptor is accessible for virus binding.

ii) IRES-dependent tissue tropism: Susceptibility to PV is also determined at the level of translation initiation of the viral protein which is controlled by the IRES (Jang *et al.,* 1988; Pelletier and Sonenberg, 1988; Trono *et al.,* 1988). IRES mediated translation of picornavirus genomes requires some non-canonical RNA-binding proteins apart from the canonical components of the eukaryotic translation initiation apparatus and they are known as IRES *trans*-activating factors (ITAFs). The known ITAFs for PV are polypyrimidine tract binding protein (PTB) (Hellen *et al.,* 1993; Pestova *et al.,* 1991), La autoantigen (Meerovitch *et al.,* 1989; Meerovitch *et al.,* 1993), poly(rC) binding protein-2 (PCBP-2) (Blyn *et al.,* 1997), and upstream of N-ras (unr) (Boussadia *et al.,* 2003). These ITAFs are believed to function as RNA chaperones. With the RNA-binding activity they probably cause structural changes in the RNA which then allow binding of initiation factors and/or ribosomal subunits.

Upon invasion of the central nervous system, PV destroys the motor neurons in the spinal cord and brainstem. The replication phenotype and/or neuropathogenic properties of PV are greatly affected by mutations in the IRES. The live attenuated Sabin vaccine strains used in the prevention of poliomyelitis carry such mutations (nt 480, 481, and 472 in types 1, 2, and 3, respectively) in their IRES elements in addition to other mutations in the structural and nonstructural proteins. The PV Sabin 3 showed a translation deficit in the CNS because of low levels of available PTB and the defect was rescued by increased expression of PTB in the CNS (Guest *et al.,* 2004). These findings indicate a definitive role of IRES sequences in the neurovirulent phenotype of PV. A solid proof of IRES contribution in PV neurovirulence came from studies where a picornavirus genomic hybrid was constructed in which the IRES element of PV1(M) was replaced with that of HRV2 and was named PV1(RIPO) (Gromeier, *et al.,* 1996) To construct this hybrid virus, a linker sequence (11 nucleotides long) present in the 5'NTR of a PV mutant virus, named PN6 (Trono *et al.,* 1988) was used to insert the rhinovirus IRES. PV1(RIPO), was viable and showed PV-like growth characteristics upon infection of HeLa cells, but did not replicate in tissue culture of human neuroblastoma derived cells (Gromeier *et al.,* 1996; Campbell *et al.,* 2005). Furthermore, this chimeric virus had lost the neurovirulence phenotype typical of the parental PV1(M) in CD155-transgenic mice and in non-human primates (Gromeier *et al.,* 1996; Gromeier *et al.,* 1999).

Later on, studies using IRES from other members of Picornaviridae family also showed evidences for the role of IRES and the cellular factors (ITAFs) in distinct tissue tropism of PV. The foot-and-mouth disease virus IRES was not functional in murine brain cells because in addition to PTB it required $ITAF_{45}$ which was not expressed in the restricted cells (Pilipenko *et al.,* 2000). Similarly, a chimeric PV containing the IRES sequence of hepatitis C virus propagated well in the liver but not in the brain of CD155tg mice (Yanagiya *et al.,* 2003). Recently a cellular protein, DRBP76 (double-stranded RNA binding protein 76) as a heterodimeric complex with NF45 (a nuclear factor), has been shown to associate with the rhinovirus IRES in neuronal but not in malignant glioma cells and to prevent PV1(RIPO) propagation in neuronal cells at the level of translation (Merrill *et al.,* 2006a, 2006b). These findings indicate that there may be differences in the requirements for cellular factors between related picornavirus IRESes and their distributions may determine the tissue- or cell-specific replication of viruses.

iii) IFN-dependent tissue tropism/IFN response-restricted tropism: It has been well established that primary tissue cultures of human or primate origin acquire susceptibility to PV over a relatively short time in culture. This had been interpreted to be a result of up-regulation of the viral receptor CD155. Recent evidence indicates that IFNα/β-system plays an important role in the acquisition of susceptibility to PV by cells in tissue culture. Differences in interferon (IFN) response among the tissues are responsible for differential susceptibility of cells

to PV. The IFN response protects the cells in some extraneural tissues (Ida-Hosonuma *et al.,* 2005). These investigators also showed that kidney cells acquired PV susceptibility during the cultivation process and the rapid loss of IFN action played an important role in the change in the susceptibility of kidney cells to PV (Yoshikawa *et al.,* 2006). Similar evidence has accumulated from other virus/host systems such as the acquisition of Myxoma Virus susceptibility in human primary fibroblasts in culture (Johnston *et al.,* 2005). Virally infected cells produce type I interferons (IFN-αs and IFN-β) through mechanisms involving activation of the interferon regulatory factor (IRF-3), NF-κB and perhaps the dsRNA-dependent protein kinase PKR and JNK-2 pathways (Garcia-Sastre *et al.,* 2006). Binding of type I IFNs to their cell surface receptors (IFNAR1/2) activates the intracellular IFN signaling pathway. Activation of the signaling pathway results in the tyrosine phosphorylation of signal transducers and activators 1, 2, and 3 (STAT1, STAT2, and STAT3) by Janus-activated kinase 1 (JAK1) and tyrosine kinase 2 (TYK2) (Reich *et al.,* 2006). The activated STATs form homo- or heterodimers and translocate to the nucleus to induce the expression of the IFN-stimulated genes (ISGs) (Reich, 2007). The function of these ISGs is to induce an antiviral state in the cell. However, many of the ISGs, for instance PKR and OAS (2'-5' oligoadenylate synthetases) are also known to facilitate killing of the virally infected cells by apoptosis (Garcia-Sastre *et al.,* 2006). However, the reason for the waning interferon response, and the resulting

increased virus susceptibility upon prolonged culture of primary tissues, is a matter of debate.

The specific topics of this dissertation

Based on the above considerations it is now clear that receptor expression is necessary but not sufficient to assure intracellular PV replication once the virion has been internalized. In order to fully understand the molecular mechanisms of PV pathogenicity, the events of virus-host interaction following PV entry must be clarified in detail. This dissertation is focused on the identification of the post entry determinants of PV that might modify PV tissue tropism and host restriction after the virus particle has successfully bound the receptor, and entered the host cell.

In Chapter II and Chapter III of this dissertation, I present experiments to elucidate the mechanism of the IRES-dependent tissue tropism of PV using a chimeric virus containing a replacement of the IRES sequence in the PV type 1 5′NTR with the corresponding sequences from HRV2. This chimeric virus, PV1(RIPO) was shown to be at least 10,000,000 times less pathogenic in CD155tg mice than the wt. While the paralytic/lethal dose 50 (PLD_{50}) (the virus titer that induces paralysis or death in 50% of the mice) for the wt is 10^2 PFU, a PLD_{50} for PV1(RIPO) could not be established, as the highest achievable dose of 10^9 PFU was still unable to kill mice. While the formidable neuroattenuation of PV1(RIPO) in CD155tg mice correlates with its inability to replicate in a human SK-N-MC neuroblastoma cell line, a crucial question has not been conclusively

answered; whether a host species specific block, that is a possible inability of PV1(RIPO) to replicate in certain or all mouse cells per se, may contribute to the attenuation phenotype. I tried to separate the possible tissue-specific block (neuronal vs non-neuronal) from the possible host species-specific block (mouse vs human) by comparing the genotypes of SK-N-MC-adapted and L20B-adapted PV1(RIPO) and analyzed their phenotypes on both cell types, respectively, as well as in CD155tg mice. In addition, I carried out experiments to examine the effect of IRES *trans*-activating factors on the growth of PV1(RIPO) in SK-N-MC cells and L20Bcells and the results are presented and discussed in Chapter III of this dissertation.

In Chapter IV, I describe the experiments that were carried out in an attempt to identify the determinants of defective replication of PV in a canine epithelial cell line, MDCK (Madin-Darby Canine Kidney) cells. Here we have a case which shows that cells of a mammalian origin in culture did not acquire susceptibility during the process of cultivation, which is thought to play an important role as a determinant in PV susceptibility of cells in culture (Ida-Hosonuma *et al.,* 2005; Yoshikawa *et al.,* 2006). In fact, this is the first report of a cell line of mammalian origin to show resistance to PV replication. The study of the defect in PV propagation in these cells is important for better understanding of PV tissue tropism and host restriction and overall PV pathogenesis in non-human primates. The proposed study was aimed to determine the intracellular stage of the virus life cycle in MDCK cells at which this restriction is exhibited.

Figure 1. Structure of PV genome and processing of PV polyprotein. (A) Schematic representation of PV genome. 5' NTR: 5' non-translated region, 3' NTR: 3' non-translated region, IRES: internal ribosomal entry site. Cleavage sites for $2A^{pro}$, $3C^{pro}$, and $3CD^{pro}$ are indicated. (B) Proteolytic processing of the poliovirus polyprotein (see text for details).

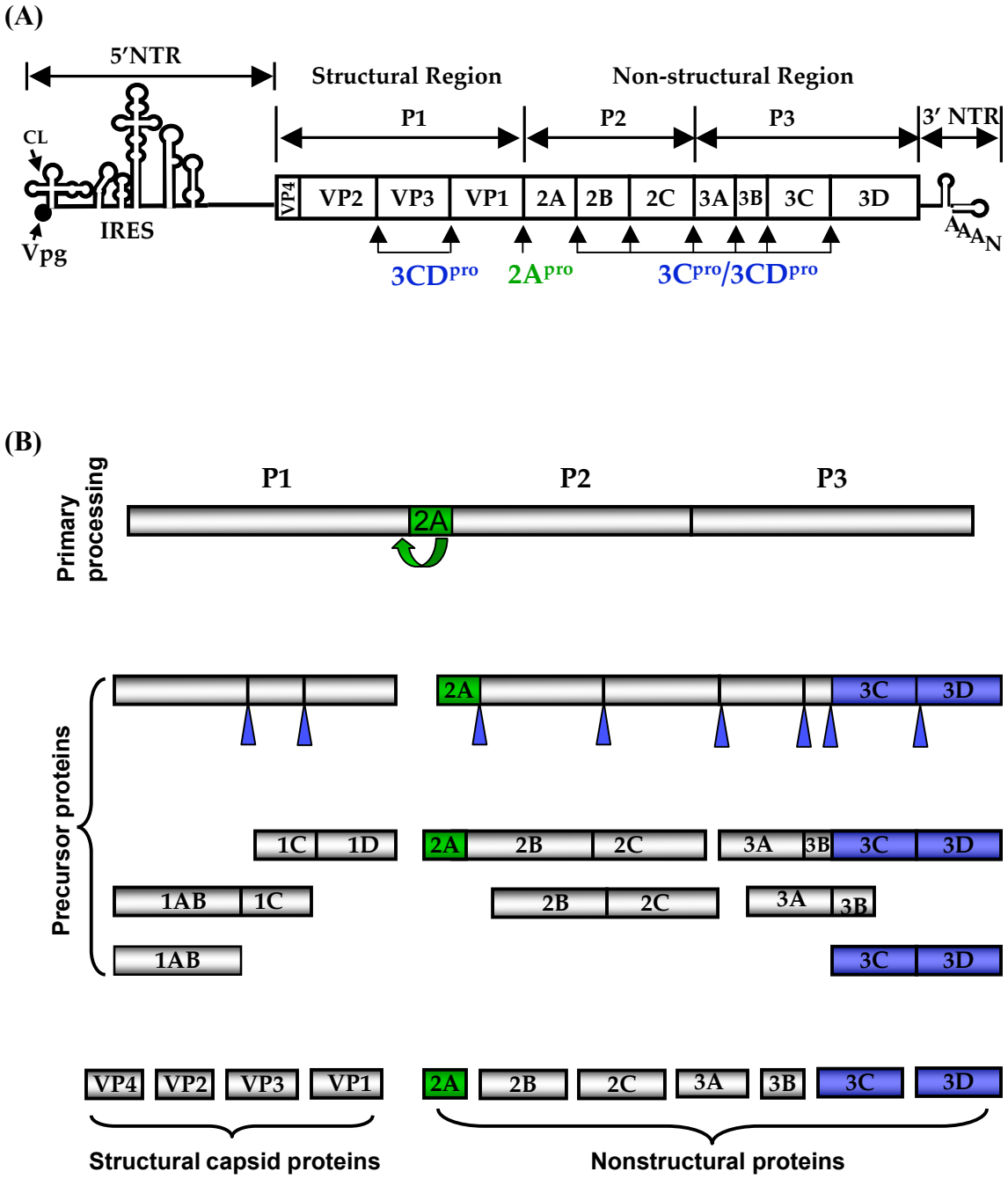
(A)
5′NTR
Structural Region
Non-structural Region
P1
P2
P3
3′ NTR
CL
VP4
VP2
VP3
VP1
2A
2B
2C
3A
3B
3C
3D
IRES
Vpg
AAAN
3CDpro
2Apro
3Cpro/3CDpro
(B)
Primary processing
P1
P2
P3
2A
Precursor proteins
1C
1D
2A
2B
2C
3A
3B
3C
3D
1AB
1C
2B
2C
3A
3B
1AB
3C
3D
VP4
VP2
VP3
VP1
2A
2B
2C
3A
3B
3C
3D
Structural capsid proteins
Nonstructural proteins

Figure 2. IRES elements of Picornaviruses. **A-C**. The figure shows the type I IRES element of PV, the type II IRES of EMCV, and the type III IRES of HAV. Figures A-C are taken from Ehrenfeld *et al.,* (2002).

(A) Type I IRES (PV).

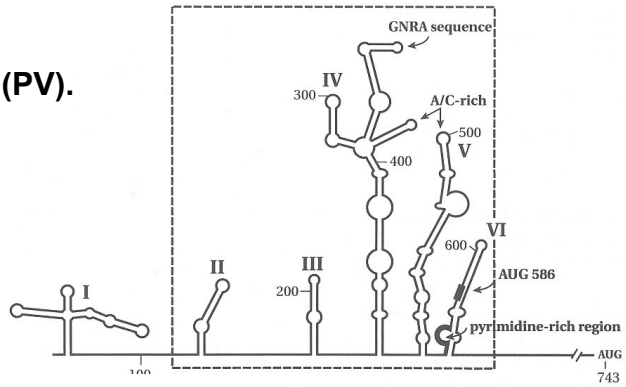

(B) Type II IRES (EMCV)

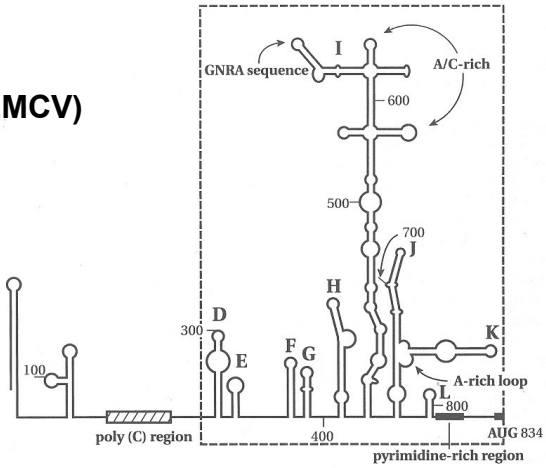

(C) Type III IRES (HAV)

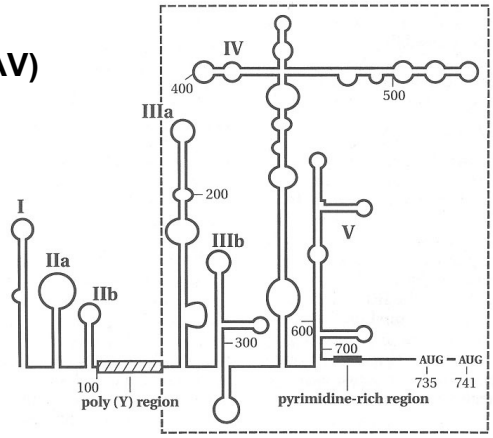

Figure 2. IRES elements of Picornaviruses. **D-E.** Type IV IRESes of Porcine kobuvirus and Porcine teschovirus, respectively. Figure D is taken from Reuter *et al.,* (2009). Figure E is taken from Chard *et al.,* (2006).

(D)

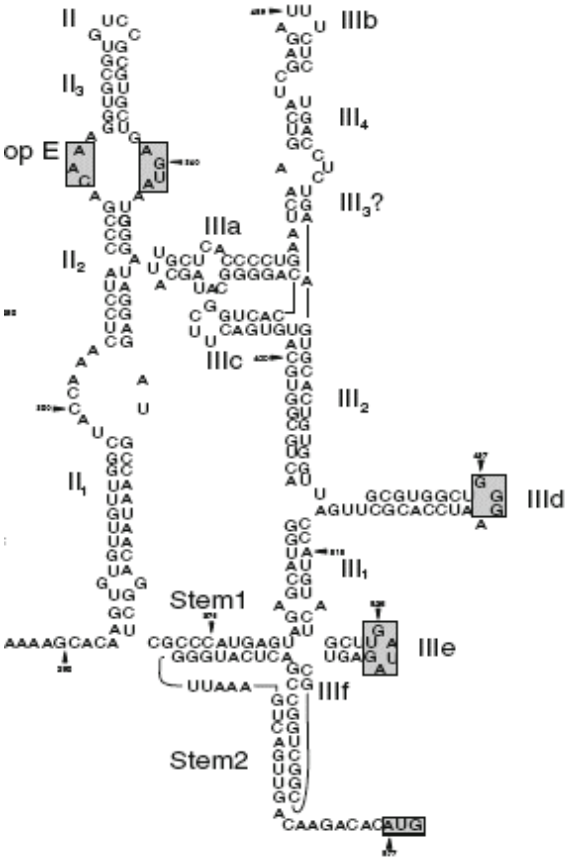
II
IIIb
III4
op E
III3?
IIIa
II2
IIIc
III2
II1
IIId
III1
Stem1
IIIe
IIIf
Stem2
AAAAGCACA
CGCCCAUGAGU
GGGUACUCA
UUAAA
GCUUA
UGAGU
GCGUGGCU
AGUUCGCACCUA
CAAGACAC
AUG

(E)

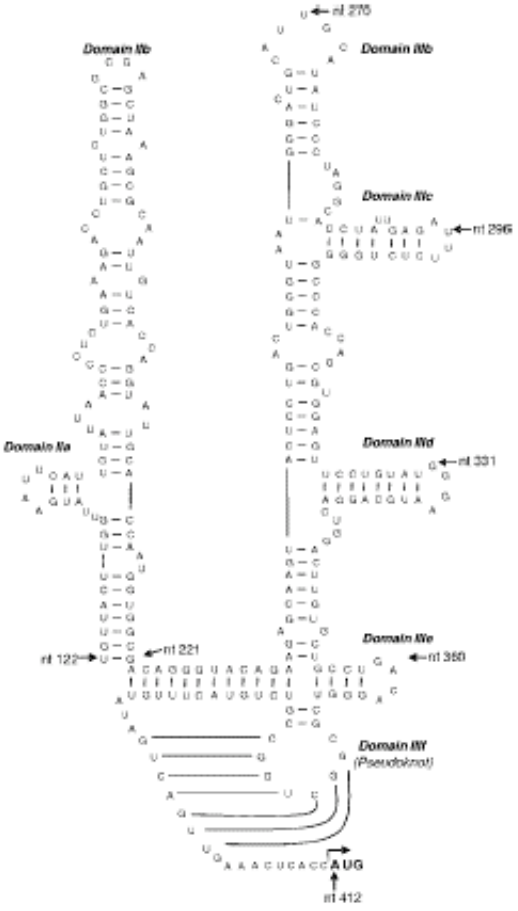
nt 275
Domain IIb
Domain IIb
Domain IIc
nt 296
Domain IIa
Domain IId
nt 331
nt 122
nt 221
Domain IIe
nt 350
Domain III
(Pseudoknot)
AUG
nt 412

Figure 3. The life cycle of poliovirus. (1) The virion binds to the receptor CD155, is transported into the cell and uncoated. (2) After cleavage of the genome linked protein VPg the RNA is translated into a polyprotein which is subsequently processed into numerous functional proteins. (3) In a membrane-associated replication complex the plus stranded genomic RNA is transcribed into a minus strand and forms a double stranded “replicative form” (RF). Minus strands then function as template for the synthesis of plus strands uner the formation of an intermediate called “replicative intermediate” (RI). (4) Newly synthesized plus stranded RNA then associates with procapsids to form mature virions. The plus stranded RNA has also the choice of re-entering genome replication or serving as mRNA in translation. (5) Finally the mature virions are released from the decaying cell. The nucleus is not involved in the replicative cycle.

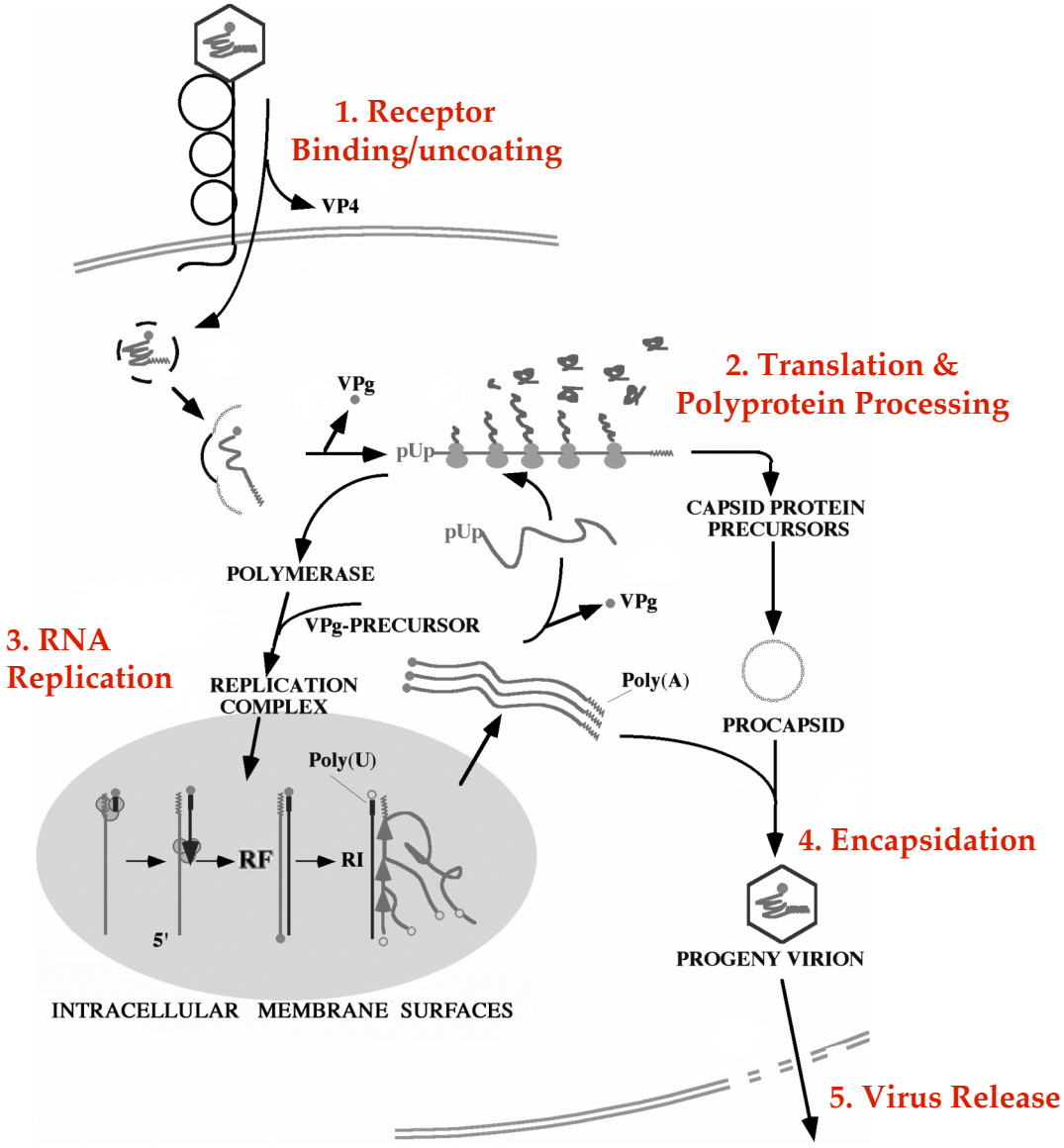
1. Receptor
Binding/uncoating
VP4
VPg
pUp
2. Translation &
Polyprotein Processing
CAPSID PROTEIN
PRECURSORS
pUp
POLYMERASE
VPg
VPg-PRECURSOR
3. RNA
Replication
REPLICATION
COMPLEX
Poly(A)
PROCAPSID
Poly(U)
RF
RI
5'
4. Encapsidation
PROGENY VIRION
INTRACELLULAR MEMBRANE SURFACES
5. Virus Release

Chapter II. A Host-specific, temperature sensitive translation defect determines the attenuation phenotype of a human rhinovirus/poliovirus chimera PV1(RIPO)

Introduction

It is generally assumed that the primary determinant of the host range of picornaviruses, a large family of plus strand RNA viruses, is the tissue specific expression of a virus' cellular receptor. In the case of PV, CD155 (also known as Pvr) (Mendelsohn *et al.,* 1989; Koike *et al.,* 1990) narrowly restricts the virus to humans and nonhuman primates. The isolation and characterization of the PV receptor CD155 made possible the construction of CD155 transgenic (tg) mice (Koike *et al.,* 1991; Ren *et al.,* 1990). These tg animals, when injected with PV, show symptoms of paralysis similar to those of human poliomyelitis. Although CD155 could be detected in various human and tg mouse tissues, many of those tissues are not necessarily sites of PV replication (Mendelsohn *et al.,* 1989; Freistadt *et al.,* 1990, Ida-Hosonuma *et al.,* 2005). This indicated that receptor expression is necessary but not sufficient for PV replication.

Picornavirus genomic RNA and mRNA are of identical sequence. However, the virion RNA is linked at its 5'-end to the small protein VPg that is cleaved off when the genome engages in translation (Wimmer *et al.,* 1993). Thus, in contrast to eukaryotic host cellular mRNAs, picornavirus genomic RNAs, that serve as mRNA lack the 5' cap structure. Instead picornaviruses control their translation with an internal ribosomal entry site (IRES) within the 5' nontranslated regions (5' NTRs) of their genome (Jang *et al.,* 1988; Pelletier and Sonenberg, 1988; Ehrenfeld *et al.,* 2002).

Picornavirus IRES elements are large, extensively structured segments of RNA (~450 nt). Although these elements are quite distinct in structure, they are interchangeable between viruses of different genera and even of different families, yielding novel chimeric infectious viruses (Alexander *et al.,* 1994; Gromeier *et al.,* 1996, 1997; Lu and Wimmer, 1996; Dobrikova *et al.,* 2003). Some of these studies with IRES-chimeric viruses illustrated the potential contribution of the IRES element toward cell tropism of the virus (Gromeier *et al.,* 1996; Dobrikova *et al.,* 2003; Kauder *et al.,* 2006).

The IRES dependent tissue tropism as a determinant of picornaviral pathogenesis was studied previously using PV1(RIPO), a chimeric virus containing the IRES of HRV2 in the background of the genome of PV, type 1 (Mahoney) [PV1(M)] (Gromeier *et al.,* 1996). PV1(RIPO) was found to replicate well in human cervical carcinoma cells (HeLa) but replication was significantly reduced in human neuroblastoma cells (SK-N-MC) at 37^{o}C. Subsequently it was observed that PV1(RIPO) exhibited a temperature-sensitive (*ts*) growth phenotype (Cello *et al.,* 2008), characterized by severely impaired viral replication on SK-N-MC cells at 39.5^{o}C. A *ts* phenotype has also been documented for all three Sabin vaccine strains and it is considered an important factor in neuroattenuation (Macadam *et al.,* 1991; Macadam *et al.,* 1992). Furthermore, PV1(RIPO) had lost the neurovirulent phenotype of PV1(M) in CD155tg mice, and in non-human primates (Gromeier *et al.,* 1996; Gromeier *et al.,* 1999). It is at least 1,000,000 times less pathogenic in CD155tg mice than

wild-type PV. Similar results were obtained when an IRES recombinant between HRV2 and the neurovirulent *wt* Leon/37 PV of type 3 was tested in the CD155tg mouse model (Chumakov *et al.,* 2001).

The question whether the IRES is an important determinant of PV pathogenesis, led to a nearly two decades long study of attenuated and neurovirulent polioviruses by different groups. Early studies showed that the reduced efficiency of *in vitro* translation of Sabin type 3 PV RNA compared to that of the neurovirulent strains of type 3 PV is the result of the known attenuating mutation (C472→U) in the IRES of Sabin type 3 PV (Svitkin *et al.,* 1985, 1990). Supporting evidence for this observation came from the work of La Monica and Racaniello (1989). Using cell culture models they showed the C472→U mutation in Sabin type 3 PV results in low titer growth and reduced translation efficiency in neuroblastoma cells but not in HeLa cells. Later on they performed experiments to test the role of IRES-mediated translation initiation as a determinant of PV tissue tropism and pathogenesis (Kauder *et al.,* 2004, 2006). Replacing the IRES of PV1(M) with that of coxsackie virus B or hepatitis C virus and using the Sabin type 3 PV IRES, Kauder and colleagues (2004) originally reported that the tropism of wild type and vaccine strains of PV is determined in a step after IRES-mediated translation. In a subsequent study, however, using a different experimental strategy, they suggested that IRES-derived translation plays an important role in replication of a chimeric virus (P1/HRV2) in an age-dependent manner in CD155tg mice (Kauder *et al.,* 2006).

The neuroattenuation of PV1(RIPO) in CD155tg mice correlated with its inability to replicate in human SK-N-MC neuroblastoma cells and in non-human primates (Gromeier *et al.,* 1996; Gromeier *et al.,* 1999). It is not yet known whether a host species specific block, may contribute to the attenuation phenotype. In this study I examined the IRES dependent tissue tropism of PV1(RIPO) with the aim of distinguishing between a tissue specific block (neuronal vs non-neuronal) and a host species specific block (mouse vs human) by comparing the growth phenotypes of PV1(RIPO) in different human and mouse cell lines of neuronal and non-neuronal origin. My results indicate that PV1(RIPO) possesses a strong temperature dependent growth defect in all the mouse cell lines tested (both neuronal and non-neuronal expressing the human PV receptor CD155), an observation suggesting that mouse tissues are generally unable to support HRV2 IRES-dependent initiation at temperatures higher than 33^{o}C. All CD155-expressing mouse cell lines, on the other hand, are perfectly susceptible to infection by wild type PV. These results correlate with high attenuation of this chimeric virus in CD155tg mice. This attenuation phenotype might be related to a mouse species specific block of PV1(RIPO) growth at higher temperatures. The CD155tg mice models therefore have their limitations to assess the neurovirulence of chimeric virus PV1(RIPO) and perhaps other similar chimeras.

MATERIALS AND METHODS

Viruses and cells. The neurovirulent PV type 1 [Mahoney; PV1(M)] is the strain being used routinely in the laboratory (Cello *et al.,* 2002). PV1(RIPO) was constructed as described previously (Gromeier *et al.,* 1996). The construction of PN6 mutant virus has been described elsewhere (Trono *et al.,* 1988). The mouse neuroblastoma cell line stably expressing CD155$_\alpha$ (Neuro-2a^{CD155}) (Mueller *et al.,* 2003; Toyoda *et al.,* 2007b), mouse fibroblast cell lines (L cells) expressing either CD155$_\alpha$ (H20A) (Mendelsohn *et al.,* 1989), or CD155$_\delta$ (L20B) (Mendelsohn *et al.,* 1989; Pipkin *et al.,* 1993) and mouse fibroblast cell line stably expressing CD155$_\alpha$ (NIH3T3^{CD155}, Mueller and Wimmer unpublished), all of which are susceptible to PV infection, were maintained in DMEM containing 1% penicillin/streptomycin and 10% fetal bovine serum. HEK293 (Ad transformed neuroepithelial) cells (A gift from M. Gromeier; Campbell *et al.,* 2005) were maintained in Dulbecco's minimal essential medium (DMEM) containing 1% penicillin/streptomycin and 10% fetal bovine serum. HeLa (human cervical cancer) cells, and human neuroblastoma cell lines SK-N-MC and SK-N-SH were obtained from the American Type Culture Collection (Manassas, VA) and were maintained according to the supplier's specification.

Serial passages of PV1(RIPO) in SK-N-MC and L20B cells. The selection of PV1(RIPO) isolates capable of efficient replication in mouse cells and human neuroblastoma cells was carried out according to the following procedure: H20A and SK-N-MC cells were infected at an MOI (multiplicity of infection) of 10

with PV1(RIPO) and incubated at 37°C for 4 days, or until the appearance of CPE. After 7 blind passages complete CPE was observed and RNA extracted from the viral cell lysate served as template for reverse transcription-PCR (RT-PCR) and the purified PCR amplicons were used for sequencing reactions.

RNA extraction, RT-PCR, and DNA sequencing. Viral RNA was extracted from infected cells using TRIzol solution (Invitrogen) and used as template for RT-PCR. Titan One-Tube RT-PCR system was used to perform RT-PCRs following the manufacturer's instructions (Roche, Mannheim), and the PCR amplicons were purified with the QIAquick gel extraction kit (QIAGEN). The sequence of the purified PCR products was determined with oligonucleotide primers in cycle sequencing (ABI Prism Big Dye terminator cycle sequencing ready reaction kit; Applied Biosystems) in an automated sequencer (model 310; Applied Biosystems).

Construction of plasmids. Several recombinant variants with phenotypes quite distinct from the parent PV1(RIPO) were constructed using different combination of mutations in the 5'NTR that had been identified in the adapted isolates. For instance, the plasmid for one of the recombinant variants, R-1235, (see below), was constructed as follows and was named R-1235r: cDNA prepared from R-1235 viral RNA was cut with *Bbrpl* and *SacI* and ligated to a similarly restricted PV1(RIPO) fragment. To construct R-2r, which has a single C133G mutation in the 5'-NTR of PV1(RIPO), site-directed mutagenesis was carried out in a two step PCR reaction. For the first-step PCR, two PCR

fragments F1 and F2 were amplified by using pT7PV1(RIPO) as template and the primer pair 5'TTAAAACAGCTCTGGGGTTGTACCCACCCC 3' and 5' TCAGTAATCTGGCTGATTACCGCCTATTGGTCTTTGTGAAAAAC 3'for F1 fragment and the primer pair 5' GTCCTGTTTCGAAGCCGCGTTACTAGC 3' and 5' AGTTTTTCACAAAGACCAATAGGCGGTAATCAGCCAGATTACTG 3' for F2 fragment. The two PCR fragments, F1 and F2 carrying overlapping ends were then used as templates for the second-step PCR. R-123r, R-12r, R-35r, R-3r, R-5r were constructed by choosing appropriate restriction endonuclease sites within R-1235r and PV1(RIPO) plasmids and exchanging fragments between these plasmids. Mutations in the final constructs were verified by sequencing using the ABI Prism DNA Sequencing kit.

***In vitro* transcription, transfection and virus isolation.** All plasmids were linearized with *Dra*I. RNAs were synthesized with phage T7 RNA polymerase, and the RNA transcripts were transfected into HeLa R19 cell monolayers by the DEAE-dextran method as described previously (van der Werf *et al.,* 1986). The incubation time was 2 to 3 days for full-length viral constructs. Virus titer was determined by a plaque assay, as described before (Molla *et al.,* 1991).

One-step growth curves at 33 ^{o}C, 37 ^{o}C, and 39 ^{o}C. One-step growth experiments in different human and mouse cell lines were carried out as follows. Cell monolayers in 35 mm plastic culture dishes were washed with DMEM and inoculated at an MOI of 10 with the virus to be tested. The dishes were rocked for

30 min at room temperature, the cells were thoroughly washed to remove unbound virus and placed at 33^{o}C or 37^{o}C or 39.5^{o}C. At 0, 2, 4, 6, 8, 12, 24 and 48 hr post infection (p.i.), the dishes were subjected to three consecutive freeze-thaw cycles, and the viral titers of the supernatants were determined by plaque assay on HeLa cells, as describe before (Molla *et al.,* 1991).

Poliovirus luciferase replicons and luciferase assays. Previously a wt replicon PV1(M)-luc was described, in which the PV capsid coding sequence was replaced by that of firefly luciferase gene (Li *et al.,* 2001). In addition two new chimeric replicons were constructed that, in analogy to their full length infectious counterparts, carrying either the wt HRV2 IRES [PV1(RIPO)-luc] or a mouse-adapted HRV2 IRES (R-1235r-luc). *In vitro* transcribed replicon RNA was transfected into monolayers (35-mm-diameter dishes) of HeLa, SK-N-MC and L20B cells using a modified DEAE-Dextran transfection method (Mueller *et al.,* 2006) and incubated at 33°C, 37°C or 39.5°C in DMEM, 2% BCS. At different time points post-transfection the growth medium was removed from the dishes, and the cells were washed gently with 2 ml of phosphate-buffered saline. The cells were lysed in passive lysis buffer (Promega) and the firefly luciferase activity was measured by methods described previously (Yin *et al.,* 2003) using a firefly luciferase substrate kit (Promega). The rate of viral translation was assayed by incubating transfected cells in the presence of 2mM guanidine hydrochloride (GuHCl), a potent inhibitor of PV replication. RNA replication of a

construct, on the other hand, can be assessed by considering the ratio of luficerase signals obtained in the absence and presence of the guanidine.

Neurovirulence assays in mice. Groups of four CD155tg mice (Koike *et al.,* 1991) were inoculated with any given amount of virus ranging from 10^2 to 10^8 plaque-forming units (pfu; 30 µL/mouse) i.c. with different viruses. Mice were examined daily for 21 days after inoculation for paralysis and/or death. The virus titer that induced paralysis or death in 50% of the mice (PLD_{50}) was calculated by the method of Reed and Muench (Reed and Muench, 1938). All experiments involving mice were conducted in compliance with institutional IACUC regulations and federal guidelines.

RESULTS

Previously a picornavirus genomic hybrid, PV1(RIPO), was constructed in which the IRES element of PV1(M) was replaced with that of HRV2 (Gromeier, *et al.,* 1996) (Fig. 4A). PV1(RIPO) was cloned by using an upstream *EcoRI* restriction site in the spacer region between the clover leaf and the IRES of the PV1(M) genome. This *EcoRI* site was originally generated through linker insertion scanning in the 5'NTR of PV1(M) resulting in PV variant PN6, which displayed wt growth characteristics in HeLa cells (Trono *et al.,* 1988) (Fig. 4A). We have previously described that modifications within this spacer region by mutation of two nearby clusters of C residues (Toyoda *et al.,* 2007a), or of the dinucleotide UA(101/102)GG (Cello *et al.,* 2002; De Jesus *et al.,* 2005), or by insertion of a stem-loop (Yin *et al.,* 2003; Toyoda *et al.,* 2007b) significantly

changed the phenotypes of the parental virus. PV1(RIPO) exhibited a replication phenotype and *ts* growth restriction in SK-N-MC neuroblastoma cells (Cello *et al.,* 2008) but the effect, if any, of the linker insertion in strain PN6 on the replication in cells of neuronal origin remained unknown.

The growth phenotype of PV1(RIPO) and PN6 in human cell lines at different temperature. Upon further analysis of the spacer region of entero and rhinoviruses we identified a previously unrecognized highly conserved sequence in the spacer region corresponding to nt position 103-112 of the PV genome (Fig. 12). The question thus arose, whether the longer spacer region artificially extended by the *EcoRI* linker was the cause for PV1(RIPO) attenuation phenotype. The growth phenotypes of PV1(RIPO) and PN6 in HeLa R19 was first analyzed at 33^{o}C, 37^{o}C and 39.5^{o}C and found to be similar to that of PV1(M) (Fig. 4B). When tested in three different human cell lines of neuronal origin (Fig. 5) PN6 replicated with similar growth kinetics as PV1(M) at all three temperatures (closed triangles) whereas the growth of PV1(RIPO) was inhibited in SK-N-MC cells (Gromeier *et al.,* 1996), and in HEK293 cells (Campbell *et al.,* 2005). A *ts* phenotype of PV1(RIPO) observed at 39.5^{o}C was particularly pronounced in SK-N-MC and HEK293 cells. For reasons that remain unknown, the growth defect at 33°C is reduced in all three human neuronal cell lines tested, and even absent in SK-N-SH (Fig. 5). In any event, the phenotypes of PV1(RIPO) observed in Fig. 5 could be the result solely of the presence of the HRV2 IRES in the PV1(M) background, or of the presence of the HRV2 IRES

plus the insertion preceding the HRV2 IRES (Fig. 4A). It should be noted that the *EcoRI* linker insertion increases the length of the spacer region, and thus the distance between cloverleaf and IRES by 12 nucleotides. The corresponding sequence changes in the spacer between clover leaf and IRES in PN6, however, exerted little, if any effect in cells of human origin.

PV1(RIPO) has a mouse cell-specific propagation defect which can be rescued by growth at lower temperature. I then tested whether the growth phenotypes of PV1(RIPO) in mouse cells of neuronal and non-neuronal origin reflects that in human cells. For the experiments I used $N2a^{CD155}$, a mouse neuroblastoma cell line stably expressing the human PV receptor CD155 (Mueller and Wimmer, 2003) as well as the two CD155- expressing mouse fibroblast cell lines L20B (Mendelsohn *et al.,* 1989; Pipkin *et al.,* 1993) and $NIH3T3^{CD155\alpha}$ (see the Materials and Methods). Infections were carried out at 33°C, 37°C and 39.5°C. Whereas PV1(M) and PN6 replicated well in all cell lines at 33°C and 37°C, PN6 expressed a *ts* phenotype at 39.5°C that was pronounced in $NIH3T3^{CD155\alpha}$ cells (Fig. 6C). Surprisingly, PV1(RIPO) did not replicate in any mouse cell at either 37°C or 39.5°C (Fig. 6A-C). In stark contrast, all three cells supported replication at 33°C. At 33°C, therefore, even cells of neuronal origin ($N2a^{CD155}$ cells) are an adequate substrate for PV1(RIPO) replication (Fig. 6A).

PV1(RIPO) is defective in IRES mediated translational initiation at the restricted temperature. After CD155 mediated internalization, the PV particle uncoats and the viral genome RNA serves as mRNA for the translation of a

single polyprotein by a cap-independent mechanism, followed by replication of the incoming genome (Wimmer *et al.,* 1993; Paul, 2002). In order to understand at which stage of replication the attenuation of PV1(RIPO) occurs in some human cell lines the functionality of PV-specific replicons expressing the Luciferase gene was analyzed. Specifically, I used PV1(M)-Luc and PV1(RIPO)-Luc, containing the firefly luciferase reporter gene in place of the PV capsid proteins, to assess their ability to be translated and replicated in SK-N-MC and L20B cells. To differentiate between the luciferase signals due to translation from the incoming viral RNA from signals due to translation from mRNA synthesized during replication the cells were grown in the presence and in the absence of 2mM guanidine hydrochloride (GuHCl). At this concentration, GuHCl inhibits viral RNA replication without any toxic effect on cellular processes or viral translation (Caliguiri *et al.,* 1968; Jackobson *et al.,* 1968; Loddo *et al.,* 1962). HRV2 IRES-mediated translation and RNA replication were measured in HeLa R19 cells, mouse L20B cells and SK-N-MC cells by transfecting the cells with *in vitro* transcribed RNA of PV luciferase replicons and incubation of the cells at 33^{o}C, 37^{o}C and 39.5^{o}C in the presence (for translation) or in the absence (for replication) of 2 mM GuHCl (Fig. 7). Translation and replication mediated by the HRV2 IRES in case of the PV1(RIPO)-luc replicon were similar to that of the PV1(M)-luc replicon in HeLa R19 cells (Fig. 7A). In contrast, in SK-N-MC cells HRV2 IRES-mediated translation, and consequently replication, was low and it decreased with increasing temperature (Fig. 7B). Most strikingly, in mouse L20B

cells the PV1(RIPO)-luc replicon failed to show any replication activity at 37^{o}C and 39.5^{o}C, likely as a result the greatly reduced translation activity (Fig. 7C), This finding is consistent with the growth characteristics of the corresponding chimeric virus, PV1(RIPO), in different mouse cell lines (Fig. 6B). Therefore, I conclude that in mouse cell lines the HRV2 IRES-mediated translation is defective in a *ts* manner, which is ultimately affecting viral RNA replication.

Genetic variants in the 5'NTR of PV1(RIPO) are adapted to growth in mouse cells and human neuronal cells. Serial passage of an attenuated strain of PV1(M) facing a replication block may result in the evolution of modified variants with increased replication properties. With the aim of isolating such adapted variants, PV1(RIPO) was serially passaged in SK-N-MC cells and in mouse H20A cells at 37^{o}C, respectively. Two variants (R-1 and R-7) were isolated from SK-N-MC passages and seven (R-1235, R-123, R-124, R-234, R-136, R-12, and R-23) from H20A passages (Fig. 8) (see Materials and Methods). These variants showed increased replication in the cell types in which their progenitor was highly restricted in growth. The 5' NTRs of the adapted isolates were sequenced and the mutations were mapped with the aim of understanding the molecular determinants of the high-titer growth phenotype (Fig. 8). The three most common changes that were observed were: i) either a 12 or a 13 nucleotide deletion in the spacer between cloverleaf and IRES (mutation 1); ii) point mutation 2; and iii) point mutation 3. Among these, mutation 1 was observed for both human SK-N-MC cells and mouse H20A cells and was either a

12 or a 13 nucleotide deletion in the spacer between the CL and the IRES (Fig. 8). Interestingly, this deletion sequence corresponds to the *EcoRI* linker insertion (originally derived from the parental PN6 virus) which was used for cloning of this virus. On the other hand point mutations 2 and 3 are most likely important for mouse-specific adaptation because they are only present in the mouse cell-adapted isolates. The isolates containing different combination of these changes (R-1235, R-123, R-12 and R-23) were then tested for their growth in different mouse cell lines at various temperatures (Fig. 9). Although they all grew very well at 33^{o}C and 37^{o}C, at 39.5^{o}C they showed growth defects similar to PV1(RIPO).

To distinguish between a tissue specific (neuronal vs non-neuronal) and/or host species specific (mouse vs human) block, the SK-N-MC-and L20B-adapted isolates were evaluated in a crosswise comparison of their growth restriction in L20B and SK-N-MC cells, respectively. The mouse cell-adapted PV1(RIPO) isolate, R-1235, with a replication phenotype nearly identical to wt PV1(M) in mouse cells, also replicated with kinetics similar to wt PV1(M) in SK-N-MC cells (Fig. 10A), whereas human neuron-adapted PV1(RIPO) isolate (R-1) still showed an attenuated phenotype in L20B cells (Fig. 10B). This result indicates that the deletion in the spacer region alone is not sufficient to restore a high titer growth phenotype in mouse cells, and that the additional point mutations identified in the HRV2 IRES are essential for overcoming the mouse-specific host restriction .

To identify the most effective point mutation(s) in variants of PV1(RIPO) leading to efficient replication in mouse cells (in addition to the deletion mutation),

several of the mouse cell-adapted isolates were reconstructed by introducing the most commonly observed point mutation(s) into the 5'NTR of PV1(RIPO). When the deletion and three point mutations were introduced into the parental PV1(RIPO), the resulting reconstructed virus named R-1235r showed growth kinetics similar to that of the adapted isolate R-1235 in L20B cells (data not shown). This observation indicates that all important adaptive mutations are confined to the 5'NTR and that no significant second site reversions exist elsewhere in the genome. A luciferase replicon of R-1235r was then used to examine whether these mutations can restore the translation and replication activity of the replicon RNA in mouse L20B cells. As expected, the PV1(RIPO)-luc replicon failed to show translation and replication activity at higher temp (37^{o}C and 39.5^{o}C) both at early (5 hour) and late (11 hour) time points post transfection (Fig. 11). The PV1(M)-luc replicon exhibited high level of luciferase activity at all the temperatures. Convincingly, the R-1235r-luc replicon exhibited a similar luciferase activity as the PV1(M)-luc replicon, indicating that translation in mouse cells was restored by the adaptive mutations (Fig. 11). This result correlated well with the restoration of the higher growth titer of R-1235r virus in mouse L20B cells.

Some additional mutants were constructed *in vitro* by introducing mutations 1, 2, 3, and 5 either singly (R-1r, R-2r, R-3r and R-5r) or in combination (R-123r, R-12r and R-35r). All these mutants were then compared with the original adapted isolates for their growth phenotypes (Table 1).

Co-variation between mouse-cell adaptive mutations and mouse neurovirulence. To further assess the relationship between the high-titer growth phenotype of the mouse cell-adapted PV1(RIPO) variants, their equivalent reconstructions, and the neurovirulence in CD155tg mice, groups of 4 CD155tg mice were inoculated via the intracerebral route with 10^2-10^8 PFU (30 μl/mouse), as previously described (Gromeier *et al.,* 1996). All mice were observed and scored daily for at least 21 days post inoculation for symptoms of poliomyelitis and/or death. Using the data obtained, the mouse paralytic/lethal dose 50 (PLD_{50}) (the virus titer that induces paralysis or death in 50% of the mice) was determined using the method of Reed and Muench (Reed and Muench, 1938) (Table 1). As was observed before, PV1(RIPO) was at least 10^6 times less pathogenic in CD155tg mice than wild type PV1(M) (Gromeier *et al.,* 1996, 1999). In fact, a PLD_{50} for PV1(RIPO) could not be established (Table 1) as the virus did not kill at the highest tested dose, whereas the PLD_{50} for PV1(M) was 10^2 PFU. This result correlates with the inability of PV1(RIPO) to replicate in mouse L20B cells (Table 1). In contrast, the mutant virus PN6 with the insertion of 11 nt between the clover leaf and IRES is attenuated in CD155tg mice with a PLD_{50} of $10^{4.7}$ [still by orders higher than PV1(RIPO)], presumably due to the slight replication defect in mouse cells, as seen in $NH3T3^{CD155}$ cells. It should be noted that the replication defect of PN6 in mouse cells is more pronounced when infections are done at a low MOI (0.01), a scenario more akin to the situation a virus might find upon encounter of a host cell in an infected animal.

PV1(RIPO) isolates, adapted to grow in mouse H20A cells, exhibited different degrees of neuropathogenicity in CD155tg mice whereas, importantly, the human SK-N-MC cell adapted isolate R-1 was still as neuroattenuated as PV1(RIPO) (Table 1). The mouse-adapted PV1(RIPO) isolates R-1235 and R-123, on the other hand, showed significantly increased neurovirulence over that of the parental PV1(RIPO), which supported the fact that the mutations are not only able to control the high titer replication phenotype in mouse cell tissue culture but also improved neurovirulence in the CD155tg mice. When reconstructed, PV1(RIPO) mutants R-1235r and R-123r show a similar trend in neuropathogenicity, an observation indicating the importance of these mutations (Table 1). Reconstructed mutants R-12r and R-35r, harboring combination of two mutations, are still capable of inducing paralysis and/or death in CD155tg mice but need a relatively higher dose of virus. Mutants R-1r, R-2r, R-3r, and R-5r, which have a single mutation are incapable of improving the neuropathogencity of PV1(RIPO). The conclusion from this study is that the important mutations in the 5'NTR have cumulative effect in neurovirulence in CD155tg mice. For example, in R-1235r they together contribute significantly to render this variant a highly neurovirulent derivative of PV1(RIPO).

The deletion of the *EcoRI* linker in PV1(RIPO) was sufficient for the complete restoration of replication in human neuronal cells. This indicates that the neuron-specific defect of PV1(RIPO) is not a result of the choice of the HRV2 IRES to drive translation. It is rather a result of suboptimal spacer length or

disruption of an unknown sequence signal or host factor binding site due to the *EcoRI* linker between cloverleaf and IRES. While deletion of *EcoRI* linker alone restored replication in human neuronal cells it did not suffice to restore neurovirulence in CD155tg mice. This is best illustrated by the phenotype of the resulting virus (R-1) retaining the mouse-specific defect, which can be overcome with additional adaptive mutations within the HRV2 IRES (see above).

DISCUSSION

The experiments reported here were designed to further shed light on the mechanism by which the PV1(M) variant PV1(RIPO), a chimera in which the IRES of PV has been exchanged with that of HRV2, expresses its remarkably attenuated phenotype in the spinal cord of non-human primates (Gromeier *et al.,* 1999; Chumakov *et al.,* 2001) and in CD155tg mice. The attenuation was discovered when it was observed that the replication of PV1(RIPO) is inhibited in human cells of neuronal origin, such as SK-N-MC (neuroblastoma) cells (Gromeier *et al.,* 1996) or HEK293 (Ad transformed neuroepithelial) cells (Campbell *et al.,* 2005) but not in non-neuronal transformed cells such as HeLa cells. It was originally suggested that a specific inhibition of translation is the major cause of attenuation of PV1(RIPO), a hypothesis that is supported by the data presented here. It was subsequently discovered that replication of PV1(RIPO) is *ts* at 39.5^{o}C in neuroblastoma cells but not in HeLa or HTB-14 glioblastoma cells (Cello *et al.,* 2008).

In addition to tissue-specific restriction (observed in human tissues of different origin) I have now found that there is also a strong species-specific restriction of the growth of PV1(RIPO) at physiological temperature: in contrast to wt PV1(M), this chimera does not replicate in NIH 3T3^{CD155}, L20B^{CD155} or N2a^{CD155} cells, three mouse cell lines stably transformed with the PV receptor CD155 (see Materials and Methods). The block in replication is enhanced at 39.5^{o}C but, remarkably, it is absent at 33^{o}C (Fig. 6). These data, which have been obtained by two different investigators with the different cell lines at different times, are highly reproducible. They are, nevertheless, at variance with a report by Kauder *et al.* (Kauder *et al.,* (2006)) in which a construct very similar to PV1(RIPO) was found to replicate in L20B cells, albeit with much delayed kinetics. The exquisite temperature sensitivity observed here, and in particular the rescue of the *ts* phenotype at temperatures below 37^{o}C, may be the reason why this phenomenon has eluded us in an earlier study (Gromeier *et al.,* 1996), during which incubation temperatures may not have been tightly controlled at perhaps less than 37^{o}C.

The replication of human rhinoviruses is broadly restricted in mouse cells. However, host range variants of HRV2 (Yin *et al.,* 1983) and HRV 39 (Lomax *et al.,* 1989) that bypassed the block in mouse L cells have been reported to produce 2C protein with altered electrophoretic mobility. Harris *et al.* (2003, 2005) have shown more recently that these host cell restrictions can be overcome by specific mutations in proteins mapping to the P2/P3 non-structural

region of the genome. However, in the background of a full length rhinovirus genome, no mouse-adaptive mutations were ever reported to localize to the IRES. The mouse specific mutations in the HRV2 IRES, observed here, suggests to us that the PV replication machinery may interact poorly with the PV1(RIPO) 5'NTR at some stage during the viral life cycle. This may also explain why the remarkable host restriction is only seen in the context of a PV genome (full length or replicon), but apparently not IRES driven reporter constructs (Kauder *et al.,* 2004, 2006; Campbell *et al.,* 2005).

This conclusion is supported by my translation experiments using Luciferase expressing PV replicons (Fig. 7) which indicate that the lack of translational activity in mouse cells is the most likely reason for the observed phenotype of PV1(RIPO). In hindsight it is perhaps not surprising that the HRV2 IRES in a PV background brings about a *ts* phenotype (at least in some cell types), as IRES function is likely to be optimized at the natural replication temperature of rhinoviruses of approximately 33^{o}C.

Assays with reporter genes, however, call for cautious interpretation of the data. Campbell *et al.* (2005) have reported that assays with IRES-driven Luciferase reporter constructs that consisted only of the HRV-2 IRES and the reporter gene, did express Luc well (or even better) in HEK293 or SK-N-MC cells than the equivalent PV IRES driven reporter constructs. The authors comment that the "results indicate that translation in a reporter context does not recapitulate the neuron-specific functional deficit of the HRV2 IRES in the context

of the PV genome" (Campbell *et al.,* 2005). If so, the results of the interesting IRES studies of Kauder *et al.* (2004, 2006) using dicistronic reporter mRNA produced by an adenovirus might not have yielded results that can be interpreted to reflect IRES tropism or attenuation. On the other hand, it is intriguing to speculate that the non-structural proteins have to cooperate with the IRES to facilitate maximal expression of the polyprotein, and that this expression is dependent also on ITAFs (N. Jahan and S. Mueller, unpublished results).

My work demonstrates that changes in the 5'NTR alone, particularly the mutations in the HRV2 IRES, are sufficient to rescue HRV2 IRES-mediated translation in mouse cells and, consequently, RNA replication in mouse L cells. Most importantly, these mutations were not only able to rescue the defective growth of PV1(RIPO) in mouse cells but also to produce a highly neurovirulent virus in CD155tg mice.

Previous studies (Gromeier *et al.,* 1996, Gromeier *et al.,* 1999) showed that the PV1(RIPO) IRES containing domains V and VI of the PV1(M) IRES exhibited the same neurovirulence as PV1(M) in CD155tg mice. This observation suggested that both of these domains of the PV1(M) IRES are required for mouse neurovirulence. Subsequently, they have extended these studies using chimeric IRES constructs and using human HEK293 cells as indicator cells for neurovirulence. In these studies, domain VI of the IRES was dispensable for the expression of attenuation but the entire domain V was required for a growth phenotype of PV1(RIPO) in HEK293 cells (Campbell *et al.,* 2005). In the study

presented here, the focus was on the genetics of the expression of conditional phenotypes (*ts*) and of the host range of PV1(RIPO). I have confirmed that PV1(RIPO) is restricted in human neuroblastoma and HEK293 cells at 37^{o}C and I describe that the replication of the chimera at 39.5^{o}C is severely inhibited. In mouse cells, however, regardless of whether they originate from neuronal (N2a^{CD155}) or non-neuronal (L20B and NIH 3T3^{CD155}) precursors, PV1(RIPO) is unable to replicate to any measurable level at 37^{o}C or 39.5^{o}C. Interestingly, PV1(RIPO) can grow in any of the mouse cells analyzed with wt PV kinetics at 33^{o}C, an observation suggesting that there is "nothing wrong" with the basic design of a replicating PV in mouse cells.

In this regard, it did not matter whether the mouse cells were of neuronal origin (N2a^{CD155}) or non-neuronal origin (L20B, NIH 3T3^{CD155}). Thus, besides the previously described defect in human neuronal cells (Gromeier *et al.,* 1996; Cello *et al.,* 2008) PV1(RIPO) displays an exquisite mouse specific block in propagation. In fact, the mouse specific defect may contribute significantly to the tremendous attenuation of PV1(RIPO) seen in CD155tg mice. My results serve to caution investigators as to the interpretation of pathogenicity data obtained with PV variants in the transgenic mouse models. Attenuation of PV variants in CD155tg mice should be corroborated by the absence of a replication block in tissue culture of CD155 expressing mouse cells, such as the widely available L20B.

In spite of the low apparent proliferation of PV1(RIPO) in mouse cells or neuroblastoma cells at 37^{o}C, serial blind passages produced novel genotypes adapted to replication in these restrictive cells to varying degrees. Sequence analyses of the 5'NTR of the new variants identified mutations responsible not only for efficient growths in mouse cells but also for inducing paralysis and/or death in CD155tg mice.

Interestingly, 6 out of 9 isolates from separate passage in human SK-N-MC cells and mouse H20A cells possess a common mutation (mutation 1), which is either a 12 or a 13 nucleotide deletion (AGGAATTCAACT or AGGAATTCAACTT) in the spacer I between the cloverleaf and IRES (Fig. 8). This deletion contains the *EcoRI* restriction site (GAATTC), which was introduced into the linker sequence between the clover leaf and the IRES (Trono *et al.,* 1988) (strain PN6), a construct used as parent virus of PV1(RIPO) (Fig. 4). While the striking neuroattenuation of PV1(RIPO) in CD155tg mice correlates with it's inability to replicate in SK-N-MC neuroblastoma cell line (Fig. 10) variant R-1 grew well in SK-N-MC cells but still replicated only poorly in mouse L20B cells (Fig. 10). In keeping with this trend, R-1 still showed high degree of neuroattenuation in CD155tg mice (Table 1). Replication in a human neuronal cell (SK-N-MC) and neurovirulence in CD155tg mice, therefore, do not co-vary. As has been pointed out before by Campbell *et al.* (2005), assays in neuronal tissue culture cells alone may not be a reliable indicator of neurovirulence.

The selection of R-1 variants indicates that the inserted linker sequence is not neutral in SK-N-MC or in mouse cells. In the context of PV propagated in HeLa cells, however, the insertion appears to be stable presumably because the advantage of deleting it is very small under these conditions. The deletion

restores both the sequence and the length of a highly conserved region (GTAACTTAGAAG) in PV and HRV genomes between the clover leaf and IRES (Fig. 12 and Fig. 13). Similar observations by De Jesus *et al.* (2005) have indicated an abundance of conserved nucleotides amongst different PV serotypes and human C-cluster coxsackie A viruses in this region although the significance of these conserved regions is not known. It should be noted that we have previously found hotspots in the short spacer that are important for RNA synthesis (Toyoda *et al.,* 2007a) or essential for neurovirulence in mice (Cello *et al.,* 2002; De Jesus *et al.,* 2005; Toyoda *et al.,* 2007b).

Mutation 2 (R-2), a C133G transversion, was observed in 5 out of 7 H20A adapted isolates (Fig. 8). It maps downstream of a highly conserved sequence of six nt (CAATAG) in domain II of the IRES that is found in different PV serotypes and different HRV serotypes (Fig. 12 and Fig. 13). Interestingly, a transition A133G was observed at the same position by Shiroki *et al.* (1995), when a heat-resistant mutant was isolated by serial passage at 40^{o} C of wild type PV in L cells expressing the PV receptor CD155. Remarkably, Toyoda *et al.* (2007b) also reported an A133G transition when a PV carrying the cis acting element *cre* in the spacer region (mono-*cre*PV) was either passaged in mouse N2a^{CD155} cells or

isolated from a mouse tumor (neuroblastoma). Again, the 133 mutation was responsible for the increased replication of this A_{133}Gmono-crePV1 variant, as compared to mono-*cre*PV in mouse N2a$^{CD155\alpha}$ cells. These observations, together with the R-2 mutation reported here, indicate that a G residue in position 133 favors replication in mouse cells and is, thus, a host range mutation.

The mechanism by which certain PV derivatives express an attenuated phenotype is poorly understood. In My view, the IRES does play an important role in this process. In the three Sabin vaccine strains, a point mutation in each of the domain V has been implicated in contributing to attenuation and there are numerous experiments in support of this assertion (Wimmer *et al.,* 1993; Kew *et al.,* 2005). Gromeier and his colleagues have dissected the HRV2 IRES in the context of the PV background (Gromeier *et al.,* 1996, 1999) and have recently come to the conclusion that the V domain alone is the structure that confers the low replication phenotype to PV1(RIPO) if "attenuation" assayed in HEK293 cells (Campbell *et al.,* 2005). Merrill *et al.* (2006a) and Merrill and Gromeier (2006b) have presented evidence that a double-stranded RNA binding protein (DRBP76) is responsible for *trans*-dominant repression of PV1(RIPO) in neuronal cells but the locus of binding of this protein to the HRV2 IRES has not yet been determined.

Is domain V of the IRES in PV1(RIPO) involved in regulating viral proliferation in mouse cells? As seen in Fig. 8 only three mutations (R-4, -5, -6) were found to map to domain V in variants isolated after blind passages. Genetic

analyses of mutant combinations showed that these mutations were not required for other variants to regain replication in mouse cells (see constructs R-12 and R-123; Fig. 9) although variant R-1235 has regained the highest replication ability. Neurovirulence tests in CD155tg mice co-varied with replication capabilities in tissue culture cells of the mutant combinations (Table 1). Because of this co-variation, neurovirulence tests of the chimeric virus in CD155tg mice do not allow us to draw conclusions about the attenuation phenotype of PV1(RIPO) in these transgenic animals. One striking point remains to be made. All the variants, isolated after serial passages and after reconstructing into cDNA, resulting viruses retain their *ts* phenotype at 39.5^{o}C. This phenotype is similar to the *ts* phenotype of PV1(RIPO) in SK-N-MC cells. Surprisingly, under the conditions of the experiments, the *ts* phenotypes of the various variants do not prevent their killing of the animals at low PLD_{50}.

Figure 4. Genetic structure of the 5'NTRs of PV1(M), PN6, and PV1(RIPO) and one step growth curves of PV1(M), PN6, and PV1(RIPO) in HeLa R19 cells. (A) Genetic structure of the 5'NTRs of PV1(M), PN6, and PV1(RIPO). Poliovirus open reading frame (open arrows), AUG initiation codon, the cloverleaf (CL), the IRES, spacer I (S-I) and spacer-II are indicated. The linker sequence (shown with a black square) of 11 nt. containing the *EcoRI* restriction site (GAATTC) was inserted in S-I of PV1(M) between nt. 108 and 109 to construct PN6 virus. (B) One step growth curves of PV1(M), PN6, and PV1(RIPO) in HeLa R19 cells. Cells were infected at an MOI of 10 and incubated at 33^{o}C, 37^{o}C, and 39.5^{o}C. The virus titers were determined by plaque assay on monolayers of HeLa R19 cells, as described in Materials and Methods.

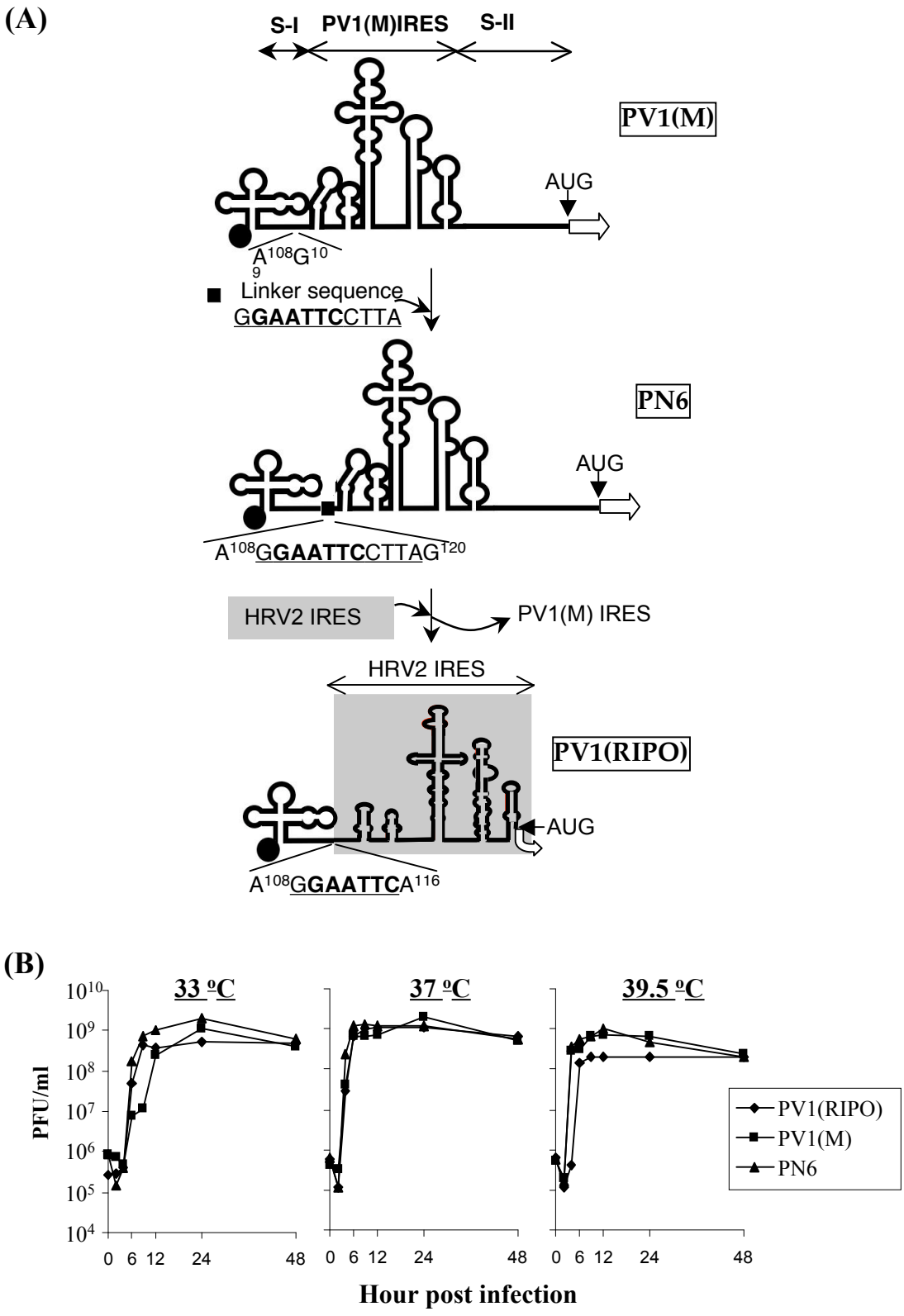
(A)
S-I
PV1(M)IRES
S-II
PV1(M)
AUG
A108G10
9
Linker sequence
GGAATTCCTTA
PN6
AUG
A108GGAATTCCTTAG120
HRV2 IRES
PV1(M) IRES
HRV2 IRES
PV1(RIPO)
AUG
A108GGAATTCA116
(B)
33 ºC
37 ºC
39.5 ºC
PFU/ml
10^10
10^9
10^8
10^7
10^6
10^5
10^4
0 6 12 24 48
PV1(RIPO)
PV1(M)
PN6
Hour post infection

Figure 5. One step growth curves of PV1(M), PN6, and PV1(RIPO) in Human neuronal cell lines. SK-N-MC cells (A), HEK293 cells (B), and SK-N-SH cells (C) were infected at an MOI of 10 and incubated at 33^{o}C, 37^{o}C, and 39.5^{o}C. The virus titers were determined by plaque assay on monolayers of HeLa R19 cells, as described in Materials and Methods.

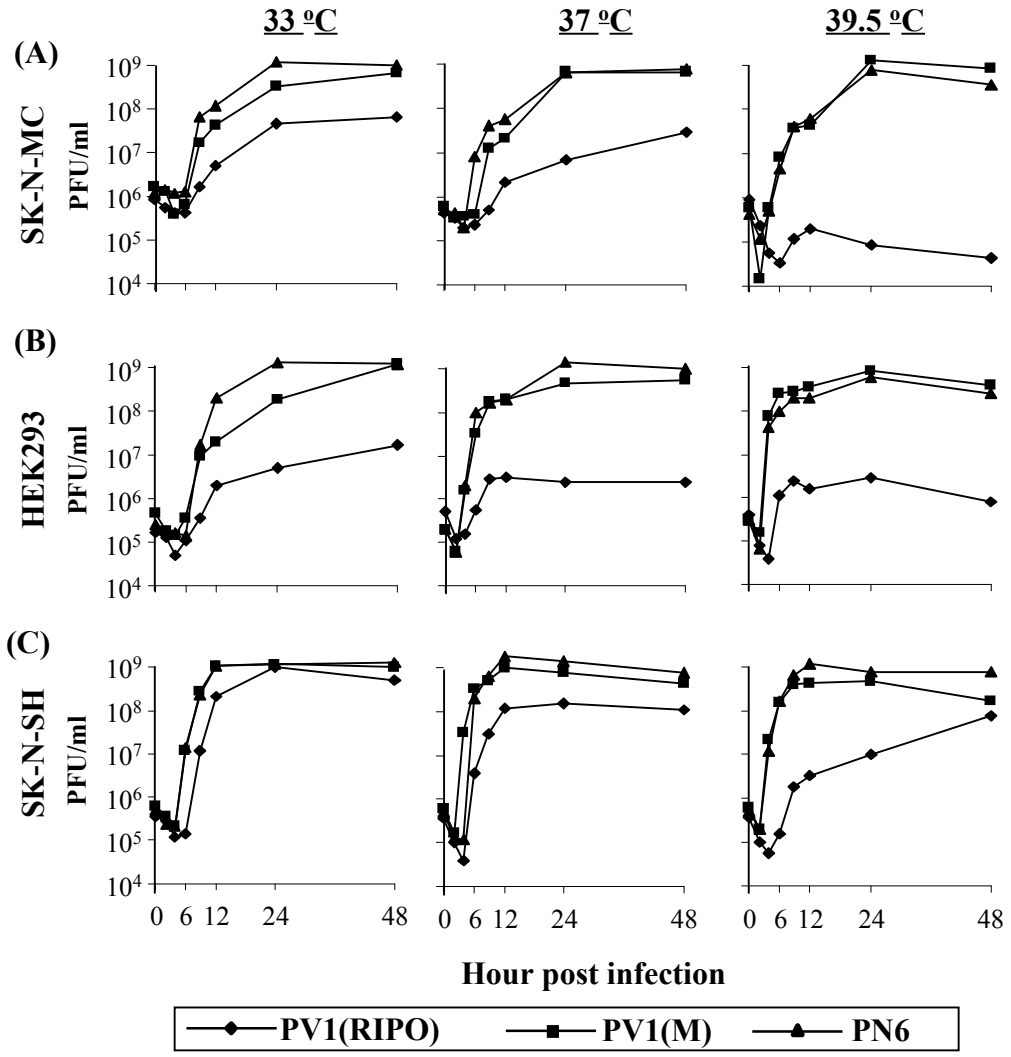
33 ºC
37 ºC
39.5 ºC
(A)
SK-N-MC
(B)
HEK293
(C)
SK-N-SH
PFU/ml
10^9
10^8
10^7
10^6
10^5
10^4
0 6 12 24 48
Hour post infection
PV1(RIPO)
PV1(M)
PN6

Figure 6. One step growth curves of PV1(M), PN6, and PV1(RIPO) in mouse cell lines. $N2a^{CD155}$ cells (A), L20B cells (B), and NIH $3T3^{CD155}$ cells (C) were infected at an MOI of 10 and incubated at 33°C, 37°C, and 39.5°C. The virus titers were determined by plaque assay on monolayers of HeLa R19 cells, as described in Materials and Methods.

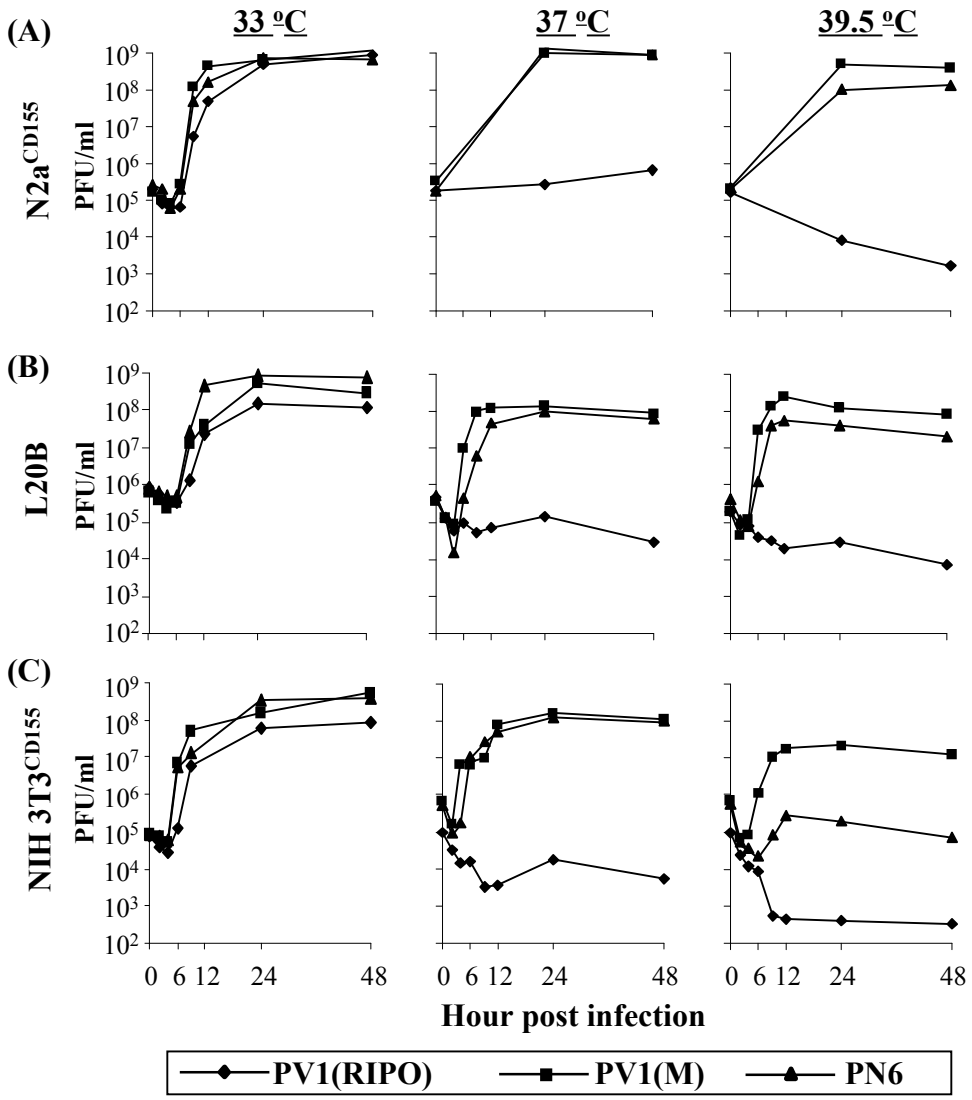
(A)
33 ºC
37 ºC
39.5 ºC
N2a^CD155
PFU/ml
(B)
L20B
PFU/ml
(C)
NIH 3T3^CD155
PFU/ml
0 6 12 24 48
Hour post infection
PV1(RIPO)
PV1(M)
PN6

Figure 7. RNA translation and replication of PV1(RIPO)-luc and PV1(M)-luc replicons. Structure of the luc-replicon is shown on the top. Monolayers of HeLa R19 cells (A), SK-N-MC cells (B), and mouse L20B cells (C) were transfected with *in vitro* transcribed RNA of poliovirus luciferase replicons and incubated at 33^{o}C, 37^{o}C and 39.5^{o}C in the presence (for translation) or in the absence (for replication) of 2mM guanidine hydrochloride (GuHCl). RNA translation and RNA replication were assessed by measuring the luciferase activity at different time point post transfection.

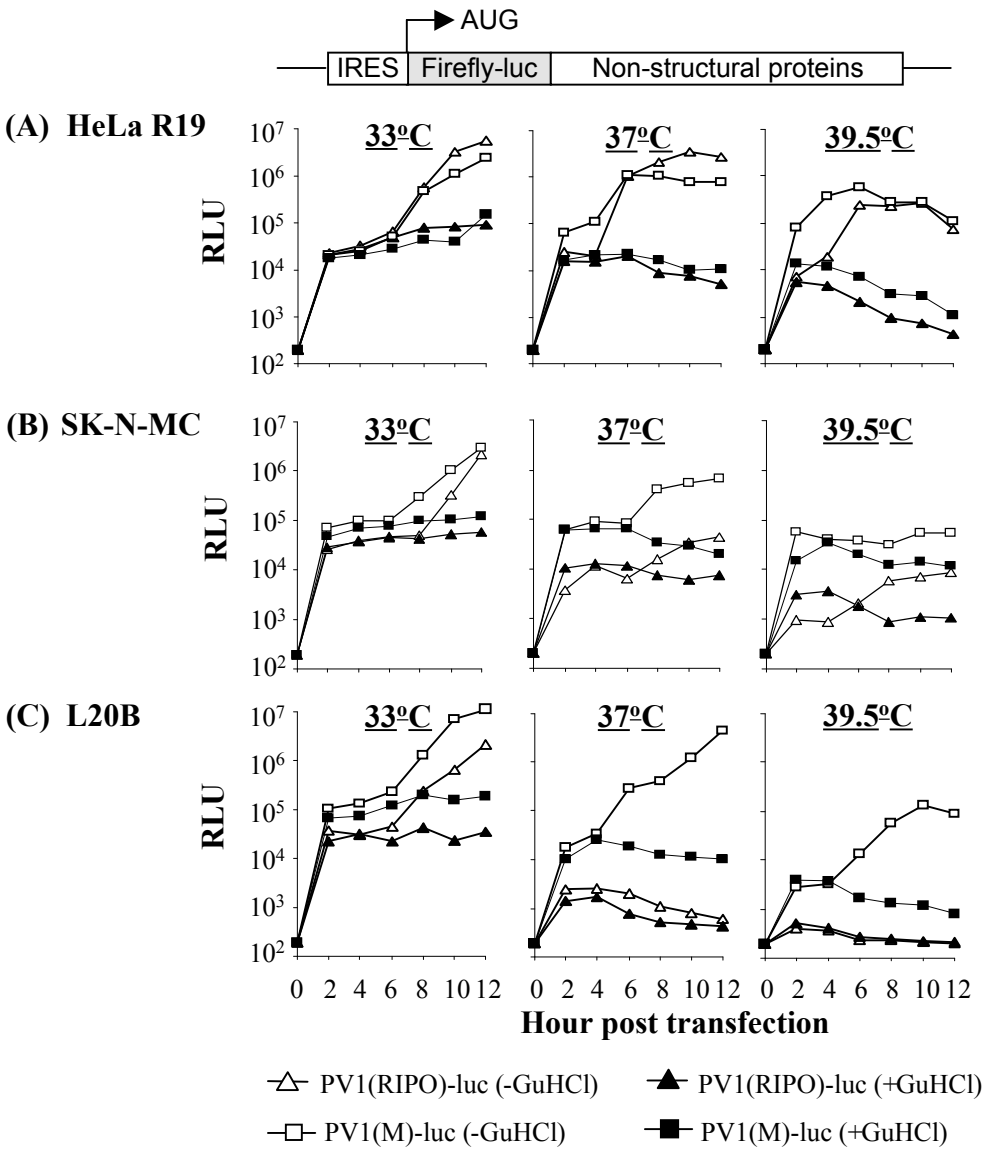
AUG
IRES
Firefly-luc
Non-structural proteins
(A) HeLa R19
(B) SK-N-MC
(C) L20B
33ºC
37ºC
39.5ºC
RLU
Hour post transfection
PV1(RIPO)-luc (-GuHCl)
PV1(RIPO)-luc (+GuHCl)
PV1(M)-luc (-GuHCl)
PV1(M)-luc (+GuHCl)

Figure 8. Genetic analyses of the 5'NTR nucleotide sequences of the adapted isolates of PV1(RIPO). (A) The isolates name and the mutation(s) they carry are indicated. The mutations found are numbered according to their position in the 5'NTR starting from the 5'end. The number in parentheses show the number of isolates out of total isolates containing any particular mutation. The sequence of deletion for mutation 1 is shown. (B) List of the mutations, including their location in the 5'NTR, and the nucleotide changes of the variants.

(A) **Isolates** **Mutations**

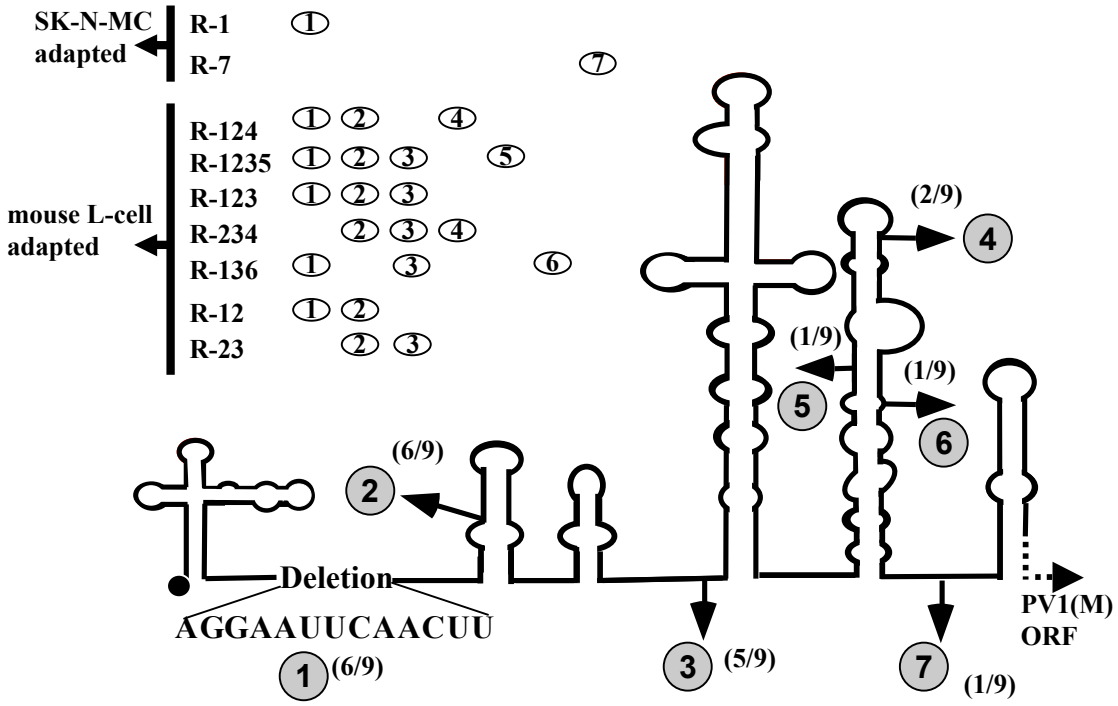

(B)

Mutation	nt. Change in PV1(RIPO)
1	Deletion of 107 to 119
2	C133G
3	A127U
4	U491C
5	U468C
6	U523C
7	C559U

Figure 9. Growth of PV1(RIPO) and selected L20B cell-adapted isolates in mouse cell lines. L20B cells (A), NIH 3T3^{CD155} cells (B), and N2a^{CD155} cells (C) were infected at an MOI of 10 and incubated at 33^{o}C, 37^{o}C, and 39.5^{o}C. The virus titers were determined by plaque assay on monolayers of HeLa R19 cells, as described in Materials and Methods.

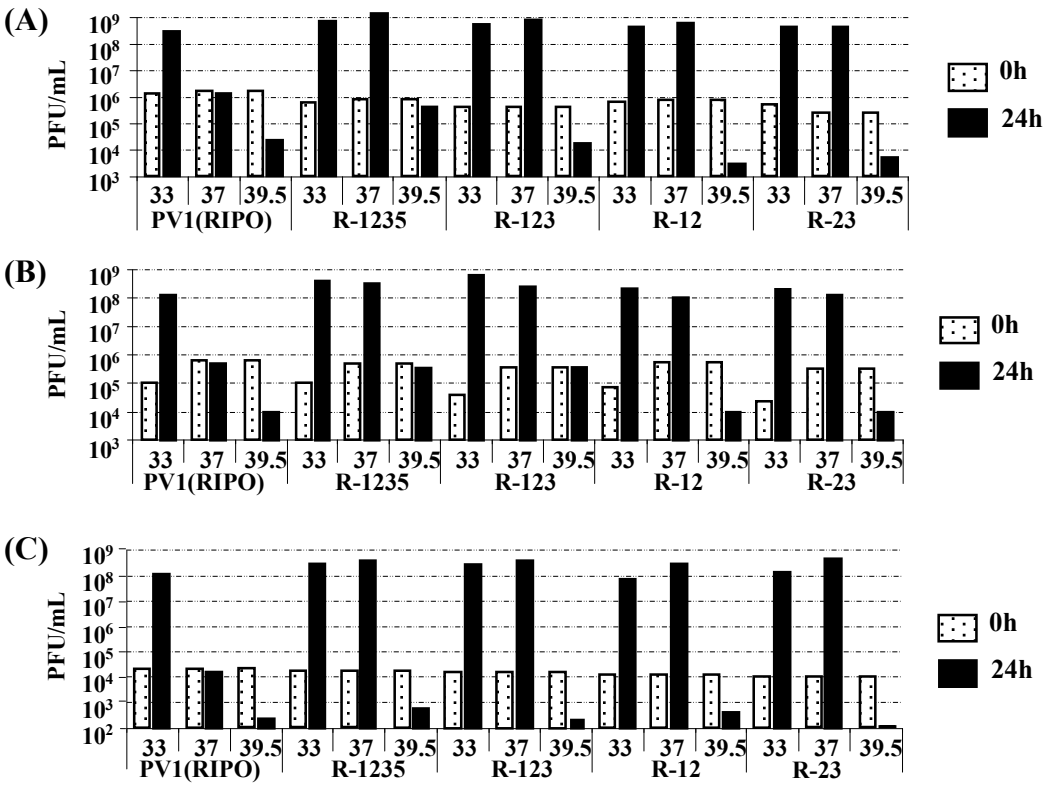
(A)
PFU/mL
10^9
10^8
10^7
10^6
10^5
10^4
10^3
33 37 39.5 33 37 39.5 33 37 39.5 33 37 39.5 33 37 39.5
PV1(RIPO) R-1235 R-123 R-12 R-23
0h
24h
(B)
PFU/mL
10^9
10^8
10^7
10^6
10^5
10^4
10^3
33 37 39.5 33 37 39.5 33 37 39.5 33 37 39.5 33 37 39.5
PV1(RIPO) R-1235 R-123 R-12 R-23
0h
24h
(C)
PFU/mL
10^9
10^8
10^7
10^6
10^5
10^4
10^3
10^2
33 37 39.5 33 37 39.5 33 37 39.5 33 37 39.5 33 37 39.5
PV1(RIPO) R-1235 R-123 R-12 R-23
0h
24h

Figure 10. Evaluation of species-specific growth restriction of mouse cell-adapted and human neuronal cell-adapted isolates of PV1(RIPO). Human neuronal cell-adapted (R-1) and mouse fibroblast-adapted (R-1235) variants of PV1(RIPO) were used to infect human SK-N-MC cells (A) or mouse L20B cell (B) at an MOI of 10 and incubated at 37^{o}C. The virus titers at various time points were determined by plaque assay on monolayers of HeLa R19 cells, as described in Materials and Methods. Mouse-adapted variant R-1235 completely restores replication competency on human neuronal cells, while neuron-adapted variant R-1 does not.

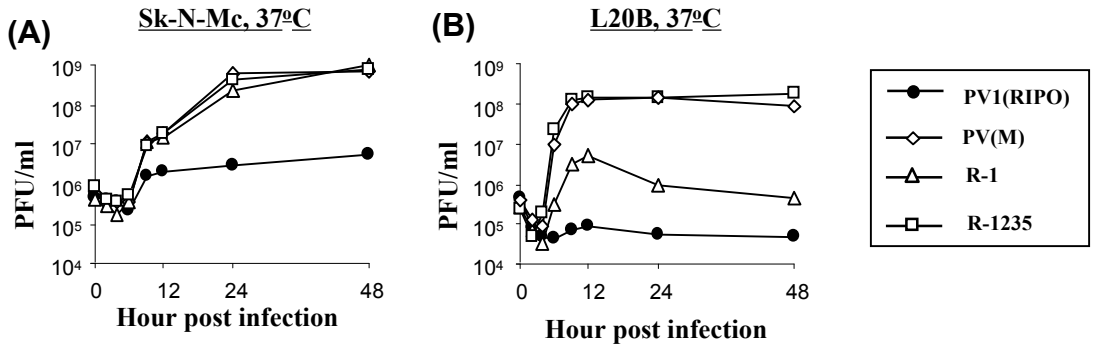
(A)
Sk-N-Mc, 37ºC
PFU/ml
10^9
10^8
10^7
10^6
10^5
10^4
0
12
24
48
Hour post infection
(B)
L20B, 37ºC
PFU/ml
10^9
10^8
10^7
10^6
10^5
10^4
0
12
24
48
Hour post infection
PV1(RIPO)
PV(M)
R-1
R-1235

Figure 11. RNA translation and replication of R-1235r-luc replicon in L20B cells. Structure of the luc-replicon is shown on the top. Monolayers mouse L20B cells were transfected with *in vitro* transcribed RNA of luciferase replicons and incubated at 33^{o}C, 37^{o}C and 39.5^{o}C in the presence (for translation) or in the absence (for replication) of 2 mM guanidine hydrochloride (GuHCl). RNA translation and RNA replication were assessed by measuring the luciferase activity at 5 and 11 hr post transfection.

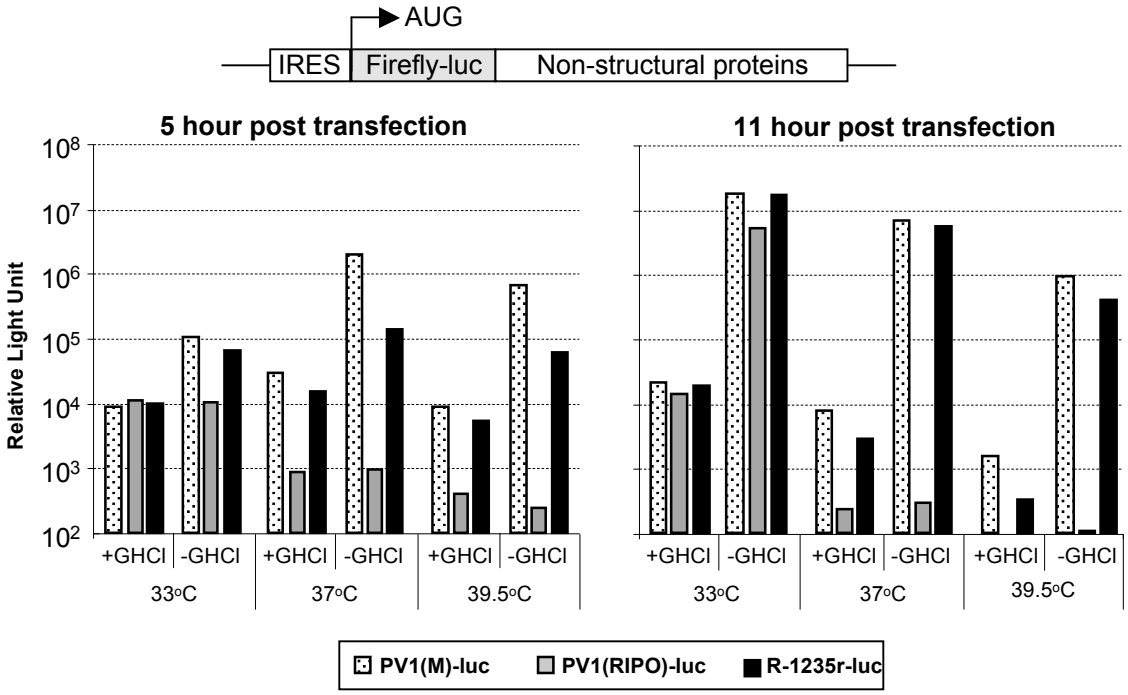
AUG
IRES
Firefly-luc
Non-structural proteins
5 hour post transfection
11 hour post transfection
Relative Light Unit
10^8
10^7
10^6
10^5
10^4
10^3
10^2
+GHCl
-GHCl
33°C
37°C
39.5°C
PV1(M)-luc
PV1(RIPO)-luc
R-1235r-luc

Table 1: Neurovirulence study in CD155tg mice

Virus(PFU)	PLD_{50} [a]	Relative increase in PLD_{50} [b]	Fold increase in virus titer on L20B cells [c]
PV1(RIPO)	**$>10^{8}$ [d]**	**1**	**0.5**
R-1	**$\geq 10^{8}$ [d]**	**≤ 1**	**960**
R-1r	**ND**	**ND**	**400**
R-2r	**$>10^{8}$ [d]**	**1**	**140**
R-3r	**$>10^{7}$ [d]**	**<10**	**0.3**
R-5r	**$>10^{7}$ [d]**	**<10**	**5.7**
R-35r	**10^{7}**	**10**	**7,500**
R-12r	**10^{6}**	**100**	**8,400**
R-23	**$10^{5.5}$**	**316**	**12,000**
R-123	**10^{5}**	**1,000**	**22,000**
R-123r	**$10^{5.3}$**	**501**	**30,000**
R-1235	**10^{3}**	**100,000**	**130,000**
R-1235r	**$10^{3.2}$**	**63,096**	**100,000**
PN6	**$10^{4.7}$**	**1,995**	**16,000**
PV1(M)	**10^{2}**	**1,000,000**	**250,000**

PLD_{50}, the virus titer that induces paralysis or death in 50% of the mice

[a] Groups of four mice were infected intracerebrally with a given amount of virus. PLD_{50} values were calculated by the method of Reed and Muench.

[b] Relative increase in PLD_{50} was calculated by considering PLD_{50} of PV1(RIPO) as 1

[c] Fold increase virus titer in L20B cells after 24 hour infection at 10 MOI as compared with titer at 0 hour post infection

[d] PLD_{50} could not be determined as no mice died at highest dose inoculated

ND: Not determined

Figure 12. Sequence alignments of spacer I and part of stem-loop-II in the 5' NTR of human enteroviruses and human rhinoviruses, reveals a highly conserved sequence motif. Nucleotides in red, blue and black color represent nucleotides highly, moderately and not conserved among the viruses respectively. Dashes denote nucleotides missing in any particular virus. Part of the PV1(RIPO) sequence, representing Mutation 1 (13 nt deletion) in the adapted isolates has been shown on the top as an extra sequence in PV1(RIPO). M, Mahoney; La, Lansing; Le, Leon. Alignments were done using Multalin (http://bioinfo.genotoul.fr/multalin/multalin.html).

**It should be noted that recently the genus Rhinovirus was incorporated into the Enterovirus genus (www.picornaviridae.com)

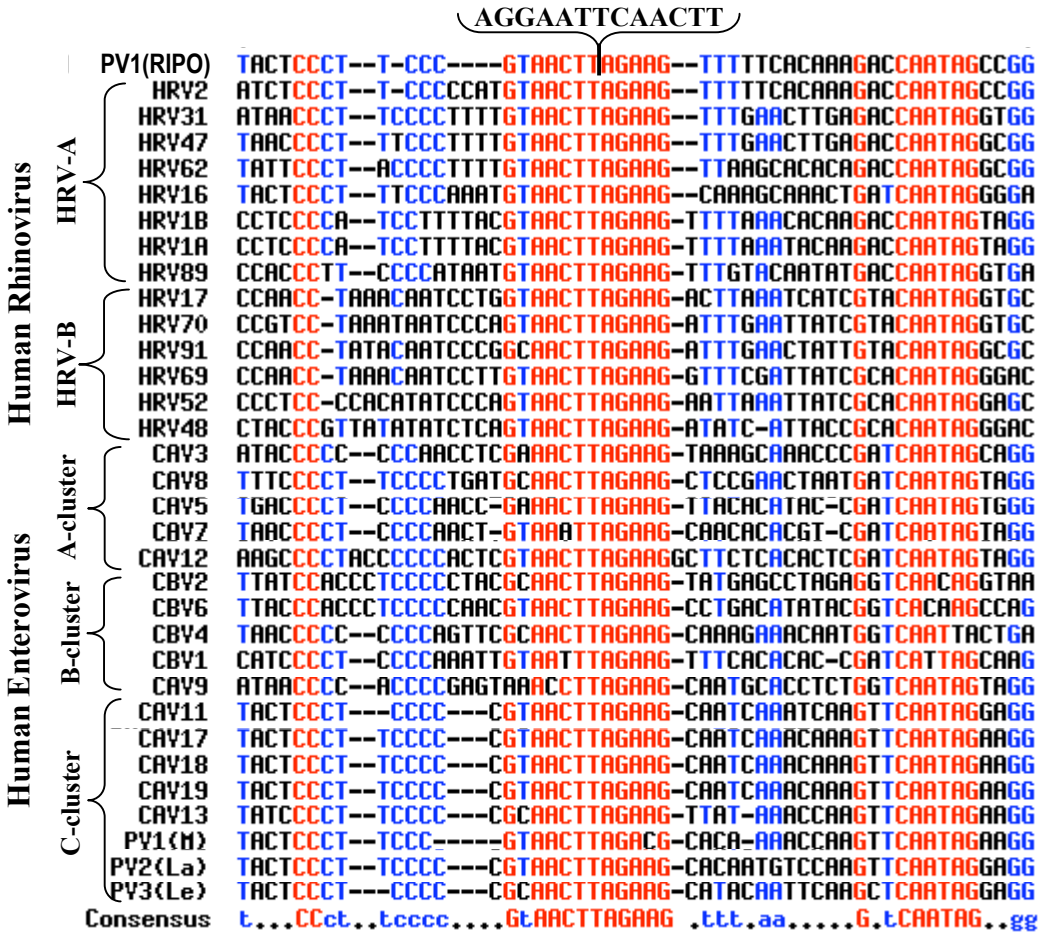
AGGAATTCAACTT
Human Enterovirus
Human Rhinovirus
A-cluster
B-cluster
C-cluster
HRV-A
HRV-B
PV1(RIPO)
HRV2
HRV31
HRV47
HRV62
HRV16
HRV1B
HRV1A
HRV89
HRV17
HRV70
HRV91
HRV69
HRV52
HRV48
CAV3
CAV8
CAV5
CBV7
CAV12
CBV2
CBV6
CBV4
CBV1
CAV9
CAV11
CAV17
CAV18
CAV19
CAV13
PV1(M)
PV2(La)
PV3(Le)
Consensus

Figure 13. Nucleotide sequence alignments of spacer I and part of stem-loop II in the 5'NTR of human enteroviruses, human rhinoviruses (HRV) and PV1(RIPO). Nucleotides in red, blue and black color represent nucleotides highly, moderately and not conserved among the viruses respectively. Dashes denote nucleotides missing in any particular virus but that are otherwise present in other polioviruses or human rhino viruses. M, Mahoney; S, Sabin; La, Lansing; Le, Leon. Alignments were done using Multalin (http://bioinfo.genotoul.fr/multalin/multalin.html).

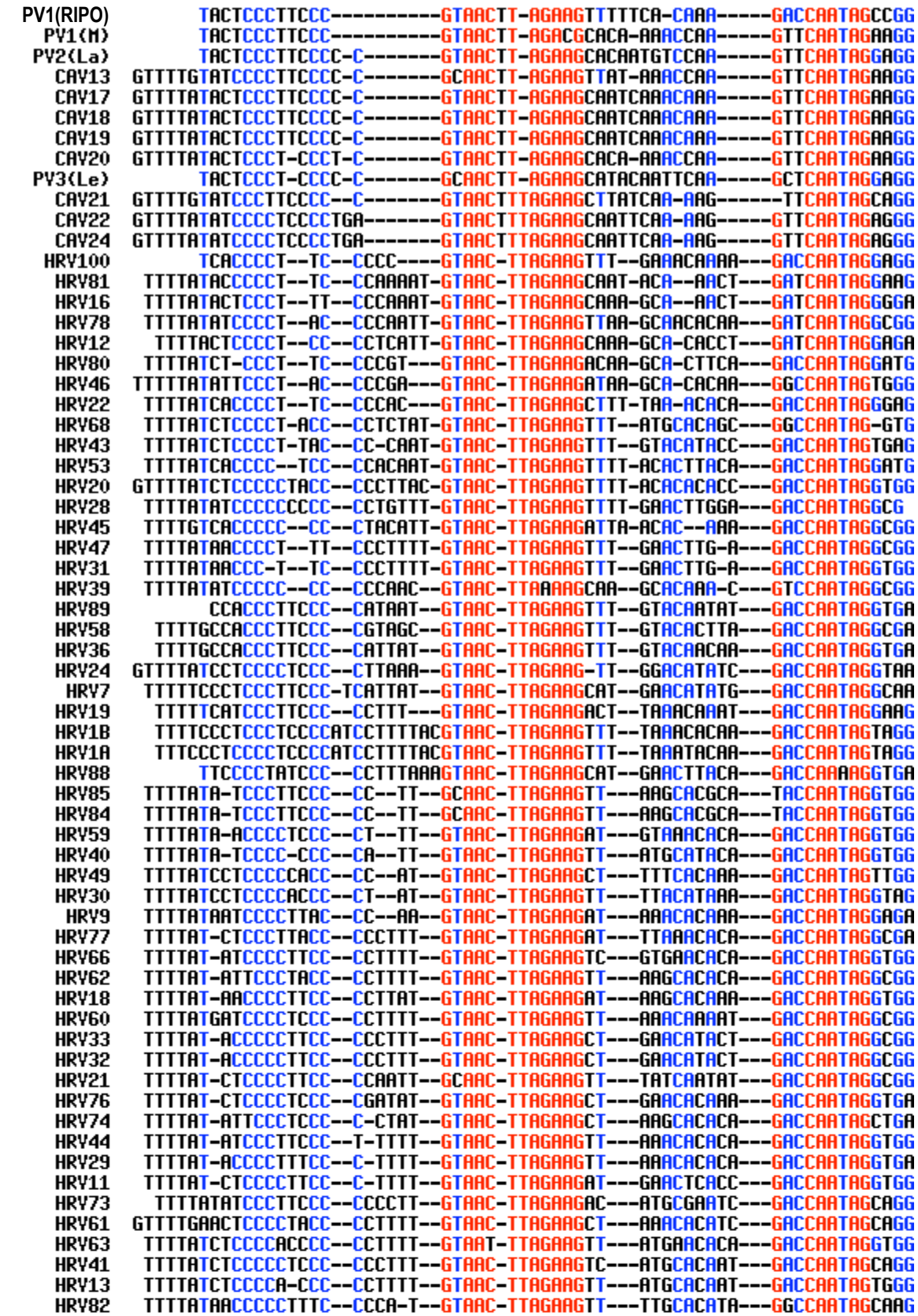
PV1(RIPO)
PV1(M)
PV2(La)
CAV13
CAV17
CAV18
CAV19
CAV20
PV3(Le)
CAV21
CAV22
CAV24
HRV100
HRV81
HRV16
HRV78
HRV12
HRV80
HRV46
HRV22
HRV68
HRV43
HRV53
HRV20
HRV28
HRV45
HRV47
HRV31
HRV39
HRV89
HRV58
HRV36
HRV24
HRV7
HRV19
HRV1B
HRV1A
HRV88
HRV85
HRV84
HRV59
HRV40
HRV49
HRV30
HRV9
HRV77
HRV66
HRV62
HRV18
HRV60
HRV33
HRV32
HRV21
HRV76
HRV74
HRV44
HRV29
HRV11
HRV73
HRV61
HRV63
HRV41
HRV13
HRV82

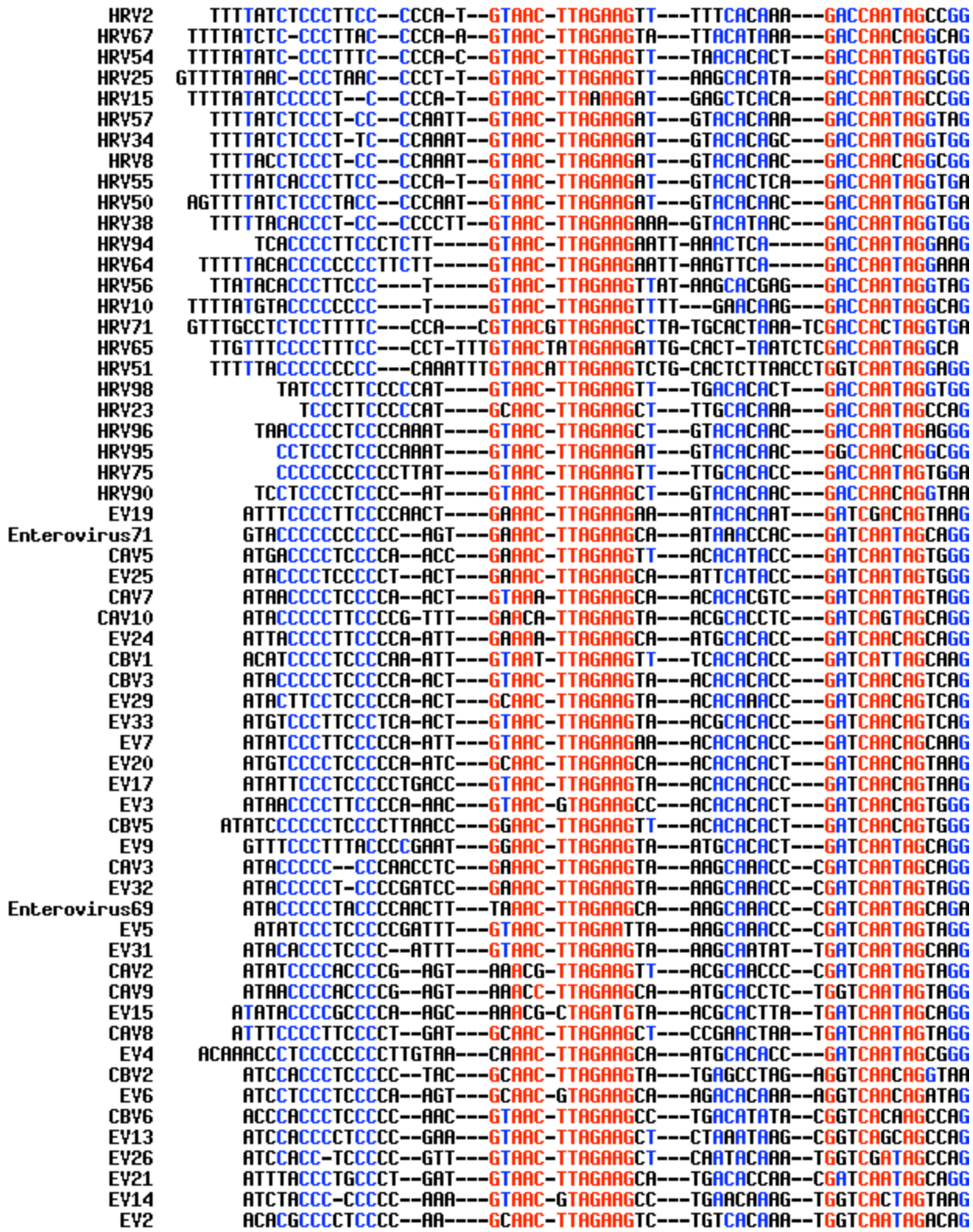
HRV2
HRV67
HRV54
HRV25
HRV15
HRV57
HRV34
HRV8
HRV55
HRV50
HRV38
HRV94
HRV64
HRV56
HRV10
HRV71
HRV65
HRV51
HRV98
HRV23
HRV96
HRV95
HRV75
HRV90
EV19
Enterovirus71
CAV5
EV25
CAV7
CAV10
EV24
CBV1
CBV3
EV29
EV33
EV7
EV20
EV17
EV3
CBV5
EV9
CAV3
EV32
Enterovirus69
EV5
EV31
CAV2
CAV9
EV15
CAV8
EV4
CBV2
EV6
CBV6
EV13
EV26
EV21
EV14
EV2

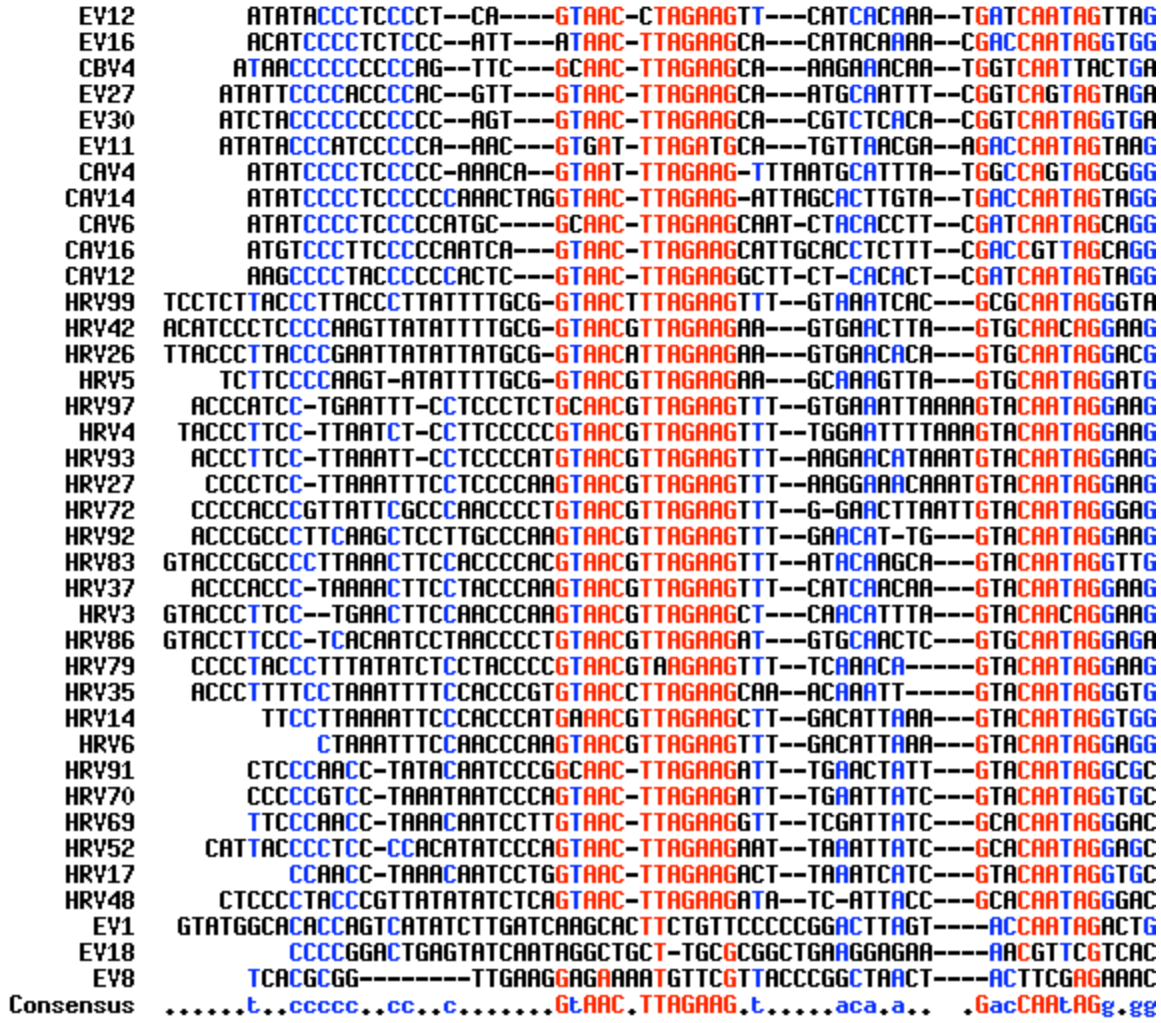
EV12 ATATACCCTCCCCT--CA----GTAAC-CTAGAAGTT---CATCACAAA--TGATCAATAGTTAG
EV16 ACATCCCCTCTCCC--ATT---ATAAC-TTAGAAGCA---CATACAAAA--CGACCAATAGGTGG
CBV4 ATAACCCCCCCCCAG--TTC---GCAAC-TTAGAAGCA---AAGAAACAA--TGGTCAATTACTGA
EV27 ATATTCCCCACCCCAC--GTT---GTAAC-TTAGAAGCA---ATGCAATTT--CGGTCAGTAGTAGA
EV30 ATCTACCCCCCCCCCC--AGT---GTAAC-TTAGAAGCA---CGTCTCACA--CGGTCAATAGGTGA
EV11 ATATACCCATCCCCCA--AAC---GTGAT-TTAGATGCA---TGTTAACGA--AGACCAATAGTAAG
CAV4 ATATCCCCTCCCCC-AAACA--GTAAT-TTAGAAG-TTTAATGCATTTA--TGGCCAGTAGCGGG
CAV14 ATATCCCCTCCCCCCAAACTAGGTAAC-TTAGAAG-ATTAGCACTTGTA--TGACCAATAGTAGG
CAV6 ATATCCCCTCCCCCATGC----GCAAC-TTAGAAGCAAT-CTACACCTT--CGATCAATAGCAGG
CAV16 ATGTCCCTTCCCCCAATCA---GTAAC-TTAGAAGCATTGCACCTCTTT--CGACCGTTAGCAGG
CAV12 AAGCCCCTACCCCCCACTC---GTAAC-TTAGAAGGCTT-CT-CACACT--CGATCAATAGTAGG
HRV99 TCCTCTTACCCTTACCCTTATTTTGCG-GTAACTTTAGAAGTTT--GTAAATCAC---GCGCAATAGGGTA
HRV42 ACATCCCTCCCCAAGTTATATTTTGCG-GTAACGTTAGAAGAA---GTGAACTTA---GTGCAACAGGAAG
HRV26 TTACCCTTACCCGAATTATATTATGCG-GTAACATTAGAAGAA---GTGAACACA---GTGCAATAGGACG
HRV5 TCTTCCCCAAGT-ATATTTTGCG-GTAACGTTAGAAGAA---GCAAGTTA---GTGCAATAGGATG
HRV97 ACCCATCC-TGAATTT-CCTCCCTCTGCAACGTTAGAAGTTT--GTGAAATTAAAAGTACAATAGGAAG
HRV4 TACCCTTCC-TTAATCT-CCTTCCCCCGTAACGTTAGAAGTTT--TGGAATTTTAAAGTACAATAGGAAG
HRV93 ACCCTTCC-TTAAATT-CCTCCCCATGTAACGTTAGAAGTTT--AAGAACATAAATGTACAATAGGAAG
HRV27 CCCCTCC-TTAAATTTCCTCCCCAAGTAACGTTAGAAGTTT--AAGGAAACAAATGTACAATAGGAAG
HRV72 CCCCACCCGTTATTCGCCCAACCCCTGTAACGTTAGAAGTTT--G-GAACTTAATTGTACAATAGGGAG
HRV92 ACCCGCCCTTCAAGCTCCTTGCCCAAGTAACGTTAGAAGTTT--GAACAT-TG---GTACAATAGGAAG
HRV83 GTACCCGCCCCTTAAACTTCCACCCCACGTAACGTTAGAAGTTT--ATACAAGCA---GTACAATAGGTTG
HRV37 ACCCACCC-TAAAACTTCCTACCCAAGTAACGTTAGAAGTTT--CATCAACAA---GTACAATAGGAAG
HRV3 GTACCCTTCC--TGAACTTCCAACCCAAGTAACGTTAGAAGCT---CAACATTTA---GTACAACAGGAAG
HRV86 GTACCTTCCC-TCACAATCCTAACCCCTGTAACGTTAGAAGAT---GTGCAACTC---GTGCAATAGGAGA
HRV79 CCCCTACCCTTTATATCTCCTACCCCGTAACGTAAGAAGTTT--TCAAACA-----GTACAATAGGAAG
HRV35 ACCCTTTTCCTAAATTTTCCACCCGTGTAACCTTAGAAGCAA--ACAAATT-----GTACAATAGGGTG
HRV14 TTCCTTAAAATTCCCACCCATGAAACGTTAGAAGCTT--GACATTAAA---GTACAATAGGTGG
HRV6 CTAAATTTCCAACCCAAGTAACGTTAGAAGTTT--GACATTAAA---GTACAATAGGAGG
HRV91 CTCCCAACC-TATACAATCCCGGCAAC-TTAGAAGATT--TGAACTATT---GTACAATAGGCGC
HRV70 CCCCCGTCC-TAAATAATCCCAGTAAC-TTAGAAGATT--TGAATTATC---GTACAATAGGTGC
HRV69 TTCCCAACC-TAAACAATCCTTGTAAC-TTAGAAGGTT--TCGATTATC---GCACAATAGGGAC
HRV52 CATTACCCCTCC-CCACATATCCCAGTAAC-TTAGAAGAAT--TAAATTATC---GCACAATAGGAGC
HRV17 CCAACC-TAAACAATCCTGGTAAC-TTAGAAGACT--TAAATCATC---GTACAATAGGTGC
HRV48 CTCCCCTACCCGTTATATATCTCAGTAAC-TTAGAAGATA--TC-ATTACC---GCACAATAGGGAC
EV1 GTATGGCACACCAGTCATATCTTGATCAAGCACTTCTGTTCCCCCGGACTTAGT----ACCAATAGACTG
EV18 CCCCGGACTGAGTATCAATAGGCTGCT-TGCGCGGCTGAAGGAGAA----AACGTTCGTCAC
EV8 TCACGCGG--------TTGAAGGAGAAAATGTTCGTTACCCGGCTAACT----ACTTCGAGAAAC
Consensus ......t..ccccc..cc..c.......GtAAC.TTAGAAG.t.....aca.a.. .GacCAAtAGg.gg

Chapter III. Analysis of the effect of over-expression of IRES *trans*-activating factors (ITAFs) in rescuing the growth defect of PV1(RIPO)

Introduction

The importance of CD155, the cellular receptor for PV, and the IRES element in determining the tissue and host tropism has been discussed in the chapter II. The IRES-mediated tropism is determined at the level of translation initiation of the viral protein, which is controlled by the IRES in concert with both canonical and non-canonical *trans*-acting cellular translation initiation factors. These non-canonical ITAFs are mostly RNA-binding proteins (Jang, 2006) (Table 2). Five cellular ITAFs, specific for picornaviral IRES elements, have been identified: the polypyrimidine tract-binding protein (PTB) (Pestova *et al.,* 1991; Hellen *et al.,* 1993; Hunt *et al.,* 1999a; 1999b; Gosert *et al.,* 2000); the poly(rC)-binding protein 2 (PCBP2) (Blyn *et al.,* 1997; Gamarnik *et al.,* 1997); the autoantigen La (Meerovitch *et al.,* 1989; Meerovitch *et al.,* 1993; Belsham *et al.,* 1995; Craig *et al.,* 1997); the upstream of N-ras protein (unr) (Hunt *et al.,* 1999a; 1999b; Boussadia *et al.,* 2003); and ITAF(45) (Pilipenko *et al.,* 2000). These factors are believed to function as RNA chaperones by binding to RNA and changing the secondary structure of RNA which then facilitates ribosome recruitment and allows binding of initiation factors and/or ribosomal subunits to RNA. Therefore, the qualitative and quantitative differences of these factors in cells may play important roles in determining the IRES-mediated tissue and host tropisms of picornaviruses. Since viral replication depends on the translation of the viral polyprotein, the intracellular abundance of these factors may be an

important determinant of the extent to which specific cell types are permissive for virus replication.

All the canonical initiation factors involved in the conventional scanning mechanism, except the cap-binding initiation factor eIF4E, are used for the internal initiation of translation of picornavirus RNAs (Jang, 2006). As mentioned earlier, for the internal initiation of RNA translation, the picornaviral IRES also needs additional *trans*-activating factors (Table 2). The different picornavirus species show differences in the requirements for such factors that parallel the differences in IRES structure. On the basis of the primary sequence and the secondary RNA structure, picornavirus IRESes can be divided into three major types: the enteroviruses and rhinoviruses contain type I IRES, the cardioviruses and aphthoviruses contain type II IRES (Wimmer *et al.,* 1993) and hepatitis A virus possess type III IRES (Fig. 15A-C, Chapter I). Members of each of these groups show high degree of homology in primary sequence and secondary structure of the IRES, but very little homology is observed between the different groups (Fernández-Miragall *et al.,*2009). Cardiovirus and apthovirus IRESes show efficient translation in a wide range of cell-free extracts, including rabbit reticulocyte lysate (RRL) (Svitkin & Agol, 1978; Kaminski *et al.,* 1990). In contrast, translation of enterovirus and rhinovirus IRESes are inefficient in RRL and need supplementation with HeLa cell factors (Brown & Ehrenfeld, 1979; Dorner *et al.,* 1984; Borman & Jackson, 1992; Bailly *et al.,* 1996). These observations led to the search for those factors that are necessary for IRES activity but that are

either completely absent from RRL or are much less abundant than in HeLa cell extracts. Interestingly, studies conducted by different groups found that a specific combination of two or three of the ITAFs is required by some picornavirus IRES elements for an efficient translational activity. The close phylogenetic relationship between PV and human rhinovirus (HRV) and the strong similarity in their IRES structures led to the speculation that the same ITAFs would be required by their IRESes (see Table 2).

La, a 52-kDa protein, is a predominantly nuclear protein. However, in PV-infected cells it is translocated to the cytoplasm and has been reported to bind specifically to the PV 5'NTR to enhance and correct aberrant translation of PV RNA in reticulocyte lysates (Meerovitch *et al.,* 1989, 1993). Poly (rC) binding protein 2 (PCBP2), 38 kDa cytoplasmic protein, binds the PV IRES with its KH domain and appears to be an essential factor required for PV translation initiation and viral RNA replication (Blyn *et al.,* 1996,1997; Walter *et al.,* 2002). In addition to La and PCBP2, the 57-kDa polypyrimidine-tract binding protein (PTB), predominantly found in the nucleus and in lower abundance in cytoplasm, binds to multiple sites in the PV 5' NTR (Hellen *et al.,* 1994). The stimulatory effect of PTB on IRES-mediated translation of PV mRNA has been claimed to depend on the C-terminal one-third of the PTB molecule containing two putative RNA recognition motifs (Gosert *et al.,* 2000). Moreover, inhibition of translation of PV mRNA has been observed by the cleavage of PTB by viral protease $3C^{pro}$ (Back *et al.,* 2002).

As was observed with PV, PTB was found to stimulate the activity of the HRV IRES (Borman *et al.,* 1993; Hunt *et al.,* 1999a). Additionally a 96- to 97-kD protein doublet, which was identified as unr, was found to act synergistically with PTB to stimulate translation dependent on the HRV IRES (Hunt *et al.,* 1999b). In contrast, unr did not significantly augment the PTB-dependent stimulation of PV IRES activity. However, a later study by another group showed that unr is required for both HRV and PV IRES activity *in vitro* and *in vivo* (Boussadia *et al.,* 2003). Unr is a cytoplasmic RNA-binding protein, containing five cold-shock domains that binds to two distinct secondary structure domains of the HRV-2 IRES (Anderson *et al.,* 2007). These investigators proposed that unr helps to maintain a complex tertiary structure by acting as a RNA chaperone, which is required for translation competency.

Various studies provided considerable genetic evidence that picornavirus IRES elements contain determinants of tissue-specific or cell-type-specific translation initiation. Analysis of PV IRES mutants showed that translation defects could be cell type specific because the mutation in some way alters the interaction of the IRES with a translation factor (s), leading to diminished translation. In support of this hypothesis it has been demonstrated that Sabin type 3 PV RNA showed reduced translation efficiency *in vitro* when compared with RNAs from neurovirulent type 3 PV RNA (Svitkin *et al.,* 1985). A preparation called “initiation-correcting factor” from HeLa cells appeared to be relatively less active in translating viral RNAs from attenuated strains than that from

neurovirulent strains (Svitkin *et al.,* 1988). Later on, Guest *et al.,* (2004) showed that the inefficient growth of the PV Sabin 3 strain in the CNS is due to low level expression of PTB coupled to a reduced binding of PTB on the Sabin3 IRES. The translation defect could be rescued by increased expression of PTB in the CNS which was done by coelectroporation of PTB expression construct and the Sabin3 IRES bicistronic construct into the chicken embryo spinal cord. A similar study showed a decreased translation capacity of attenuated PV RNA in cell extracts of neuronal origin, but not in HeLa cells (La Monica and Racaniello, 1989). Experiments using viruses with chimeric genomes confirmed the importance of IRES as cell-specific determinant. This has been discussed to some extent in the previous chapter. Chimeric PV harboring IRES sequences of HRV type 2 or hepatitis C virus instead of the PV IRES do not propagate in the CNS of CD155tg mice (Gromeier *et al.,* 1996**;** Yanagiya *et al.,* 2003). The translation initiation by the IRES of foot-and-mouse disease virus (FMDV) is not active in neurons because it requires $ITAF_{45}$, which is expressed only in proliferating cells (Pilipenko *et al.,* 2000). These are good examples of IRES-dependent restriction of viral gene expression in a tissue-specific manner, which might be due to a lack of or shortage of ITAFs resulting in tissue- or cell-specific failure of replication of viruses. However, Kauder and Racaniello (2004) reported results, which contradict this, even their own previous hypothesis. They performed experiments to test the role of IRES-mediated translation initiation as a determinant of PV tissue tropism and pathogenesis (Kauder *et al.,* 2004, 2006).

Replacing the IRES of PV1(M) with that of coxsackie virus B (CVB) or hepatitis C virus (HCV) and using the Sabin type 3 PV IRES, Kauder and colleagues (2004) originally reported that the tropism of wild type and vaccine strains of PV is determined in a step after IRES-mediated translation. In a subsequent study, however, using a similar experimental strategy, they suggested that IRES-mediated translation plays an important role in the replication of a chimeric virus (P1/HRV2) in an age-dependent manner in CD155tg mice (Kauder *et al.,* 2006). They concluded that greater expression of ITAFs, synthesized during neonatal development may facilitate HRV2 IRES-mediated translation in neonates.

Campbell *et al.* (2005) have reported that assays with IRES-driven Luciferase reporter constructs that consisted only of the HRV-2 IRES and the reporter gene, did express Luc well (or even better) in HEK293 or SK-N-MC cells than the equivalent PV IRES driven reporter constructs. Therefore, data obtained from assays with reporter genes must be interpreted with caution (Campbell *et al.,* 2005). IRES-mediated propagation defects in neuronal cells cannot be explained by translation efficiency at the IRES alone. If so, the results of the IRES studies of Kauder *et al.* (2004, 2006) where they used dicistronic reporter mRNA produced by an adenovirus, to reflect cell type-specific growth of PV1(RIPO), might be misleading. On the other hand, it is intriguing to speculate that the non-structural proteins have to cooperate with the IRES to facilitate maximal expression of the polyprotein, and that this expression is dependent also on ITAFs.

As described in the previous chapter, the chimeric virus PV1(RIPO) harboring the IRES of HRV2 instead of PV1(M), shows a distinct tissue and host tropism when the growth of this virus in different human neuronal cells and mouse cells was compared with that of wild type PV1(M). One reason for the observed phenotype might be the qualitative or the quantitative differences of ITAFs present in different cells of human and mouse origin. PV1(RIPO) possesses the IRES of HRV2 which might have different requirements of the ITAFs than the IRES of PV1(M). One way to explore the role of the quantitative differences in ITAFs on tissue-specific failure of PV1(RIPO) replication is to over-express the ITAF(s) in the restricted human neuronal cells and examine the ability of the ITAFs over-expressing cells to rescue the growth defect of PV1(RIPO). On the other hand, to gain insight into the role of qualitative differences in ITAFs on host-specific failure of PV1(RIPO) replication is to express the human cell factor(s) in mouse cells in which this chimeric virus showed defective growth.

In this study, I demonstrate that over-expression of human PTB1 (hPTB1), PCBP2 and unr stimulated the HRV2 IRES-mediated translation of viral protein resulting in increased growth of PV1(RIPO) in human neuronal cells SK-N-MC. In addition, hPTB1 expression in mouse cells rescued the translation defect of PV1(RIPO) in these restricted cells and the virus was able to replicate and grow in mouse cells. Interestingly, a variant of PV1(RIPO) adapted to grow in mouse cells no longer required hPTB1 supplementation in mouse cells. These results

suggest that there are quantitative differences in the requirements of the HRV2 IRES and the PV IRES for different ITAFs in human neuronal cells. In addition, hPTB1 and possibly other unknown cellular factors may be important determinants of the host range of PV1(RIPO) in mouse cells. The restriction of rhinovirus type 2 IRES activity in mouse cells could be exploited as a functional assay to identify those factors that are necessary for HRV2 IRES activity but that are either completely absent, less abundant, or otherwise functionally inadequate in mouse cells (difference between human and mouse homologs).

MATERIALS AND METHODS

Viruses and cells. The neurovirulent PV type 1 [Mahoney; PV1(M)] is the strain being used routinely in the laboratory (Cello *et al.,* 2002). PV1(RIPO) was constructed as described previously (Gromeier *et al.,* 1996). R-1235 virus is mouse L20B cell-adapted PV1(RIPO) which was obtained after 7 serial passages at 37^{o}C. The mouse fibroblast cell lines (L cells) expressing CD155δ (L20B) (Mendelsohn *et al.,* 1989; Pipkin *et al.,* 1993) were maintained in DMEM containing 1% penicillin/streptomycin and 10% fetal bovine serum. HeLa (human cervical cancer) cells, and human neuroblastoma cell lines SK-N-MC were obtained from the American Type Culture Collection (Manassas, VA) and were maintained according to the manufacturer's specification.

Expression of ITAFS. SK-N-MC cells were transfected using Lipofectamine (Invitrogen) with a mammalian expression plasmid pCDNA3 containing the gene for hPTB1, PCBP2, and unr under the control of

cytomegalovirus promoter. The transfection procedure was followed as outlined by the manufacturer. Stable cell clones resistant to G418 were selected. L20B cells were transfected in a similar way with the same expression plasmid containing cDNA for hPTB1 and stable cell clones resistant to G418 were selected.

Antibodies. Anti-PTB monoclonal antibodies DH1, DH3, DH7 and DH17 (Grossman *et al.,* 1998) and anti-PCBP2 polyclonal antiserum (Walter *et al.,* 1999; Walter *et al.,* 2002) (a generous gift of Bert L. Semler, University of California, Irvine) and anti-actin mouse mAb (Calbiochem) were used as primary antibodies for Western blot analysis. Anti-unr polyclonal antibody (Chang *et al.,* 2004) was a generous gift of Ann-Bin Shyu, The University of Texas Medical School, Houston, Texas.

Immunoblot analysis. For immunoblot analysis, 30-μg aliquots of the total cell extract was separated by SDS gel (12% acrylamide). Following electrotransfer to polyvinylidene difluoride membranes, membranes were blocked with 5 % skim milk in 0.1% Tween-PBS for 0.5 h. Membranes were probed either with anti-PTB monoclonal antibodies at 1:200 dilution or with anti-PCBP2 polyclonal antiserum at 1:1000 dilution for overnight at 4^{o} C. The membranes were washed three times and incubated with horseradish peroxidase-conjugated anti-mouse (for PTB) or anti-rabbit (for PCBP2) immunoglobin G for 2 h. After three washes, proteins were visualized with an enhanced chemiluminescence reagent kit (Amersham International Plc.) according to the manufacturer's

recommended procedure. The same blot was re-used and the same steps were repeated to detect actin. For this purpose, anti-actin(Ab-1) mouse mAb (JLA20) (Calbiochem) was used as primary antibody and goat anti-mouse IgM conjugated to horseradish peroxidase (Calbiochem) as secondary antibody.

Growth of virus at 37 °C and 39 °C. One-step growth experiments in different human and mouse cell lines were carried out at different temperatures. Cell monolayers in 35 mm plastic culture dishes were washed with Dulbecco's minimal essential medium (DMEM) and inoculated at an MOI of 10 with the virus to be tested. The dishes were rocked for 30 min at room temperature, the cells were thoroughly washed to remove unbound virus and placed at 37°C or 39.5°C. At 0, 2, 4, 6, 8, 12, 24 and 48 hr post infection (p.i.), the dishes were subjected to three consecutive freeze-thaw cycles, and the viral titers of the supernatants were determined by plaque assay, as describe before (Molla *et al.,* 1991).

Poliovirus luciferase replicons and luciferase assay. Previously a wt replicon PV1(M)-luc was described, in which the PV capsid coding sequence was replaced by that of firefly luciferase gene (Li *et al.,* 2001). In addition a new chimeric replicon was constructed that, in analogy to their full length infectious counterparts, carries the wt HRV2 IRES [PV1(RIPO)-luc]. The plasmids containing these replicons were linearized with *Dra*I and used for RNA synthesis using phage T7 RNA polymerase. *In vitro* transcribed replicon RNA was transfected into monolayers (35-mm-diameter dishes) of HeLa, SK-N-MC and L20B cells using a modified DEAE-Dextran transfection method (Mueller *et al.,*

2006) and incubated at 37°C and 39.5°C in DMEM, 2% BCS. At different time points post-transfection the growth medium was removed from the dishes, and the cells were washed gently with 2 ml of phosphate-buffered saline. The cells were lysed and the firefly luciferase activity was measured by methods described previously (Yin *et al.,* 2003).

RESULTS

PV1(RIPO) was found to replicate well in human cervical carcinoma cells (HeLa) but replication was significantly reduced in human neuroblastoma cells (SK-N-MC) at 37^{o}C. Furthermore, PV1(RIPO) had lost the neurovirulent phenotype of PV1(M) in mice transgenic for the human PV receptor gene, *CD155* (CD155tg mice), and in non-human primates (Gromeier *et al.,* 1996; Gromeier *et al.,* 1999). The relationship between genotype and phenotype(s) became even more complex when I found that a variant of PV1(RIPO) (R-1) grew well in SK-N-MC cells but still showed high neuroattenuation in CD155tg mice (see chapter II). Therefore, I concluded that replication in SK-N-MC cells and neurovirulence in CD155tg mice do not co-vary. Additionally, I found, as I described in chapter II, that PV1(RIPO) possesses a strong temperature dependent growth defect in all of the mouse cell lines tested (both neuronal and non-neuronal expressing the human PV receptor CD155). The high attenuation of PV1(RIPO) in CD155tg mice, therefore, co-varied with the inability of this chimeric virus to replicate in mouse cells. These observations suggest that PV1(RIPO) shows a distinct tissue and host tropism. My aim was to study the influence of the quantitative and

qualitative differences of the ITAFs for the observed tissue and host specificity of PV1(RIPO).

Over-expression of known ITAFS in SK-N-MC cells stimulates proliferation of chimeric poliovirus PV1(RIPO). To determine whether a quantitative difference in the ITAFs could help PV1(RIPO) to grow better in human neuronal cells, cell lines of SK-N-MC stably over-expressing the ITAFs hPTB1 or PCBP-2, or unr were generated (see Materials and Methods). To assess the level of over-expression of the proteins hPTB1 and PCBP2 in SK-N-MC cells, immunoblot assays were carried out with appropriate antibodies and compared with patterns obtained from the parental SK-N-MC cells (Fig. 14A and14C respectively). In the regular SK-N-MC cells, PTB was visualized as a doublet band migrating with an apparent molecular mass of ~57 kDa (indicated with arrows numbered 1 and 2 in Fig. 14A). Transfection with the hPTB1-expressing plasmid resulted in significant increase in the PTB content of SK-N-MC-hPTB1 cells as reflected by the increased intensity of the doublet bands numbered 1 and 2 (Fig. 14A). Interestingly, a new minor PTB species migrating with a slightly smaller apparent mass than the major doublet bands (indicated with arrow numbered 3 in Fig. 14A) was observed in SK-N-MC cells over-expressing hPTB1. It seems likely therefore that this variant form is derived from the transfected hPTB1, and represents a post-translational modification that results in altered gel mobility (cleavage product, phosphorylation etc.). To what extent the over-expression of hPTB1 rescues the growth defect of PV1(RIPO)

was examined by growing PV1(RIPO) in the over-expressing cells and comparing the growth phenotype in these cells with that in the restricted parental cells. The results shown in Fig. 14B show that an increase in PTB content significantly enhanced the growth of PV1(RIPO) in SK-N-MC cells at 37^{o}C. Furthermore, the increased level of PTB partially rescued the restricted growth of PV1(RIPO) in SK-N-MC cells at 39.5^{o}C (Fig. 14B).

It was of interest to me to see whether a second ITAF, PCBP2 was also capable of stimulating the growth of PV1(RIPO) in SK-N-MC cells. A significantly increased expression of PCBP2 was observed when SK-N-MC cells over-expressing recombinant PCBP2 (SK-N-MC-PCBP2) were compared with parental SK-N-MC cells by Western blotting (Fig. 14C). As was observed previously, our anti-PCBP2 polyclonal antiserum has affinity for different PCBP subtypes (Walter *et al.,* 1999; Walter *et al.,* 2002; Toyoda *et al.,* 2007a). Moreover, Toyoda *et al.,*(2007a) showed that PCBP1 and PCBP2 isoforms migrate with the same apparent mass. This observation suggests PCBP1 and PCBP2 species are co-migrating both in SK-N-MC and SK-N-MC-PCBP2 (Fig. 14C). Multiple bands (indicated with arrows) with different molecular mass were observed for both cell types (Fig. 14C). These bands might be differentially post-translationally modified forms of PCBP1 and PCBP2 (Walter *et al.,* 1999; Walter *et al.,* 2002; Toyoda *et al.,* 2007a). The effect of PCBP2 over-expression in stimulating the growth of PV1(RIPO) were next examined by comparing the growth of PV1(RIPO) and of wt PV in SK-N-MC-PCBP2 cells with that in regular

SK-N-MC cells (Fig. 14D). Interestingly, over-expression of PCBP2 showed a marked stimulation of PV1(RIPO) growth in SK-N-MC cells at 37^{o}C. Moreover, similar to hPTB1 over-expression in SK-N-MC cells, at 39.5^{o}C, a rescue of PV1(RIPO) growth was also observed with PCBP2 over-expression (Fig. 14D).

Unr, a cytoplasmic RNA-binding protein, was previously found to stimulate HRV IRES activity (Hunt *et al.,* 1999b). As PV1(RIPO) possesses the IRES of HRV2, I also assessed the effect of over-expression of unr on the stimulation of PV1(RIPO) growth in SK-N-MC cells (Fig. 14E). As with hPTB1 and PCBP2, over-expression of unr in SK-N-MC cells stimulated the growth of PV1(RIPO) at 37^{o}C. But unlike hPTB1 and PCBP2, unr over-expression did not rescue the growth of PV1(RIPO) in SK-N-MC-unr cells at 39.5^{0}C (compare Fig.14E with Fig 14B and Fig.14D). Although I worked with SK-N-MC cells that were pool-selected for over-expression of unr, I could not independently verify the level of unr expression in the resulting cell pool, as the only antibody available to me produced very high background levels of non-specific signal upon Western blotting. Rather, I took the functional rescue of PV1(RIPO) replication in SK-N-MC-unr as an indication of the expression of the recombinant human unr protein in the cells.

hPTB1, PCBP2, and unr over-expression enhances HRV2 IRES-mediated translation in SK-N-MC cells. The functionality of subgenomic PV replicons, specifically, PV1(M)-Luc and PV1(RIPO)-Luc, expressing the firefly luciferase reporter gene in place of the PV capsid proteins was analyzed and

reported in Chapter II. To differentiate between the luciferase signals due to translation from the incoming viral RNA from signals due to translation from mRNA synthesized during replication the cells were grown in the presence and in the absence of 2mM guanidine hydrochloride (GuHCl). At this concentration, GuHCl inhibits viral RNA replication without any toxic effect on cellular processes or viral translation (Caliguiri *et al.,* 1968; Jacobson *et al.,* 1968; Loddo *et al.,* 1962). HRV2 IRES-mediated translation and RNA replication were measured in parental SK-N-MC cells and SK-N-MC cells over-expressing hPTB1, PCBP2 and unr by transfecting the cells with *in vitro* transcribed RNA of PV luciferase replicons and incubating the cells at 37^{o}C and 39.5^{o}C in the presence (for translation) or in the absence (for replication) of 2 mM GuHCl) (Fig. 15). Translation and replication mediated by the HRV2 IRES in case of the PV1(RIPO)-luc replicon was low and it decreased with increasing temperature when compared to that of the PV1(M)-luc replicon in SK-N-MC cells (Fig. 15A). In contrast, in SK-N-MC-hPTB1 cells (Fig. 15B), in SK-N-MC-PCBP2 cells (Fig. 15C), and SK-N-MC-unr cells (Fig. 15D) a significant increase in HRV2 IRES-mediated translation activity, and consequently replication was observed (Fig. 17B). Consistent with the lack of rescuing effect of unr on PV1(RIPO) virus growth (Fig. 14E), only a insignificantly small increase in translation activity of PV1(RIPO)-luc replicon was noticed by the over-expression of unr at 39.5^{o}C (Fig. 15D).

Expression of hPTB1 rescues the growth defect of PV1(RIPO) in mouse L20B cells. PV1(RIPO) showed a severe propagation defect in mouse cells, which has been described in Chapter II. Since the quantitative differences in ITAFs in SK-N-MC cells have showed a marked influence on HRV2-IRES-mediated translation and the growth of PV1(RIPO), I was interested to examine the effect of hPTB1 on PV1(RIPO) growth in L20B cells, a mouse fibroblast cell line expressing the PV receptor. The expression of hPTB1 in L20B-hPTB1 cells was assessed by immunoblot assays using different monoclonal antibodies to hPTB1 and was compared with PTB expression in parental L20B cells (Fig. 16A). As was observed earlier in SK-N-MC cells, PTB was visualized as a doublet band migrating with an apparent molecular mass of ~57 kDa (indicated with arrows numbered 1 and 2 in Fig. 16A). Among four different monoclonal antibodies to hPTB1, three antibodies, anti-PTB DH1 ((Fig. 16A, right blot), DH7 and DH17 (not shown) were able to detect both the recombinant hPTB1 (expressed in L20B-hPTB1cells) and endogenous mouse PTB (mPTB, in L20B cells) (Fig. 16A, right blot). Interestingly, a fourth monoclonal antibody, anti-PTB DH3 only detected the recombinant hPTB1 expressed in L20B cells, but not the endogenous mPTB isoforms (Fig. 16A, left blot). Thus, it can be inferred that mAb DH3 is specific for the hPTB1, which represents the antigen used for production of this series of anti PTB mAbs (Grossman, Helfman, *et al.* 1998).

To determine whether the production of hPTB1 in L20B cells plays a role in the growth of PV1(RIPO), the growth of this virus was compared with that of

PV1(M) in L20B cells and L20B-hPTB1 cells (Fig. 16). Consistent with the over-expression of hPTB1 in SK-N-MC cells, expression of this protein in L20B cells rescued the defective growth of PV1(RIPO) at 37^{o}C (Fig. 16B) but no rescue was observed at 39.5^{o}C (Fig. 16C). Qualitative changes in PTB, i.e., the expression of hPTB1 in L20B cells appeared to significantly enhance the growth of PV1(RIPO) in L20B-hPTB1 cells.

Rescue of HRV2 IRES-mediated translation defect by expression of hPTB1 in L20B cells. Qualitative differences in the ITAFs, which interact differently with HRV2 IRES in mouse L20B cells than in human cells, resulting in a translational defect might play an important role in the outcome of PV1(RIPO) infection in mouse cells. Therefore, I was interested to determine the extent to which hPTB1 expression mediates enhancement of translation directed by the HRV2 IRES in L20B cells. For this purpose, the functionality of PV- subgenomic luciferase replicons was analyzed in L20B and L20B-hPTB1 cells as described above for SK-N-MC cells. HRV2 IRES-mediated translation and RNA replication were measured in regular L20B cells and L20B-hPTB1 cells by transfecting the cells with *in vitro* transcribed RNA of PV1(M)-Luc and PV1(RIPO)-Luc PV luciferase replicons and incubation of the cells at 37^{o}C and 39.5^{o}C in the presence (for translation) or in the absence (for replication) of 2 mM GuHCl) (Fig. 17). The results of these experiments closely paralleled those obtained in SK-N-MC cells over-expressing different ITAFs. A 10-fold enhancement of HRV2-directed translational activity was obtained in L20B-hPTB1 cells (Fig. 17). This

resulted in more than 100-fold increase in replication of PV1(RIPO)-luc replicon in L20B-hPTB1 cells. However, unlike PTB and PCBP2 over-expression in SK-N-MC cells, hPTB1 could not rescue the defective HRV2-directed translational activity and consequently replication in L20B-hPTB1 cells at 39.5^{o}C (Fig. 17). These results are consistent with the effect of hPTB1 on PV1(RIPO) growth in L20B-hPTB1 cells (Fig. 16B and 16C). The increase in HRV2 IRES-directed translation in the presence of hPTB1 in L20B cells again suggests that mPTB present in L20B cells is insufficient for optimal function of the HRV2 IRES. These results also indicate that the expression of hPTB1 compensates for the intrinsically poor activity of mPTB on HRV2 IRES activity in L20B cells.

The growth of PV1(M) is non-responsive to the over-expression or expression of ITAFs. The growth of PV1(M) was unaffected by the over-expression of hPTB1 (Fig. 14B), PCBP2 (Fig. 14D), and unr (Fig. 14E) in SK-N-MC cells. In contrast, the PV IRES activity was increased significantly with the over-expression of these ITAFs in SK-N-MC cells (Fig. 15). These results suggest that the amount of ITAFs in SK-N-MC cells are sufficient enough for the optimal growth of PV1(M) in these cells. In addition, increase in PV-mediated translational initiation as a result of over-expression of ITAFs has no further effect on PV1(M) growth in SK-N-MC cells. In L20 B cells the expression of hPTB1 also failed to show any influence on PV1(M) growth (Fig. 16B). Consistent with the growth of the PV1(M), PV IRES activity is non-responsive to the absence or presence of hPTB1 in L20B or L20B-PTB cells, respectively (Fig. 17). This

observation suggests that the PV IRES is either capable of using mPTB or, less likely, is independent of PTB in mouse cells.

Mouse L20B cell adapted PV1(RIPO) is non-responsive to hPTB1 supplementation. A variant of PV1(RIPO) adapted to grow in mouse cells, described in Chapter II, showed high neurovirulence in CD155tg mice. This variant, which was named R-1235, contains four mutations in the 5'NTR (Fig. 18A). As R-1235 showed wt PV1(M) like growth in SK-N-MC cells and L20B cells it was interesting to examine the effect of hPTB1 supplementation on the growth of this virus in these cells. As was observed with wt PV1(M), over-expression or expression of hPTB1 in SK-N-MC cells or L20B cells, respectively, had no influence on the growth of R-1235 in these cells (Fig. 18B and 18C). Therefore, similar to PV1(M), R-1235 either adapted to using the endogenous mPTB or became independent of PTB in L20B cells.

DISCUSSION

IRES-dependent tropism between cell types of different hosts can be determined largely by the quantitative and qualitative differences in some non-canonical RNA binding cellular factors. These factors, commonly ITAFs are believed to act as RNA chaperones that aid in folding the IRES into the correct conformation and promote the process of ribosome internal binding to IRES. In this chapter of my dissertation, I have presented the findings from my study about the role of ITAFs as important determinant for type I IRES function in human cells and mouse cells. These human ITAFs were introduced into cells

deficient of propagating the chimeric virus PV(RIPO) thereby rescuing the growth defect. Specifically, PV1(RIPO) if supplied with an excess of ITAFs, can grow in a human neuronal cell line (SK-N-MC) and in a mouse cell line (L20B). Two different types of functional assays were performed: (i) viral propagation in these cells and (ii) translation and replication activity of a luciferase replicon in these cells.

Over-expression of the ITAFs stimulated significantly the replication of the chimeric virus PV1(RIPO). Numerous experiments have shown that the ITAFs directly act on the IRES elements (Jang, 2006; Fernández-Miragall *et al.,* 2009). It is, therefore, reasonable to assume that the over-expression of PCBP2, hPTB1, and unr, separately, in human neuronal cells stimulated on HRV2 IRES activity. A quantitative increase in any one of these factors is enough to favor the HRV2 IRES activity in these cells. The over-expression of hPTB1 and PCBP2 in human neuronal cells, in contrast to unr, rescued viral proliferation even at 39.5^{o}C. It is noteworthy that at this high temperature these proteins are still capable of helping the HRV2 IRES to function properly. A 100-fold increase in translational activity of HRV2 IRES was observed in over-expression of unr at physiological temperature but not at 39.5^{o}C. This observation suggests that temperature also has differential influence on the interaction of these proteins with the HRV2 IRES.

In HeLa cells, the concentration of the hPTB1 is sufficient for HRV2 IRES activity. In contrast, neuronal cells might be enriched with nPTB and deficient in

hPTB1 (Kikuchi *et al.,* 2000; Markovtsov *et al.,* 2000; Polydorides *et al.,* 2000; and Lillevali *et al.,* 2001). The growth deficiency of PV1(RIPO) in SK-N-MC cells can be explained if the HRV2 IRES cannot function (or function only very poorly) with endogenous hPTB, a deficiency not apparent for the PV IRES. Consistent with this idea, an increase in the relative amount of hPTB1 in neuronal cells therefore showed a great stimulation of HRV2 IRES-mediated translation and as a result growth of PV1(RIPO) as efficient as wt PV in SK-N-MC cells. A similar observation with a different picornavirus (IRES type II) was reported in a study by Pilipenko *et al.,* (2001). The investigators showed that, a mutation in the PTB/nPTB binding sites in IRES of Theiler's murine encephalomyelitis virus, a member of Picornavirus family, preferentially impaired nPTB binding compared with PTB binding. The changes in the binding of nPTB resulted in decreased neurovirulence of the mutant virus. nPTB has >70% amino acid identity with PTB (Polydorides *et al.,* 2000). Therefore, it is possible that PTB expression detected with anti-PTB in SK-N-MC cells represent the neuronal PTB (nPTB) which might not interact with HRV2 IRES as efficiently as it interacts with PV IRES. Unfortunately, we do not have antibodies capable to differentiate between hPTB1 and nPTB. In addition to the qualitative difference (nPTB vs. hPTB1) there may also be a quantitative difference in that only very small amounts of hPTB1 are expressed in SK-N-MC cells.

The observed phenotypes of PV1(RIPO) in mouse cells and in CD155tg mice makes the mouse cell lines an excellent system for the isolation of *trans*-

acting factors required for the function of HRV IRES. In the mouse cells the phenotype of PV1(RIPO) is more severe than in human neuronal cells which was reflected by absence of viral growth and translational activity even at physiological temperature. There might be several reasons for the differences in the phenotype. The mPTB, although abundantly expressed in L20B cells, does not seem to be able to activate the HRV2 IRES. In sharp contrast, the expression of hPTB1 in L20B cells increased the activity of HRV2 IRES-mediated translation and as a result the growth of PV1(RIPO). A 10-fold increase in IRES activity resulted in more than 100-fold increase in viral RNA replication (Fig. 17) and about 100-fold increase in PV1(RIPO) growth in L20B cells (Fig. 16B). However, the expression of the hPTB1 in L20B cells could not completely restore the HRV2 IRES activity as the IRES-mediated translation (Fig. 17) and the viral growth (Fig. 16) did not reach as high as the wt PV in these cells. These results strongly indicate that in addition to hPTB1, HRV2 IRES requires additional factors for efficient internal initiation of translation. Earlier studies by Hunt *et al.,* (1999 a, b) support my results where they found that unr and another protein p38 act synergistically with PTB to promote translation dependent on the HRV IRES at highest level.

It was not surprising that only few mutations in the IRES of PV1(RIPO) changed the PTB requirement of the IRES of the mouse cell-adapted PV1(RIPO), R-1235 in mouse cells. This observation strongly suggests that the interaction of protein must have been changed because i) of the changes in the

structure of IRES due to the introduction of mutations or ii) the creation of a potential mouse protein binding site (s) by the introduction of mutations. A similar observation was reported in a study with TMEV where introduction of a second site mutation in the viral IRES generated a binding site for PTB(nPTB) leading to efficient translation initiation and restoration of neurovirulence to wt levels (Pilipenko *et al.,* 2001).

It is obvious from the data presented here that, although both the PV IRES and the HRV IRES are type I IRES elements, their requirements for PTB are different in mouse cells. On the basis of these observations three interpretations were made: (i) PV1(RIPO) is using hPTB1 in L20B-hPTB cells and can not use mPTB in L20B cells, or (ii) PV1(M) and R-1235 are using mPTB in L20B cells, or (iii) PV1(M) and R-1235 are independent of PTB in L20B cells. To fully understand the role of either hPTB1 in L20B-hPTB cells or mPTB in L20B cells, these interpretations must be clarified. Following should be done to prove these hypotheses:

(i) For the first hypothesis, I have to show that HRV2 IRES is binding the hPTB1 in L20B-hPTB cells but not binding the mPTB in L20B cells.

(ii) For the second hypothesis, I have to show that PV IRES and IRES of R-1235 virus are binding the mPTB in L20B cells.

(iii) For the third least likely hypothesis, I have to show that PV IRES and IRES of R-1235 virus are not binding any PTB in L20B cells.

Therefore, to fully support these potential roles of the ITAFs obtained from these functional assays, the physical interaction of these proteins with the PV IRES and HRV2 IRES must be compared in parallel by performing some binding assays.

Table 2. Known IRES *trans*-activating factors (ITAFs) for the members of Picornaviridae family (Fitzgerald and Semler, 2009)

Virus	**Known ITAFs**
Poliovirus (PV)	PTB, PCBP2, PCBP1, La, unr, SRp20
Coxsackievirus B3 (CVB3	PCBP2, La
Enterovirus 71 (EV71)	Not known
Hepatitis A virus (HAV)	PTB, PCBP2
Human rhinovirus (HRV)	PTB, PCBP2 , La, unr, hnRNP A1
Foot-and-mouth disease virus (FMDV)	PTB, ITAF45, La
Encephalomyocarditis virus (EMCV)	PTB, La
Theiler's murine encephalomyelitis virus (TMEV)	PTB
Porcine teschovirus serotype 1 (PTV-1)	Not known

Figure 14. Comparison of the growth phenotype of PV1(M), and PV1(RIPO) virus in SK-N-MC cells and Sk-N-MC cells over-expressing hPTB-1, PCBP-2 and Unr. (A) Expression of PTB in parental SK-N-MC cells and SK-N-MC-hPTB1 cells was detected by immunoblot analysis as described in Materials and Methods section. PTB was visualized as a doublet band migrating with an apparent molecular mass of ~57 kDa which is indicated with arrows numbered 1 and 2. A new minor PTB species migrating with a slightly smaller apparent mass than the major doublet bands is indicated with arrow numbered 3. (B) Comparison of the growth phenotype of PV1(RIPO) and PV1(M) in the parental SK-N-MC cells and with that in SK-N-MC-hPTB1 cells at 37ºC and 39.5ºC. (C) Expression of PCBP2 in parental SK-N-MC cells and SK-N-MC-PCBP2 cells was detected by immunoblot analysis as described in Materials and Methods section. Our anti-PCBP2 polyclonal antiserum has affinity for different PCBP subtypes (Walter *et al.,* 1999; Walter *et al.,* 2002; Toyoda *et al.,* 2007). Multiple bands (indicated with arrows) represents differentially post-translationally modified forms of PCBP1 and PCBP2. (D) Comparison of the growth phenotype of PV1(RIPO) and PV1(M) in the parental SK-N-MC cells and with that in SK-N-MC-PCBP2 cells at 37ºC and 39.5ºC. (E) Comparison of the growth phenotype of PV1(RIPO) and PV1(M) in the parental SK-N-MC cells and with that in SK-N-MC-unr cells at 37ºC and 39.5ºC. For the comparison of the growth phenotype of PV1(RIPO) and PV1(M) [(B), (D), and (E)] cells were infected at an MOI of 10 and incubated at 37ºC and 39.5ºC. The virus titers were determined by plaque assay on monolayers of HeLa R19 cells, as described in Materials and Methods. Actin was detected as a loading control.

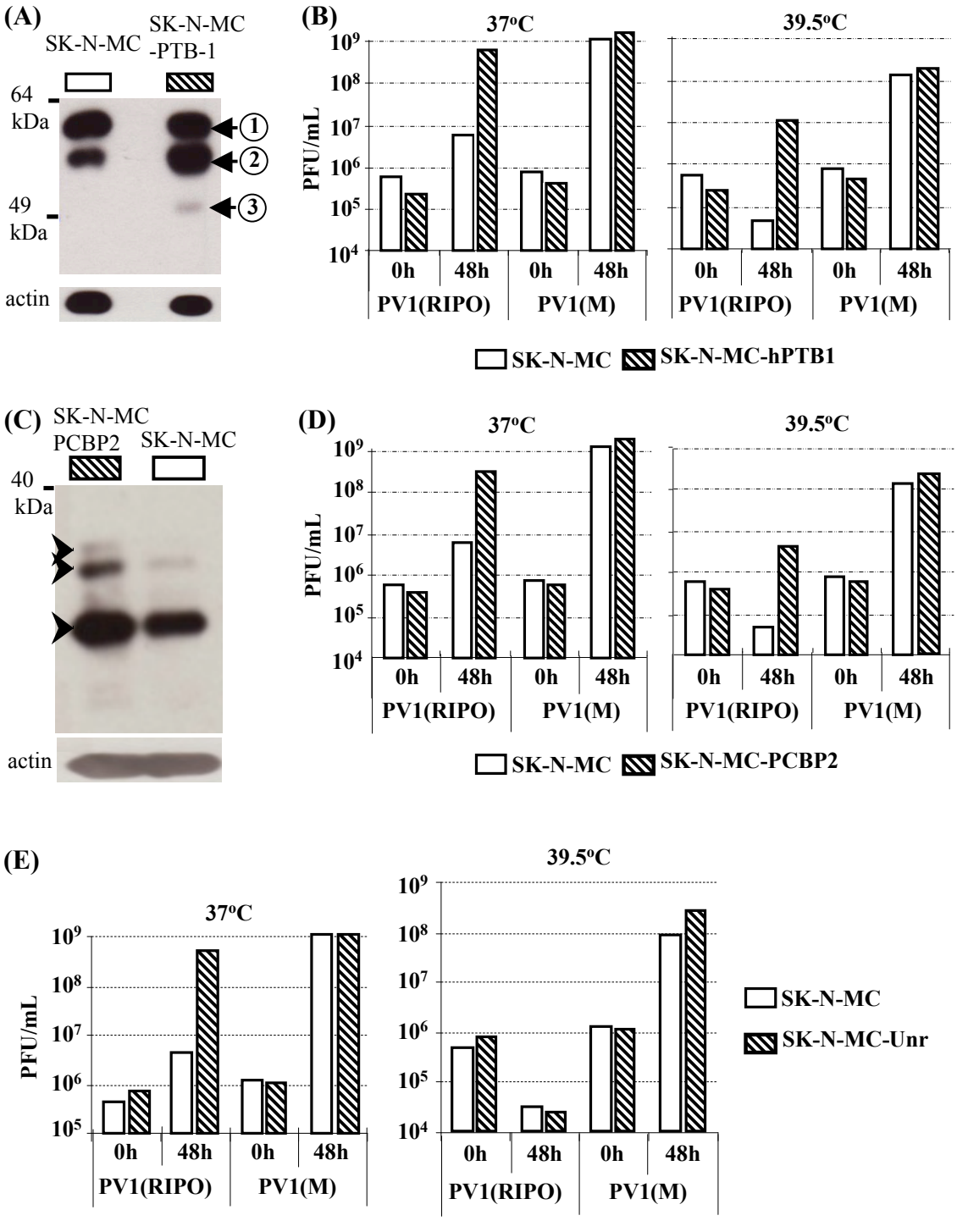
(A)
SK-N-MC
SK-N-MC -PTB-1
64 kDa
49 kDa
actin
1
2
3
(B)
37°C
39.5°C
PFU/mL
0h
48h
PV1(RIPO)
PV1(M)
SK-N-MC
SK-N-MC-hPTB1
(C)
SK-N-MC PCBP2
SK-N-MC
40 kDa
actin
(D)
37°C
39.5°C
PFU/mL
SK-N-MC
SK-N-MC-PCBP2
(E)
37°C
39.5°C
PFU/mL
SK-N-MC
SK-N-MC-Unr

Figure 15. RNA translation and replication of PV1(M)-luc and PV1(RIPO)-luc replicons in SK-N-MC cells and SK-N-MC cells over-expressing hPTB-1, PCBP-2 and Unr. Structure of the luc-replicon is shown on the top. Monolayers of SK-N-MC (A), SK-N-MC-hPTB1 (B), SK-N-MC-PCBP2 (C) and SK-N-MC-Unr (D) cells were transfected with *in vitro* transcribed RNA of luciferase replicons and incubated at either 37^{o}C or 39.5^{o}C in the presence (for translation) or in the absence (for replication) of 2mM guanidine hydrochloride (Gu HCl). RNA translation and RNA replication were assessed by measuring the luciferase activity (Relative Light Unit) at 10h post transfection.

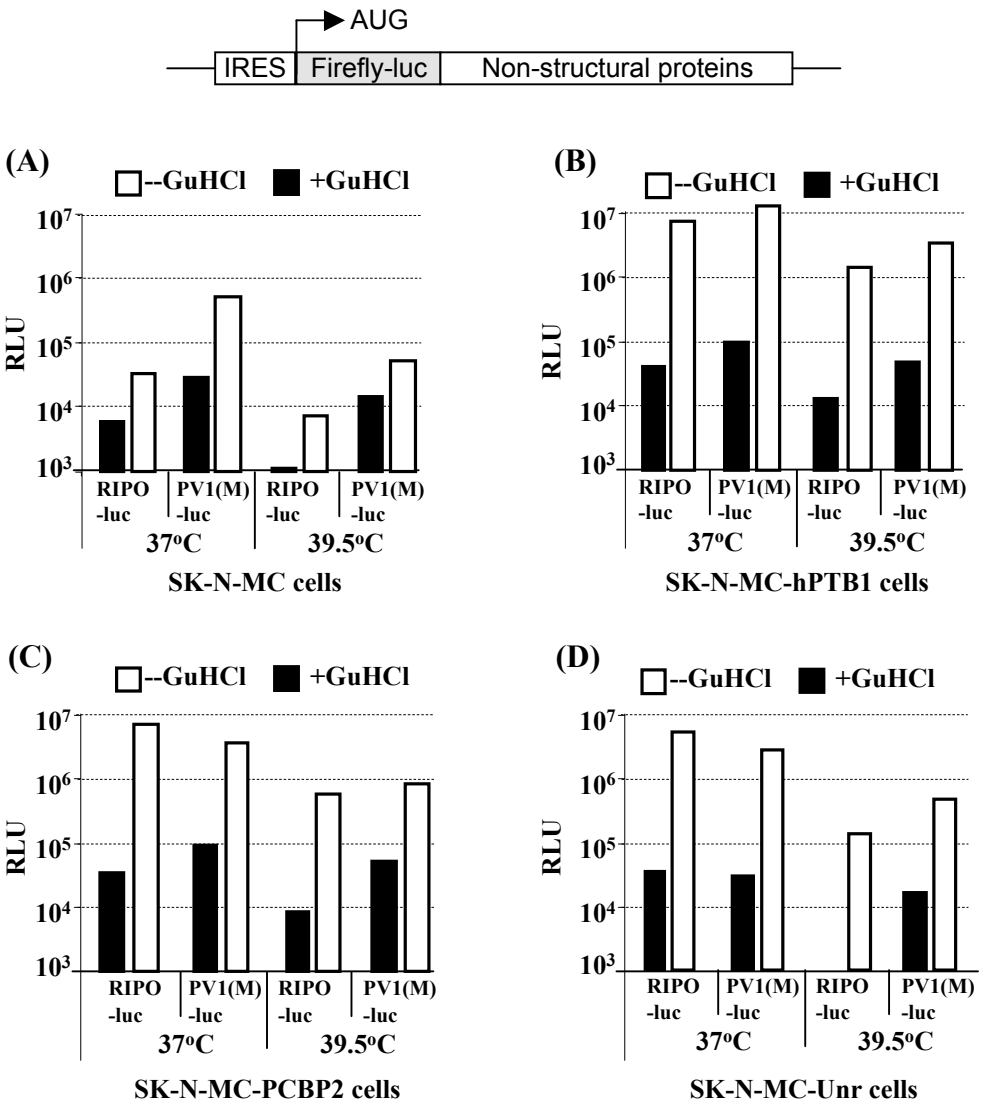
AUG
IRES
Firefly-luc
Non-structural proteins
(A)
--GuHCl
+GuHCl
RLU
10^7
10^6
10^5
10^4
10^3
RIPO -luc
PV1(M) -luc
RIPO -luc
PV1(M) -luc
37°C
39.5°C
SK-N-MC cells
(B)
--GuHCl
+GuHCl
RLU
RIPO -luc
PV1(M) -luc
RIPO -luc
PV1(M) -luc
37°C
39.5°C
SK-N-MC-hPTB1 cells
(C)
--GuHCl
+GuHCl
RLU
RIPO -luc
PV1(M) -luc
RIPO -luc
PV1(M) -luc
37°C
39.5°C
SK-N-MC-PCBP2 cells
(D)
--GuHCl
+GuHCl
RLU
RIPO -luc
PV1(M) -luc
RIPO -luc
PV1(M) -luc
37°C
39.5°C
SK-N-MC-Unr cells

Figure 16. Comparison of the growth phenotype of PV1(M), and PV1(RIPO) virus in L20B cells and L20B-hPTB1 (cells over-expressing hPTB-1) cells. (A) Expression of PTB in parental L20B cells and L20B-hPTB1 cells was detected by immunoblot analysis as described in Materials and Methods section. Two different monoclonal antibodies to PTB were used which are indicated on the bottom of each blot. PTB was visualized as a doublet band migrating with an apparent molecular mass of ~57 kDa which is indicated with arrows numbered 1 and 2. (B) and (C), Comparison of the growth phenotype of PV1(RIPO) and PV1(M) in the parental L20B cells and with that in L20B-hPTB1 cells at 37^{o}C and 39.5^{o}C, respectively. Cells were infected at an MOI of 10 and incubated at 37^{o}C and 39.5^{o}C. The virus titers were determined by plaque assay on monolayers of HeLa R19 cells, as described in Materials and Methods. Actin was detected as a loading control.

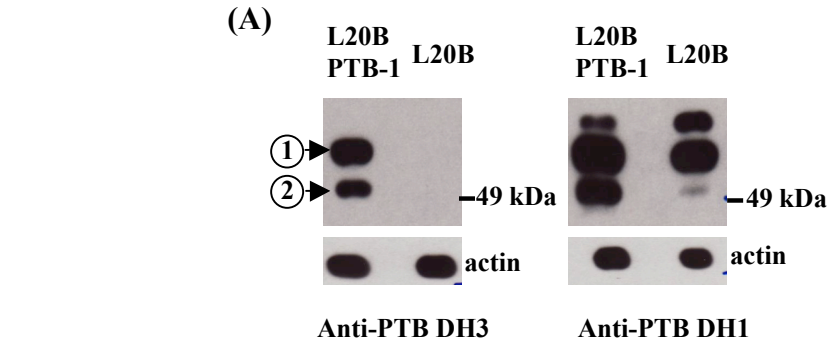
(A)
L20B
PTB-1
L20B
L20B
PTB-1
L20B
1
2
49 kDa
49 kDa
actin
actin
Anti-PTB DH3
Anti-PTB DH1

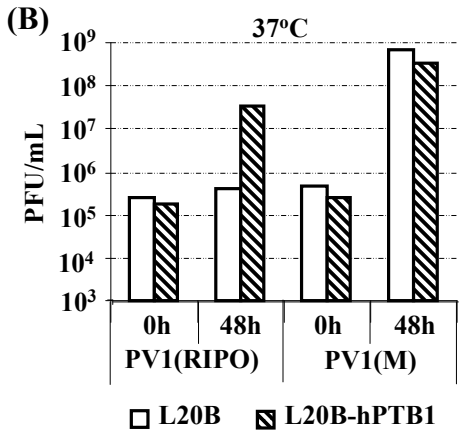
(B)
37°C
PFU/mL
10^9
10^8
10^7
10^6
10^5
10^4
10^3
0h
48h
0h
48h
PV1(RIPO)
PV1(M)
L20B
L20B-hPTB1

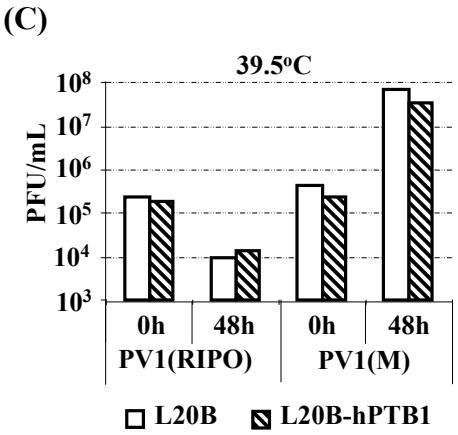
(C)
39.5°C
PFU/mL
10^8
10^7
10^6
10^5
10^4
10^3
0h
48h
0h
48h
PV1(RIPO)
PV1(M)
L20B
L20B-hPTB1

Figure 17. RNA translation and replication of PV1(RIPO)-luc and PV1(M)-luc replicons in L20B cells and L20B-hPTB1 cells. Structure of the luc-replicon is shown on the top. Monolayers of L20B and L20B-hPTB1 cells were transfected with *in vitro* transcribed RNA of luciferase replicons and incubated at 37^{o}C and 39.5^{o}C in the presence (for translation) or in the absence (for replication) of 2mM guanidine hydrochloride (GuHCl). RNA translation and RNA replication were assessed by measuring the luciferase activity at 11h post transfection.

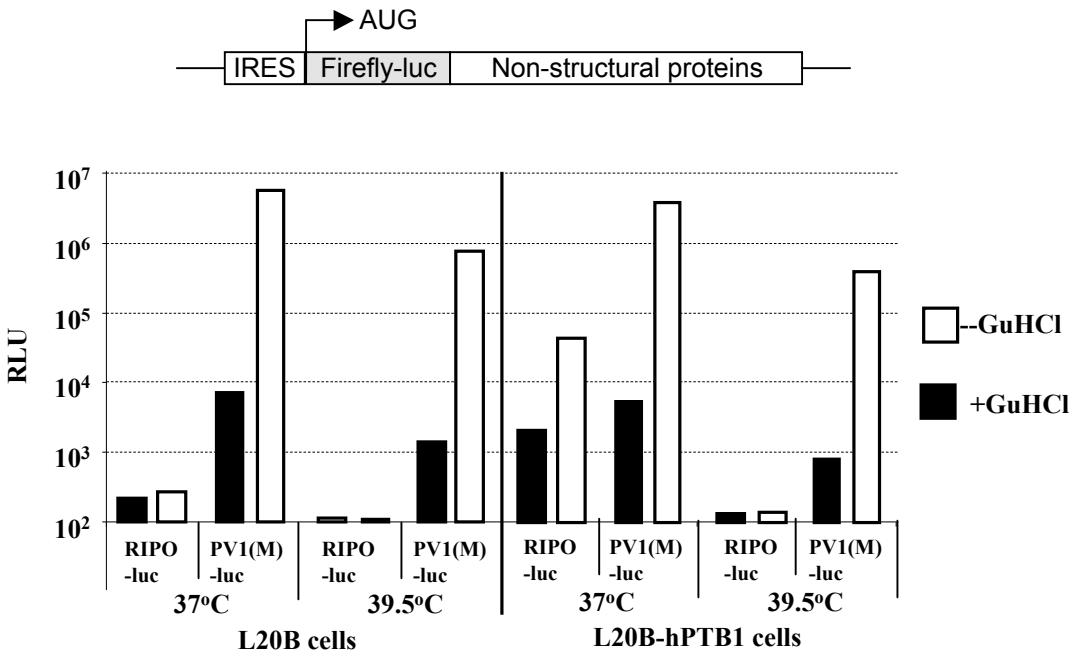
AUG
IRES
Firefly-luc
Non-structural proteins
RLU
10^7
10^6
10^5
10^4
10^3
10^2
--GuHCl
+GuHCl
RIPO -luc
PV1(M) -luc
RIPO -luc
PV1(M) -luc
RIPO -luc
PV1(M) -luc
RIPO -luc
PV1(M) -luc
37°C
39.5°C
37°C
39.5°C
L20B cells
L20B-hPTB1 cells

Figure 18. Effect of human PTB-1 over-expression (in SK-N-MC cells) and expression (L20B cells) on the growth of R-1235 virus. (A) Schematic representation of IRES of R-1235 virus. The changes in nucleotides in the 5'NTR and in the IRES are indicated and they are numbered as 1, 2, 3, and 5. (B) Comparison of the growth phenotype of R-1235 virus in the parental SK-N-MC cells and with that in SK-N-MC-hPTB1 cells at 37^{o}C. (C) Comparison of the growth phenotype of R-1235 virus in the parental L20B cells and with that in L20B-hPTB1 cells at 37^{o}C. Cells were infected at an MOI of 10 and incubated at 37^{o}C. The virus titers were determined by plaque assay on monolayers of HeLa R19 cells, as described in Materials and Methods.

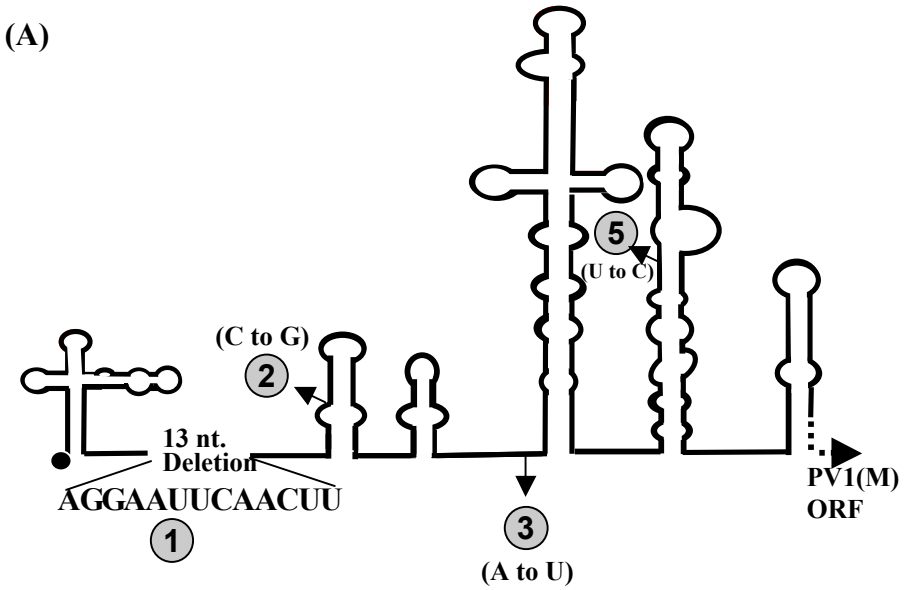
(A)
5
(U to C)
(C to G)
2
13 nt.
Deletion
AGGAAUUCAACUU
1
3
(A to U)
PV1(M)
ORF

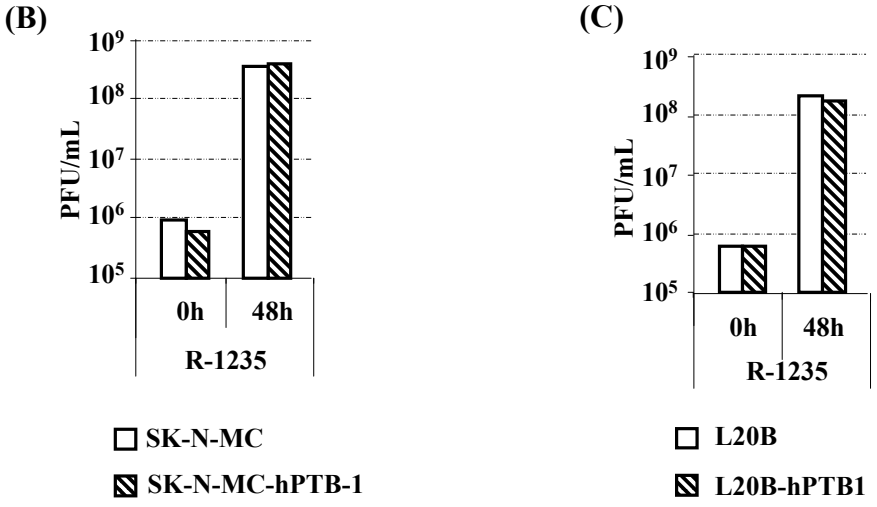
(B)
PFU/mL
10^9
10^8
10^7
10^6
10^5
0h
48h
R-1235
SK-N-MC
SK-N-MC-hPTB-1
(C)
PFU/mL
10^9
10^8
10^7
10^6
10^5
0h
48h
R-1235
L20B
L20B-hPTB1

Chapter IV: Identification of the determinants of the replication defect of PV in MDCK cells

Introduction

In chapters II and III I have shown that, concomitantly with PV receptor expression, other factors like IRES structure and availability of essential ITAFs determine tissue tropism of wt PV and PV1(RIPO), a chimeric PV. I found that the overexpression of exogenous ITAFs rescued the defective growth of PV1(RIPO) in human neuronal cells and in mouse cells, attesting to the crucial impact of ITAFs on IRES function in various intracellular environments. The scenarios investigated in chapters I and II represent cases where the lack of a certain component (a host factor) led to a disruption of viral function. In contrast, it is also plausible that the presence of certain host factors or cellular responses actively restricts PV replication.

Recent evidence indicates that the innate immunity, more specifically IFNα/β-system, plays an important role in the acquisition of susceptibility to PV by cells in host organisms like the mouse. Differences in interferon (IFN) response among the tissues in the host organism are responsible for differential susceptibility of cells. A strong IFN response protects the cells in some extraneural tissues from PV infection, while a weak or delayed interferon response in the central nervous system, appears to facilitates infection by PV (Ida-Hosonuma *et al.,* 2005). These same investigators also showed that primary kidney cells acquired PV susceptibility during the *in vitro* cultivation process concomitantly with the rapid loss of IFN action (Yoshikawa *et al.,* 2006).

Elimination of virally infected cells is crucial for the establishment of an antiviral state. Two types of death of PV infected cells have been reported: cytopathic effects (during productive infections) or apoptosis (under restrictive conditions) (Agol *et al.,* 1998). PV has been shown to induce apoptosis in a human colon carcinoma cell line (Ammendolia *et al.,* 1999), a human promonocytic cell line U937 (Lopez-Guerrero *et al.,* 2000), and in nerve cell primary cultures from the cerebral cortex of CD155tg mice (Couderc *et al.,* 2002). A more complex response was observed in HeLa cells where two oppositely directed sets of reactions were turned on by PV infection: development of an apoptotic reaction and suppression of its own apoptosis-inducing activity (Tolskaya *et al.,* 1995). Thus there is variability in the apoptotic response to PV infection that may be significant for the pathogenesis of poliomyelitis. It could be speculated that apoptosis is the default cell response to PV infection, which is counteracted more or less efficiently in different types of cells. The outcome of infection may thus depend on the virus' ability to suppress the apoptosis pathway.

Here I am presenting an example of cells of a mammalian origin in culture, known as MDCK$^{CD155\alpha}$ cells (Madin-Darby canine kidney cells expressing the human PV receptor CD155), which is a first known example of CD155 expressing mammalian cell line that cannot be infected by wild type PV. Surprisingly, this cell line did not acquire susceptibility to PV infection during the process of cultivation, which is thought to play an important role as a determinant

in PV susceptibility of cells in culture (Ida-Hosonuma *et al.,* 2005; Yoshikawa *et al.,* 2006). My results indicate that once inside the cell the IRES driven translation of viral RNA is fully functional but the cells either fail to support or actively prevent the viral RNA replication resulting in a nonproductive infection. Most perplexingly, despite the lack of replication and the absence of any progeny virus, MDCK$^{CD155\alpha}$ cells exposed to PV die within hours. The defect of viral RNA replication is probably the result of some unknown interactions between PV and MDCK cells. The study of this unknown interaction is important for the better understanding of PV tissue tropism, host restriction and overall PV pathogenesis. The proposed study is aimed to determine the intracellular stage of the virus life cycle in MDCK cells at which this restriction is exhibited after the stage of translation initiation mediated by the PV IRES.

MATERIALS AND METHODS

Viruses and cells. The neurovirulent PV type 1 [Mahoney; PV1(M)] is the strain being used routinely in the laboratory (Cello *et al.,* 2002). HeLa R19 (human cervical cancer) cells and MDCK (Madin-Darby canine kidney) cells were obtained from the American Type Culture Collection (Manassas, VA) and were maintained according to the supplier's specification. Two canine cell lines, A72 (canine fibroma) and Cf2Th (Canine thymus) were a generous gift from Dr. Colin Parish (Cornell University). A72 cells were maintained in a medium that is made up of 50% Mcoy's 5A medium and 50% Leibovitz L15, with 5% bovine calf serum. Cf2Th cells were maintained in DMEM containing 5% FBS.

Generation of MDCK$^{CD155\alpha}$ stable cell lines. MDCK cells were transfected using Lipofectamine (Invitrogen) with a mammalian expression plasmid pCDNA3 containing the gene for CD155α under the control of cytomegalovirus promoter. The transfection procedure was followed as outlined by the manufacturer. Stable cell clones resistant to G418 were selected and screened for CD155 expression by immunostaining.

Immunostaining of MDCK$^{CD155\alpha}$ cells. Expression of CD155α molecules in MDCK$^{CD155\alpha}$ cells was detected by immunostaining. The cells were grown on coverslips and were fixed in cold 1:1 methanol/acetone for 90 min at −20 °C. They were next washed 3 times with PBS. The fixed cells were then incubated with primary rabbit polyclonal antibody (Iwasaki *et al.,* 2002) at a dilution of 1:2000 in PBS containing 10% bovine calf serum (PBS/BCS) at 37^{o}C for 1h. After six washes with PBS the cells were subsequently incubated with secondary horse raddish peroxidase (HRP) conjugated goat anti-rabbit antibody (Jackson ImmunoResearch Laboratories) at a dilution of 1:2000 in PBS/BCS for 1 h at 37 °C, followed by six washes with PBS, and developed with the Vector® VIP substrate kit (Vector Labs, California) and visualized under a light microscope. Alternatively, for the immunoflurescence detection of CD155, primary antibody treated cells were incubated with secondary Alexa-488 conjugated goat anti-rabbit antibody (Molecular Probes) at a dilution of 1:2000 in PBS/BCS for 1 h at 37 °C and were visualized with a Zeiss Axioplan II fluorescence microscope equipped with a model SP401 camera (Diagnostic Instruments Inc.) microscope.

Virus growth. Cell monolayers in 35 mm plastic culture dishes were washed with 1X Hanks Balanced Salt solution (HBSS) and inoculated at an MOI of 10 with PV1(M). The dishes were rocked for 30 min at room temperature, the cells were thoroughly washed to remove unbound virus and 37^{o}C. At different time points post infection (p.i.), the dishes were subjected to three consecutive freeze-thaw cycles, and the viral titers of the supernatants were determined by plaque assay, as describe before (Molla *et al.,* 1991).

***In vitro* transcription, transfection and virus isolation.** pT7PVM plasmid (to make the viral RNA) and PV-luc replicon (to make the replicon RNA) were linearized with *Dra*I. RNAs were synthesized with phage T7 RNA polymerase, and the RNA transcripts were transfected into cell monolayers by the DEAE-dextran method as described previously (van der Werf *et al.,* 1986). The incubation time was 24 hour post transfection for virus isolation, or until virus-specific cytopathic effect (CPE) appeared. Virus titers were determined by a plaque assay on HeLa R19 monolayers, as described before (Molla *et al.,* 1991).

Luciferase assay. After being transfected with replicon RNA, the cell monolayers (35-mm-diameter dishes) of HeLa and MDCK cells were incubated at 37°C. At different time points post-transfection the growth medium was removed from the dishes, and the cells were washed gently with 2 ml of phosphate-buffered saline. The cells were lysed and the firefly luciferase activity was measured by methods described previously (Yin *et al.,* 2003).

Binding of ^{35}S-labelled PV1(M). PV1(M) proteins were labeled with [^{35}S] methionine and the viruses were purified by CsCl gradient centrifugation, as previously described (Bibb *et al.,* 1994b). For binding assay, 1X10^6 cells were incubated with 10^8 PFU of labeled virus at 25^{o}C for 30 min. After incubation, the virus-cell complex was pelleted by microcentrifugation and the cell pellets were washed 3 times with PBS. The amount of readioactivity of the cell pellet was quantitated with a liquid scintillation counter (Packard Tri-Carb) in counts per minute (cpm). All samples were done in triplicate.

FACS Analysis. MDCK cells and MDCK$^{CD155\alpha}$ cells were brought to a concentration of 1 x 10^6 cells/ml in suspension and incubated for 30 min at room temperature with or without mAb p286 at a concentration of 20μg/ml. mAb recognizes an epitope of the V-domain of CD155 (Yanagiya *et al.,* 2005). Each sample was washed with PBS and then stained with FITC-conjugated goat anti-mouse IgG (BD bioscience). After washing, 10^3 cells were analyzed by a Becton, Dickinson (Rutherford, NJ) FACS caliber. Excitation was at 488 nm and emission at 585 nm. Three parameters were measured for each cell: forward scatter (FSC-H); side scatter (SSC-H); and total fluorescence emitted from the cell (FL2-A).

Viable or non-viable cell counts using trypan blue. MDCK$^{CD155\alpha}$ cells were infected with PV1(M) at an MOI of 10 in the presence or absence of 2 mM Guanidine HCl. 24 hpi the medium was collected and the cells still attached were trypsinized. The dead cells in the medium and the trypsinized cells were mixed 1:1 with trypan blue solution. The cells were counted using a hemocytometer.

Viable cells excluded trypan blue, while non-viable cells stained blue due to trypan blue uptake.

RESULTS

MDCK cells form polarized epithelial cell layers when grown as monolayers to confluence (Barman *et al.,* 2003; Blank *et al.,* 2000; Mora *et al.,* 2002). Thus, this cell line was originally planned to be used as a source of epithelial cells to analyze the polarized transport of PV in the presence or absence of virus replication. MDCK cells do not express the cellular receptor for PV, which is known as CD155 (Mendelsohn *et al.,* 1989). Therefore, it was necessary to express CD155 in MDCK cells to assess the polarized transport of PV using this cell line.

Determination of CD155α expression in MDCK cells. MDCK cells were transfected with a mammalian expression plasmid containing the gene for CD155α, as outlined in the Materials and Methods. Several stable cell lines were selected and screened for CD155 expression by immunostaining. The CD155 expression of one of these cell lines is shown in Fig. 19. Flow Cytometric analysis revealed that more than 97% cells were positive for CD155 expression in this cell line (Fig. 20). Therefore, this cell line was chosen for infection with PV.

Although the MDCK$^{CD155\alpha}$ cells showed very good expression of the PV receptor CD155α, they were unable to produce any new progeny virus when they were infected with wild-type PV1(M) (Table 3). This was highly unexpected, as various similarly produced mouse cell lines expressing human CD155α are a

very good substrate for PV infection (Mendelsohn *et al.,* 1986; Nathanson, 2008). The question arose whether a block in virus uptake or uncoating prevents infection of this cell with PV. To bypass the cell entry and RNA release steps, PV infection was initiated by transfection of a PV(M) RNA transcript into MDCK$^{CD155\alpha}$ and HeLa R19 cells. Using a similar method Holland *et al.* (1959) had shown much earlier, that mouse, rabbit, guinea pig, swine, and chicken cells all supported PV replication upon introducing naked virion RNA. MDCK$^{CD155\alpha}$ however, even after transfection with PV1(M) RNA transcript still failed to produce any virus, while HeLa R19 cells did so very efficiently (Table 3). These results present the first report of any mammalian cell that is completely incapable of replicating, or perhaps capable of completely blocking, poliovirus synthesis. Interestingly, despite the total inability of PV to proliferate, ~95% of the MDCK$^{CD155\alpha}$ cells were killed by infection with PV, which as evidenced by the rounding up, detachment from the dish, and lysis of the infected cells [Fig. 21 (A)(iv)]. Since the cell killing did not occur in parental MDCK cells identically incubated with PV1(M) [Fig. 21 (A)(iii)] or the uninfected parental MDCK cells [Fig. 21 (A)(i)] and MDCK$^{CD155\alpha}$ cells [Fig. 21 (A)(ii)], it can be surmised that a step in the PV1(M) life cycle following virus binding to its receptor, is either the active cause or the passive trigger of cell death. The killing of MDCK$^{CD155\alpha}$ cells was dependent on the dose of PV1(M) [Fig. 21(B)] and the number of killed cells increased with longer incubation of MDCK$^{CD155\alpha}$ cells with PV1(M) [Fig. 21(C)].

Confirmation of the binding of PV to CD155α. In an attempt to understand the restriction of PV1(M) replication in MDCK$^{CD155\alpha}$ cells the binding of PV1(M) was examined. MDCK$^{CD155\alpha}$ cells showed very efficient binding of ^{35}S-labelled PV1(M) when compared to the binding of the same virus to HeLa R19 cells (Table 4). Thus the restriction of PV1(M) replication in MDCK$^{CD155\alpha}$ cells is not in the adsorption of PV1(M) but at a later stage of viral life cycle.

Since PV is not able to grow in MDCK cells, this cell line was no longer considered suitable for the study of the polarized transport of PV. However, I was interested to learn more about the intracellular stage of PV life cycle in MDCK cells at which this restriction is exhibited.

Analyses of the ability of MDCK$^{CD155\alpha}$ cells to support the translation and replication of viral RNA. The failure of the MDCK$^{CD155\alpha}$ cells to support virus production even after the introduction of viral or transcript RNA into these cells indicated that there might be some intracellular block(s) of PV1(M) in MDCK$^{CD155\alpha}$ cells. The steps following the entry of RNA into the cytoplasm is the IRES-mediated translation and replication of PV genome. As I have shown in earlier chapters the picornavirus IRES elements can be extremely sensitive to the assortment of ITAFs in the cell. As such the absence of a crucial ITAF, or the inability to utilize the corresponding dog homolog, may cause a defective viral translation. Therefore, I analyzed the translation and replication activity of the viral RNA in these cells.

A very sensitive assay for detecting RNA translation and replication is monitoring the luciferase signals from the cellular expression of a PV replicon (PV1(M)-luc) RNA that contains the firefly luciferase gene in place of the virus capsid encoding region (Fig. 22A). MDCK$^{CD155\alpha}$ and HeLa R19 (used as a control) cells were transfected with RNA transcript prepared from PV1(M)-luc. To differentiate the luciferase signals due to viral RNA translation from signals from newly replicated RNA the cells were grown in the presence or in the absence of 2mM guanidine hydrochloride (GuHCl). At this concentration, GuHCl completely inhibits viral RNA replication without any toxic effect on cellular processes or viral translation. After introducing the transcript RNA into MDCK$^{CD155\alpha}$ and HeLa R19 cells the luciferase activity was measured at different times post transfection (Fig. 22B). In the presence of GuHCl the luciferase signals were similar at different times post transfection for both MDCK$^{CD155\alpha}$ and HeLa R19 cells (Fig. 22B (i)) whereas in the absence of GuHCl the luciferase signals increased dramatically over time post transfection in HeLa R19 cells but not in MDCK$^{CD155\alpha}$ cells (Fig. 22B(ii)). This result indicates that IRES-dependent translation is functional in MDCK$^{CD155\alpha}$ cells but there is a complete block of viral RNA replication. HeLa R19 cells, on the other hand, supported both the translation and replication of the transfected RNA.

Two other canine cell lines, A72 and Cf2TH were next tested for the activity of PV replicon (PV1(M)-luc) RNA, as described above. The luciferase activity of PV1(M)-luc in different canine cells was compared to that in HeLa R19

cells (Fig. 23). As was observed with MDCK cells, luciferase signals from (PV1(M)-luc) RNA translation in the other two canine cell lines were similar to that in HeLa R19 cells at 10h post transfection in the presence of GuHCl. The luciferase signals increased dramatically at 10h post transfection in HeLa R19 cells but not in the canine cells in the absence of GuHCl. Thus, it appears, though perfectly capable of carrying out IRES mediate translation, PV RNA replication cannot proceed in any of the canine cells tested.

Inhibition of the killing of MDCK$^{CD155\alpha}$ cells by blocking PV RNA replication with guanidine hydrochloride. As shown above, despite the complete absence of viral RNA replication, MDCK$^{CD155\alpha}$ cells are killed in response to PV infection. Throughout the PV-replicon transfection experiments described above, it appeared that the luciferase signal in the presence of GuHCl was slightly higher than in the absence of the drug. Although the difference was small, it seemed to be reproducible across at least (5) experiments. Since GuHCl inhibits the formation of minus-strand RNA synthesis, and therefore the formation of the double-stranded replicative form (dsRF), it is possible that more single stranded viral mRNA is available as template for viral protein translation. This in turn may be an indication that within MCDK cells PV RNA can perhaps complete certain aspects of minus strand RNA synthesis. I hypothesized that the RNA replication process in MDCK cells is interrupted at a stage following the formation of double-stranded replicative form (dsRF). Ultimately the formation of these dsRNA forms may be responsible for triggering an antiviral response in

MDCK cells, which leads to cell death. I explored this aspect of cell killing by using an inhibitor of viral RNA replication, guanidine hydrochloride (GuHCl).

GuHCl (2 mM concentration) inhibits the NTPase action of protein 2C of PV, which ultimately blocks the initiation of minus strand RNA synthesis (Caliguiri *et al.,* 1968; Jackobson *et al.,* 1968; Loddo *et al.,* 1962). MDCK$^{CD155\alpha}$ cells were infected with PV in the presence or in the absence of 2mM GuHCl and the number of viable and non-viable cells at 20h post exposure were quantitated. As presented in Fig. 24, a marked decrease in the number of non-viable cells by PV exposure was observed in the presence of GuHCl. 44% cells were killed in the presence of GuHCl (Fig. 24B) whereas 94.2% cells were killed in the absence of GuHCl (Fig. 24A). This confirms that cell killing is predominantly caused by "cellular choice" rather than a result of viral protein toxicity, since in the presence of GuHCl the viral translation is equal to, if not higher than, that in the absence of GuHCl.

DISCUSSION

Studies using the chimeric virus PV1(RIPO) have already revealed that, PV replication in nonsusceptible tissues might be controlled at stages beyond virus entry (described in Chapter II). It was concluded that a translation defect associated with HRV2 IRES is the major determining factor for restricted growth of PV1(RIPO) in mouse cells and in CD155tg mice. The other stages of PV life cycle beyond cell entry and viral RNA translation, such as replication or assembly, might be important for PV host tropism as well. This possibility has been

generally ignored in the long past because of two main reasons: (i) intracerebral inoculation of viral RNA into rabbits, chicks, guinea pigs, and hamsters resulted in production of infectious virus (Holland *et al.,* 1959), and (ii) although PV was found unable to propagate well in the extraneural tissues *in vivo*, PV could replicate in cells of monolayer cultures that are originated from almost any mammalian tissue (Enders *et al.,* 1949; Dulbecco *et al.,* 1954). By taking the findings into consideration that the IFN response of the cells and tissues controls PV tropism (Ida-Hosonuma *et al.,* 2005), Yoshikawa *et al.,* (2006) tried to explain the situation: why is PV replication *in vivo* restricted to few tissues, though PV is able to grow in almost any tissue of primates *in vitro*? They suggested that, cells from the non-target tissues when grown in culture, acquire the susceptibility to PV infection because of losing rapid interferon response that was functional in the host cell. However, what causes such a rapid and robust immune response in the non-target tissues, has not been addressed yet. In this section of my dissertation, I have presented some evidences which can provide a possible explanation for this little explored aspect of PV tropism.

Here, I have presented a first report of a mammalian cell line grown in culture, named MDCK^{CD155} (a canine cell line expressing the CD155), which is unable to support the propagation of PV (Table 1). As mentioned earlier, it was generally believed that, any CD155 expressing cell line of primate origin can be infected with PV, when the cells are grown in culture (Enders *et al.,* 1949; Dulbecco *et al.,* 1954; Ida-Hosonuma *et al.,* 2005; Yoshikawa *et al.,* 2006). This

realization was extended by Holland *et al.* (1959) to various other mammalian and even chicken cell lines, after they sidestepped the receptor requirement, by delivering into the cells the naked PV RNA. MDCK is a canine kidney epithelial cell line and does not express the PV receptor CD155. Therefore, stable cell lines of MDCK expressing the CD155 were generated. More than 97% cells expressed the CD155 (Fig. 19 and Fig. 20) and expressed receptors bound PV very efficiently (Table 4). Activity of a PV-luc replicon showed that the PV IRES-mediated translation is functional in MDCK cells but the replication is defective.

Most likely explanations for the failure of PV to replicate in $MDCK^{CD155}$ cells is that these cells may be particularly fast or efficient in mounting an antiviral response, therefore actively blocking PV from replicating. Indeed, one study showed that murine fibroblast cells expressing stably canine Mx2 protein had an antiviral activity (Nakamura *et al.,* 2005). Mx (Myxovirus-resistance) protein is one of the type 1 IFN-induced proteins and interferes with replication of various RNA viruses (for a review, see Haller *et al.,* 2007). Type 1 IFNs are induced by viral replication products such as double-stranded (ds) RNA (for a review, see Katze *et al.,* 2002). A question unanswered, as mentioned earlier is: what causes such a rapid and robust immune response during PV infection in the MDCK cells? It is possible that an initiation of PV RNA replication in MDCK results in the formation of replicative form (RF) which is a dsRNA intermediate (Fig. 3 of Chapter I). This ds RF form might triggers a very rapid and robust IFN response, which eventually induces the expression of IFN-stimulated genes, such as Mx

protein in MDCK cells. Finally, the Mx proteins set up an antiviral state in these cells inhibiting further proliferation of PV. Alternatively, a host cell factor required in viral RNA replication may be missing or otherwise be inadequate in MDCK, and perhaps other dog cells. As a result the virus cannot complete the program it initiated, and therefore, is unable to suppress the cell's antiviral response it inadvertently triggered.

An interesting observation which gave this study a new dimension was that despite the lack of replication and the absence of any progeny virus, $MDCK^{CD155\alpha}$ cells exposed to PV die within hours. The mechanism by which PV infected MDCK cells are killed could conceivably fall into any of four separate categories: (i) The cells may be killed by the cytotoxic action of viral proteinases, foremost the two viral proteinases $2A^{pro}$ and $3C^{pro}$ (Buenz *et al.,* 2006). (ii) A crucial *trans*-acting host factor may be missing in MDCK cells preventing the replication of PV (a passive block). As a result not enough PV proteins can be synthesized to unfold the virus' antiapoptotic program therefore permitting the cell to clear the virus infection via apoptosis. (iii) Although all host cell requirements may be met for PV replication, MDCK may be particularly fast or efficient in mounting an antiviral response, therefore actively blocking PV from replicating and proceeding with the apoptotic program, before a productive infection of PV can take hold of the cell. (iv) Binding of the virus to the receptor alone may trigger a signal that leads to the killing of the cells (apoptosis). In this scenario, neither

virus uptake nor viral protein translation would be required for the killing to take place.

An important question is whether studying PV tropism in CD155tg mice is comparable to the tropism of the virus in primates. In primates, the situation might be completely different than in the CD155tg mice as is observed in my study. It is possible that the basis of PV tropism in non-human primates and in humans differs from that in CD155tg mice and is determined by factors yet to be discovered. Unfolding this complex area of PV tropism in non-human primates will undoubtedly enable us to better understand the PV pathogenesis in humans.

In the future, it will be interesting to investigate whether this cell line shows rapid IFN response, which will emphasize the role of IFN response as an important post-entry and post-translational determinant of PV tissue and host tropism. As of today, the neurotropism i.e., restricted growth of PV is not conserved in cultured cells. Almost any mammalian tissue was shown to be susceptible to PV replication after they were cultivated *in vitro*. Therefore, the resistance of MDCK cell line to PV replication should be considered as an important *in vitro* tool to use as a model system, which will allow investigation of PV pathogenesis in extraneural tissues that behaves exactly the same way as cells *in vivo*.

Figure 19. Expression of CD155α molecules in transfected MDCK cells. Expression of CD155α in parental MDCK cells [(A) and (c)] and a stable cell line of MDCK$^{CD155\alpha}$ cells [(B) and (D) MDCK$^{CD155\alpha}$ was monitored by immunostaining as described in Materials and Methods section. IF: Immunofluorescence view and PC: Phase-Contrast view.

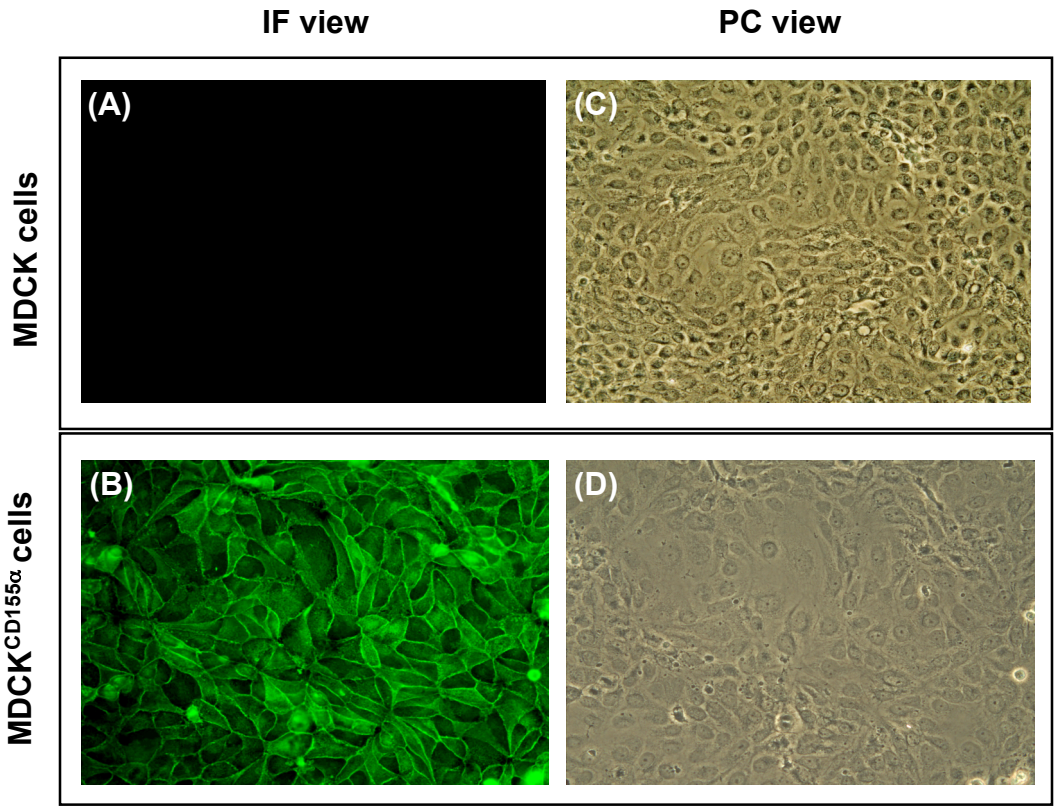
IF view
PC view
MDCK cells
MDCK$^{CD155\alpha}$ cells
(A)
(C)
(B)
(D)

Figure 20. FACS analysis of the expression levels of CD155α on the cell surface of MDCK$^{CD155\alpha}$ cells. (A) Distribution of the cells according to size (FSC-H) and cellular granularity (SSC-H). (B) A histogram that represents the number of cells at each fluorescence level. Location of gated groups is marked by their group number (M1 and M2).

(A)

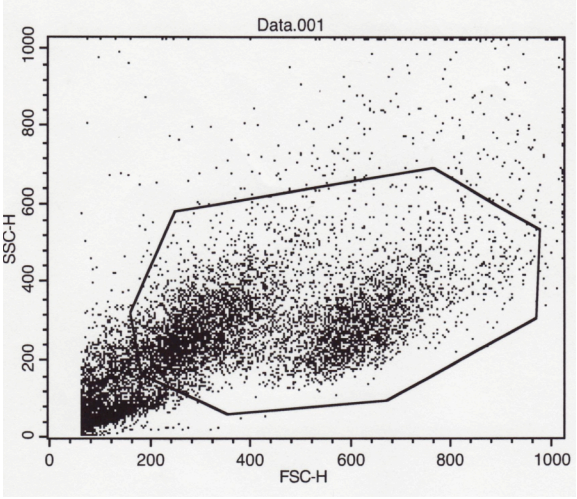
Data.001
SSC-H
FSC-H
0
200
400
600
800
1000

(B)

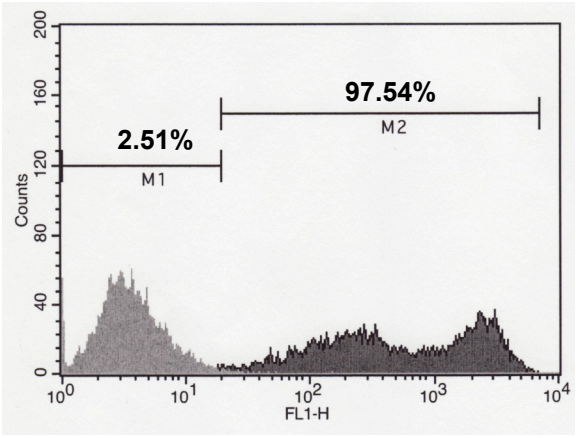
97.54%
M2
2.51%
M1
Counts
FL1-H
0
40
80
120
160
200
10^0
10^1
10^2
10^3
10^4

Table 3. Virus yield from the infection and transfection of HeLa R19, MDCK, and MDCK$^{CD155\alpha}$ cell lines with wild-type PV1(M) and PV1(M) RNA transcript

Cell lines	Infection with PV1(M) virus		Transfection with PV1(M) RNA transcript 24 h.p.t.
	0 h.p.i.	24 h.p.i.	
HeLa R19	$7.2X10^4$	$12X10^8$	$4X10^8$
MDCK	$8.8X10^4$	$2.8X10^4$	None detected
MDCK$^{CD155\alpha}$	$7.2X10^4$	$4X10^3$	None detected

h.p.i., hour post infection; h.p.t., hour post transfection

Figure 21. Killing of the MDCK$^{CD155\alpha}$ cells by infection with poliovirus. (A) Microscopic view of the MDCK and MDCK$^{CD155\alpha}$ cells infected with PV1(M). MDCK$^{CD155\alpha}$ cells were killed by infection with PV1)M), which as evidenced by the rounding up, detachment from the dish, and lysis of the infected cells [(iv)]. The cell killing did not occur in parental MDCK cells identically incubated with poliovirus [(iii)] or the uninfected parental MDCK cells [(i)] and MDCK$^{CD155\alpha}$ cells [(ii)]. (B) Dose-dependent killing of MDCK$^{CD155\alpha}$ cells by PV1(M). (C) Time course of killing of MDCK$^{CD155\alpha}$ cells by PV1(M).

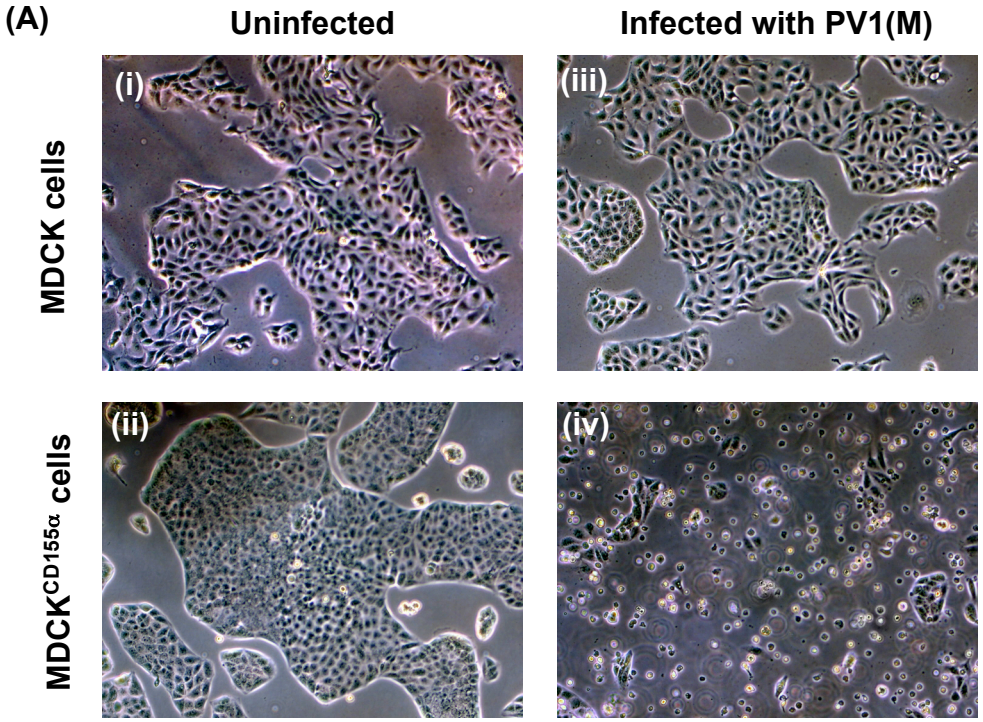
(A)
Uninfected
Infected with PV1(M)
MDCK cells
MDCK$^{CD155\alpha}$ cells
(i)
(ii)
(iii)
(iv)

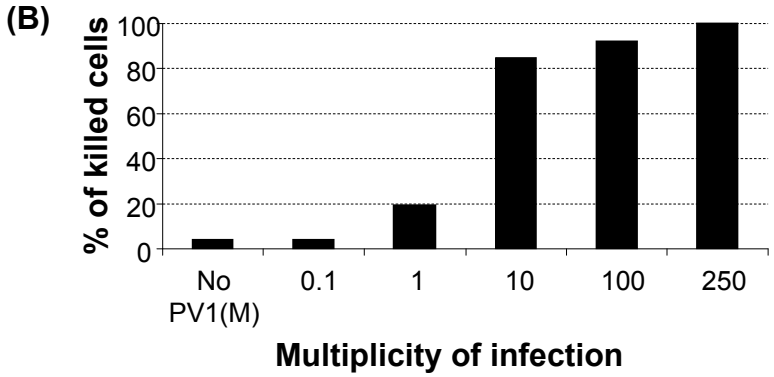
(B)
% of killed cells
100
80
60
40
20
0
No PV1(M)
0.1
1
10
100
250
Multiplicity of infection

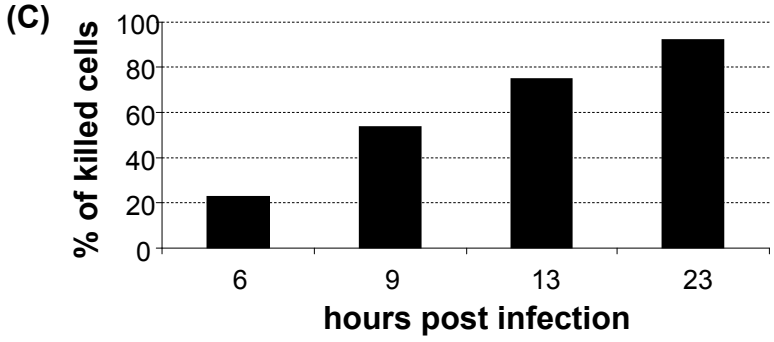
(C)
% of killed cells
100
80
60
40
20
0
6
9
13
23
hours post infection

Table 4. Binding of ^{35}S-labelled PV1(M) to different cell lines

Cell lines used	HeLa R19	MDCK	MDCK$^{CD155\alpha}$	Mock
% of binding	100	0.85	504	0.41

Figure 22. RNA translation and replication of PV1(M)-luc replicon in MDCK and HeLa R19 cells. (A) Schematic diagram of PV1(M)-luc replicon that contains Fire-fly luciferase (F-luc) gene in place of the virus capsid encoding region. (B) Cells grown in the presence (i) or in the absence (ii) of 2mM guanidine hydrochloride (GuHCl) were transfected with PV1(M)-luc RNA transcript and the luciferase signals were measured. RLU, Relative Light Unit.

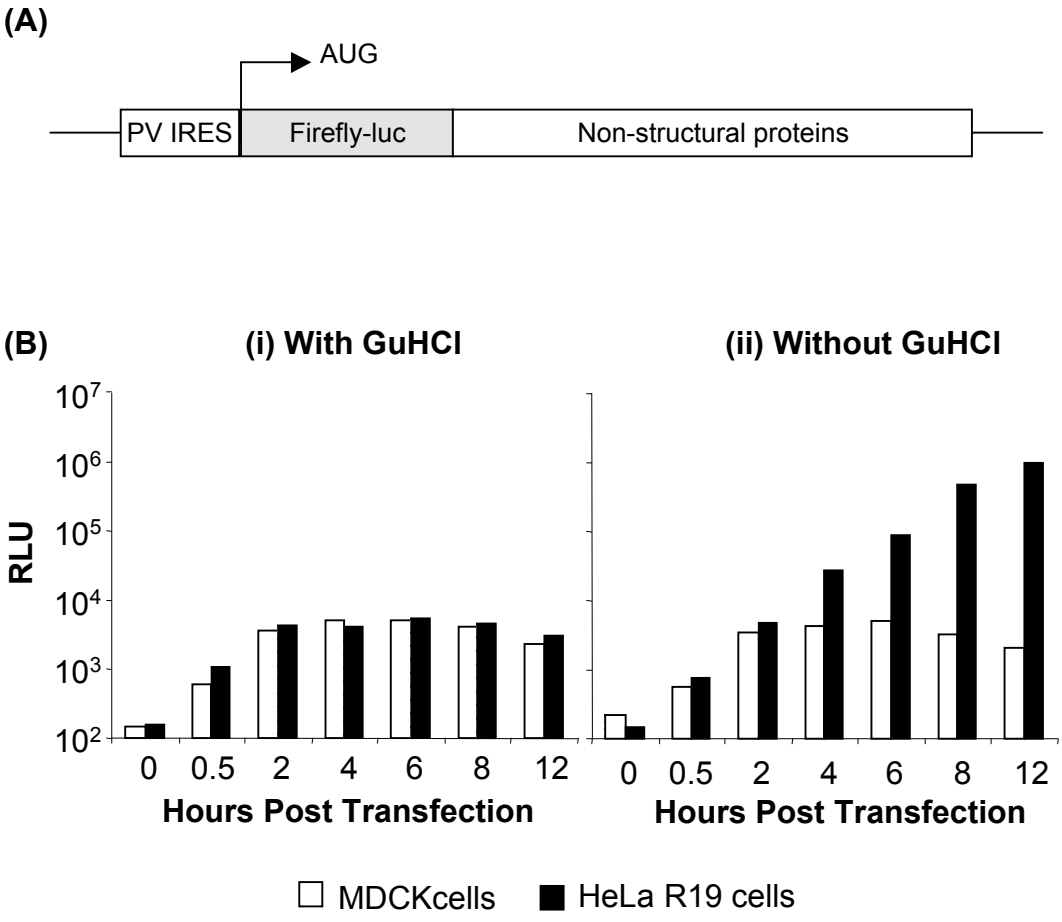
(A)
AUG
PV IRES
Firefly-luc
Non-structural proteins
(B)
(i) With GuHCl
(ii) Without GuHCl
RLU
10^7
10^6
10^5
10^4
10^3
10^2
0 0.5 2 4 6 8 12
Hours Post Transfection
0 0.5 2 4 6 8 12
Hours Post Transfection
MDCKcells
HeLa R19 cells

Figure 23. RNA translation and replication of PV1(M)-luc replicon in different canine cells and HeLa R19 cells. Cells grown in the presence or in the absence of 2mM guanidine hydrochloride (GuHCl) were transfected with PV1(M)-luc RNA transcript and the luciferase signals were measured 10 hour post transfection. RLU, Relative Light Unit; w/o, without.

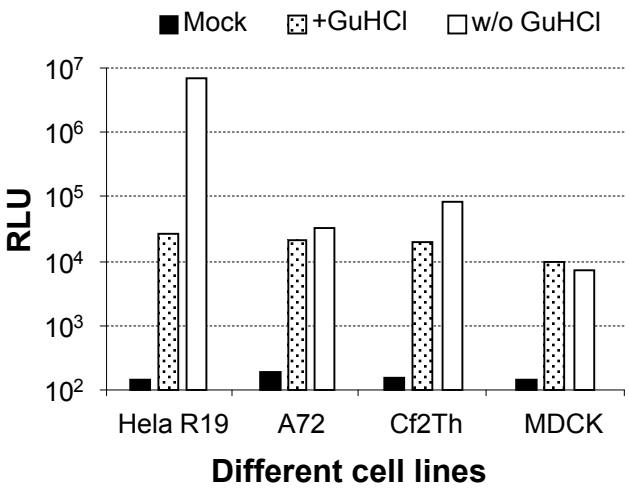
Mock
+GuHCl
w/o GuHCl
RLU
10^7
10^6
10^5
10^4
10^3
10^2
Hela R19
A72
Cf2Th
MDCK
Different cell lines

Figure 24. Inhibition of the PV1(M) induced death of the MDCK$^{CD155\alpha}$ cells by Guanidine hydrochloride. (A) MDCK$^{CD155\alpha}$ cells were infected with PV1(M) in the absence of 2mM GuHCl. (i) total cells (viable and non-viable) and (ii) viable cells were quantitated at 20h post exposure as described in Materials and Methods and (iii) the number of viable cells and that of non-viable cells were plotted. (B) MDCK$^{CD155\alpha}$ cells were infected with PV1(M) in the presence of 2mM GuHCl. (i) total cells (viable and non-viable) and (ii) viable cells were quantitated at 20h post exposure as described in Materials and Methods and (iii) the number of viable cells and that of non-viable cells were plotted.

(A) Without GuHCl

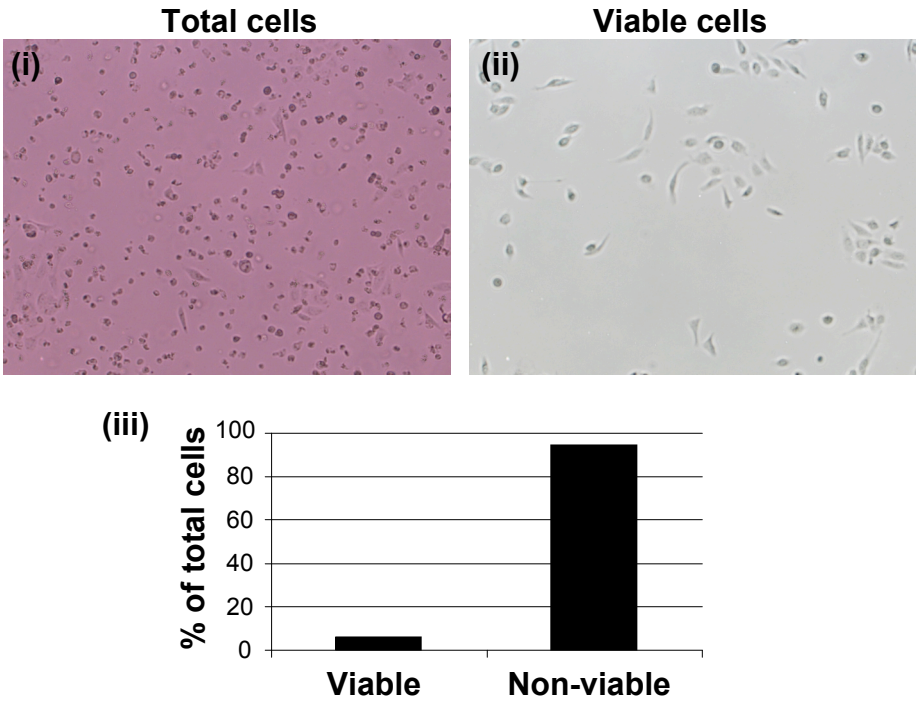

(B) With GuHCl

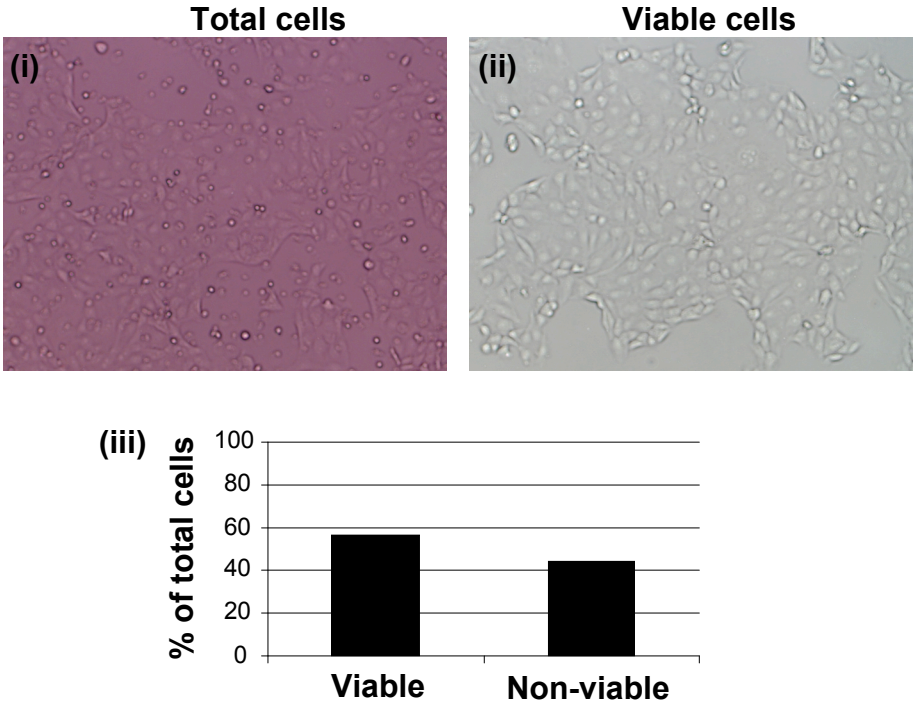

Chapter V. Discussion and Conclusion

IRES and IRES *trans*-activating factors as important determinants of PV1(RIPO) tissue and host tropism.

In chapters II and III of this dissertation, I have presented the results of my experiments designed to identify the role of the IRES and of cellular factors interacting with the IRES in PV tissue tropism and host restriction.

Varying degrees of attenuation of PV1(RIPO), a chimeric virus that contains HRV2 IRES in the PV background, were observed when the growth of this virus was compared with that of wt PV in human cells of neuronal origin and mouse cells. The extent of attenuation co-varied with the temperature sensitive (*ts*) phenotype of PV1(RIPO) in these cells. Previously PV1(RIPO) was shown to be highly attenuated in CD155tg mice and in non-human primates, which correlated with a *ts* growth defect of the virus in human neuronal cells (Gromeier *et al.,* 1996; Gromeier *et al.,* 1999; Campbell *et al.,* 2005; Cello *et al.,* 2008). However, it was not clear that a mouse cell associated growth restriction of PV1(RIPO) contributed to the inability of this virus to cause disease in CD155tg mice. Here I have shown that PV1(RIPO) has a severe propagation defect in different mouse cell lines at physiological temperature or above.

My work demonstrated that changes in the 5'NTR alone, particularly the mutations in the HRV2 IRES, are sufficient to rescue HRV2 IRES-mediated translation in mouse cells and, consequently, RNA replication in mouse L cells. Most importantly, these mutations were not only able to rescue the defective

growth of PV1(RIPO) in mouse cells but also to produce a highly neurovirulent virus in CD155tg mice.

By over-expressing some ITAFs in human cells and expressing one of them (hPTB1) in mouse cells I have shown that the tissue tropism of PV1(RIPO) can be changed or modified. More specifically, when supplied with an excess of ITAFs, the growth of PV1(RIPO) was stimulated in a human neuronal cell line (SK-N-MC) and the growth defect of PV1(RIPO) was rescued in a mouse cell line (L20B). In contrast, ITAFs expression in these cells did not affect the growth of wt PV and that of R-1235, a mouse cell-adapted PV(RIPO). More strikingly, in the absence of hPTB1 in mouse L20B cells wt PV grew as well as they grew in the other human cells examined. I suggest that wt PV and R-1235 either depend on the mPTB or do not need any PTB at all for their growth in mouse L20B cells. In the future, it would be interesting to test the binding affinities of mPTB and hPTB1 for the IRESes of wt PV, PV1(RIPO) and R-1235.

Molecular basis of PV1(RIPO) temperature sensitivity and attenuation.

The correlation between the *ts* nature of the Sabin strains and their attenuation is a matter of debate (Omata *et al.,* 1986; Tardy-Panit *et al.,* 1993; Bouchard *et al.,* 1995). Conflicting results were observed from the studies establishing a link between neuroattenuation and *ts* phenotype. Taking these earlier observations into consideration, the observed *ts* phenotype of PV1(RIPO) in mouse cells may correlate with its attenuation in CD155tg mice.

Attenuation of PV1(RIPO) in mouse cells resulted from a defect in HRV2 IRES-mediated translation defect. This process is the probable reason for temperature sensitivity. At the restricted temperature either the IRES is in a different conformation, unable to interact with mouse cell factors, or the mouse factors are non-functional. However a highly neurovirulent variant of PV1(RIPO), named R-1235, was obtained by serial passages of PV1(RIPO) in mouse L20B cells under the restrictive temperature (37^{o}C). The result obtained with the R-1235 virus supports the first possibility. This virus with its altered IRES conformation, due to the adapted mutations, presumably correctly interacts with the mouse factors. In this case the restrictive temperature (37^{o}C) is suitable for the mouse factors function.

Interestingly, all the variants isolated after serial passages and after reconstruction into cDNA, resulted in viruses that retained their *ts* phenotype at 39.5^{o}C. This phenotype is similar to the *ts* phenotype of PV1(RIPO) in SK-N-MC cells. Therefore, in the future it will be interesting to obtain adapted mutants of R-1235, which can grow better at or above 39.5^{o}C. Isolation of such variants will be helpful for the understanding of the *ts* phenotype and its relationship to virus neurovirulence.

Post-IRES step: an important determinant of PV tissue-host tropism.

In chapter IV of this dissertation I described the results of experiments that were carried out in an attempt to identify the determinants of defective replication of PV in a canine epithelial cell line, MDCK (Madin-Darby Canine Kidney) cells.

Cells in culture are believed to acquire susceptibility to PV infection during the process of cultivation (Ida-Hosonuma *et al.,* 2005; Yoshikawa *et al.,* 2006). Here I have presented a canine cell line expressing CD155, as an example of a cell line of mammalian origin grown in culture that shows resistance to PV replication. Moreover, soon after exposure to PV the cells started to die. Smura *et al.,* (2007) reported a similar observation in MDCK cells with a different virus, namely Enterovirus 94, from the Enterovirus family. This phenomenon could be explained in two different ways. Firstly, it is possible that viral proteins, expressed solely by translation of in the incoming viral RNA, are sufficient to kill the cell. Indeed, at sufficiently high multiplicity of infection (MOI), PV-infected cells get killed in the presence of GuHCl, and thus in the absence of RNA replication. This is thought to be a consequence of the cytotoxic effects of the viral proteinase $2A^{pro}$. Secondly, a very fast host cell innate immune response against the foreign invader may be responsible for blocking viral replication and for initiating an apoptotic pathway.

It is of great interest to identify the intracellular stage of the PV life cycle in MDCK cells at which this restriction occurs. This will help out understanding of PV tissue tropism and host restriction and overall PV pathogenesis in non-human primates. In the future, experiments can be done to explore the role of an innate immune response in the killing of $MDCK^{CD155\alpha}$ cells following exposure to PV. Recent evidence indicates that the IFNα/β system plays an important role in the susceptibility of cells to PV infection and it is an important determinant of PV

tissue tropism and host restriction (Ida-Hosonuma *et al.,* 2005; Yoshikawa *et al.,* 2006). A type I IFN response in MDCK$^{CD155\alpha}$ cells may contribute to the killing of these cells to protect the spread of the virus in other cells. Many of the IFN stimulated genes have a role in killing virally infected cells through apoptosis. Therefore future studies may also include experiments to determine whether or not apoptosis is the mechanism by which these cells die since PV has been shown to induce apoptosis in a variety of cells (Agol *et al.,* 1998; Ammendolia *et al.,* 1999; Lopez-Guerrero *et al.,* 2000; Couderc *et al.,* 2002).

Conclusions and Prospects.

It is not clear whether PV1(RIPO) is generally attenuated in human neuronal cell lines because it is defective in some neural-specific function, or is simply reduced in its overall efficiency of replication. However, the susceptibility of mouse L20B cells and the CD155tg mice to mouse cell-adapted PV1(RIPO) infection clearly demonstrates that the IRES, not CD155, is the determinant of PV host range in mouse cells. Therefore, the use of CD155tg mice to judge the neuropathogenicity of chimeric viruses in the PV background may be misleading. The results presented here also establish that the different replication capacity of PV1(RIPO) in different human and mouse cells may be due to differences in host factors, in quality or in quantity.

Surprisingly, PV replication was not detected in CD155-expressing MDCK cells, a cell line of mammalian origin, although the PV IRES-directed translation of PV RNA was fully functional in these cells. PV tissue tropism, therefore, is not

governed solely by the expression of CD155 or the PV IRES-mediated translation of viral RNA. The observed PV host range restriction (species tropism) is most likely to be determined at a post-translational level. Therefore, an important question, which needs to be addressed, is whether studying PV tropism in PVR transgenic mice provides information on tropism of the virus in primates. Identifying the internal block(s) to PV infection in nonsusceptible tissues will certainly advance an interesting area of PV research, which is the role of tissue-host tropism in PV pathogenesis.

References

Agol, V. I., S. G. Drozdov, T. A. Ivannikova, M. S. Kolesnikova, M. B. Korolev, and E. A. Tolskaya. 1989. Restricted growth of attenuated poliovirus strains in cultured cells of a human neuroblastoma. J. Virol. **63(9):**4034-4038.

Agol, V. I., G. A. Belov, K. Bienz, D. Egger, M. S. Kolesnikova, N. T. Raikhlin, L. I. Romanova, E. A. Smirnova, and E. A. Tolskaya. 1998. Two types of death of poliovirus-infected cells: caspase involvement in the apoptosis but not cytopathic effect. Virology **252(2):**343-353.

Alexander, L., H. H. Lu, and E. Wimmer. 1994. Polioviruses containing picornavirus type 1 and/or type 2 IRES elements: genetic hybrids and the expression of a foreign gene. Proc. Natl. Acad. Sci. USA **91:**1406-1410.

Anderson, E. C., S. L. Hunt, and R. J. Jackson. 2007. Internal initiation of translation from the human rhinovirus-2 internal ribosome entry site requires the binding of Unr to two distinct sites on the 5' qauntranslated region. J. Gen. Virol. **88(Pt 11):**3043-3052.

Andino, R., G. E. Rieckhof, and D. Baltimore. 1990. A functional ribonucleoprotein complex forms around the 5' end of poliovirus RNA. Cell **63(2):**369-380.

Ammendolia, M. G., A. Tinari, A. Calcabrini, and F. Superti. 1999. Poliovirus infection induces apoptosis in CaCo-2 cells. J. Med. Virol. **59(1):**122-129.

Armstrong, C. 1939. The experimental transmission of poliomyelitis to the eastern cotton rat, *Sigmodon hispidus hispidus*. Public Health Rep. **54:**1719-1721.

Back, S. H., Y. K. Kim, W. J. Kim, S. Cho, H. R. Oh, J. E. Kim, and S. K. Jang. 2002. Translation of polioviral mRNA is inhibited by cleavage of polypyrimidine tract-binding proteins executed by polioviral 3C(pro). J. Virol. **76(5):**2529-2542.

Bailly, J. L., A. M. Borman, H. Peigue-Lafeuille, and K. M. Kean . 1996. Natural isolates of ECHO virus type 25 with extensive variations in IRES sequences and different translational efficiencies. Virology **215(1):**83-96.

Barman, S., L. Adhikary, Y. Kawaoka, and D. P. Nayak. 2003. Influenza A virus hemagglutinin containing basolateral localization signal does not alter the apical budding of a recombinant influenza A virus in polarized MDCK cells. Virology **305:**138-152.

Baury, B., D. Masson, B. M. McDermott, Jr. A. Jarry, H. M. Blottiere, P. Blanchardie, C. L. Laboisse, P. Lustenberger, V. R. Racaniello, and M. G. Denis. 2003. Identification of secreted CD155 isoforms. Biochem. Biophys. Res. Commun. **309:**175-182.

Belsham, G. J., N. Sonenberg, and Y. V. Svitkin. 1995. The role of the La autoantigen in internal initiation. Curr. Top. Microbiol. Immunol. **203:**85-98.

Bernhardt, G., J. A. Bibb, J. Bradley, and E. Wimmer. 1994. Molecular characterization of the cellular receptor for poliovirus. Virology **199:**105-113.

Bibb, J. A., G. Bernhardt, and E. Wimmer. 1994a. Cleavage site of the signal sequence of the poliovirus receptor. J. Gen. Virol. **75:**1875-1881.

Bibb, J. A., G. Witherell, G. Bernhardt, and E. Wimmer. 1994b. Interaction of poliovirus with its cell surface binding site. Virology **201(1):**107-115.

Blyn, L. B., K. M. Swiderek, O. Richards, D. C. Stahl, B. L. Semler, and E. Ehrenfeld. 1996. Poly(rC) binding protein 2 binds to stem-loop IV of the poliovirus RNA 5' noncoding region: identification by automated liquid chromatography-tandem mass spectrometry. Proc. Natl. Acad. Sci. USA **93(20):**11115-20.

Blyn, L. B., J. S. Towner, B. L. Semler, and E. Ehrenfeld. 1997. Requirement of poly(rC) binding protein 2 for translation of poliovirus RNA. J. Virol. **71(23):**6243-6246.

Blank, C. A., D. A. Anderson, M. Beard, and S. M. Lemon. 2000. Infection of polarized cultures of human intestinal epithelial cells with hepatitis A virus: vectorial release of progeny virions through apical cellular membranes. J. Virol. **74:**6476-6484.

Bodian, D. 1955. Emerging concept of poliomyelitis infection. Science **122:**105-108.

Borman, A., and R. J. Jackson. 1992. Initiation of translation of human rhinovirus RNA: mapping the internal ribosome entry site. Virology **188(2):**685-696.

Borman, A., M. T. Howell, J. G. Patton, and R. J. Jackson. 1993. The involvement of a spliceosome component in internal initiation of human rhinovirus RNA translation. J. Gen. Virol. **74(Pt 9):**1775-1788.

Bouchard, M. J. , D. H. Lam, and V. R. Racaniello. 1995. Determinants of attenuation and temperature sensitivity in the type 1 poliovirus Sabin vaccine. J. Virol. **69(8):**4972-4978.

Boussadia, O., M. Niepmann, L. Créancier, A.C. Prats, F. Dautry, and H. Jacquemin-Sablon. 2003. Unr is required in vivo for efficient initiation of translation from the internal ribosome entry sites of both rhinovirus and poliovirus. J. Virol. **77(6):**3353-3359.

Brandenburg, B., L. Y. Lee, M. Lakadamyali, M. J. Rust, X. Zhuang, J. M. Hogle. 2007. Imaging poliovirus entry in live cells. PLoS Biol. **5(7):**1543-1555.

Brown, B. A., and E. Ehrenfeld. 1979. Translation of poliovirus RNA in vitro: changes in cleavage pattern and initiation sites by ribosomal salt wash. Virology **97(2):**396-405.

Buenz, E. J., and C. L. Howe. 2006. Picornaviruses and cell death. Trends. Microbiol. **14(1):**28-36.

Caliguiri, L. A., and I. Tamm. 1968. Action of guanidine on the replication of poliovirus RNA. Virology **35(3):**408-417.

Campbell, S. A., J. Lin, E. Y. Dobrikova, and M. Gromeier. 2005. Genetic determinants of cell type-specific poliovirus propagation in HEK 293 cells. J. Virol. **79(10):**6281-6290.

Cello, J., A. Paul, and E. Wimmer. 2002. Chemical synthesis of poliovirus cDNA: generation of infectious virus in the absence of natural template. Science **297:**1016-1018.

Cello, J., H. Toyoda, N. De Jesus, E. Y. Dobrikova, M. Gromeier, and E. Wimmer. 2008. Growth phenotypes and biosafety profiles in poliovirus-receptor transgenic mice of recombinant oncolytic polio/human rhinoviruses. J. Med. Virol. **80:**352-359.

Chang, T., A. Yamashita, C. A. Chen, Y. Yamashita, W. Zhu, S. Durdan, A. Kahvejian, N. Sonenberg and A. Shyu. 2004. UNR, a new partner of poly(A)-binding protein, plays a key role in translationally coupled mRNA turnover mediated by the c- fos major coding-region determinant. Genes & Dev. **18:** 2010-2023.

Chard, L.S., Y. Kaku, B. Jones, A. Nayak, and G. J. Belsham. 2006. Functional analyses of RNA structures shared between the internal ribosome

entry sites of hepatitis C virus and the picornavirus porcine teschovirus 1 Talfan. J. Virol. **80:**1271-1279.

Christodoulou, C., F. Colbere-Garapin, A. Macadam, L. F. Taffs, S. Marsden, P. Minor, and F. Horaud. 1990. Mapping of mutations associated with neurovirulence in monkeys infected with Sabin 1 poliovirus revertants selected at high temperature. J. Virol. **64(10):**4922-4929.

Chumakov, K., E. Dragunsky, A. Ivshina, J. Enterline, V. Wells, T. Nomura, M. Gromeier, and E. Wimmer. 2001. Inactivated vaccines based on alternatives to wild-type seed virus. Dev. Biol. (Basel) **105:**171-177.

Coleman J. R, D. Papamichail, S. Skiena, B. Futcher, E. Wimmer, and S. Mueller. 2008. Virus attenuation by genome-scale changes in codon pair bias. Science **320(5884):**1784-1787.

Couderc, T., F. Guivel-Benhassine, V. Calaora, A. S. Gosselin, and B. Blondel. 2002. An ex vivo murine model to study poliovirus-induced apoptosis in nerve cells. J. Gen. Virol. **83(Pt 8):**1925-1930.

Craig, A. W., Y. V. Svitkin, H. S. Lee, G. J. Belsham, and N. Sonenberg. 1997. The La autoantigen contains a dimerization domain that is essential for enhancing translation. Mol. Cell Biol. **17(1):**163-169.

De Jesus, N., D. Franco, A. Paul, E. Wimmer, J. Cello. 2005. Mutation of a single conserved nucleotide between the cloverleaf and internal ribosome entry site attenuates poliovirus neurovirulence. J. Virol. **79(22):**14235-14243.

Dobrikova, E., P. Florez, S. Bradrick, and M. Gromeier. 2003. Activity of a type 1 picornavirus internal ribosomal entry site is determined by sequences within the 3' nontranslated region. Proc. Natl. Acad. Sci. USA **100(25):**15125-15130.

Dorner, A. J., B. L. Semler, R. J. Jackson, R. Hanecak, E. Duprey, and E. Wimmer. 1984. In vitro translation of poliovirus RNA: utilization of internal initiation sites in reticulocyte lysate. J. Virol. **50(2):**507-514.

Dulbecco, R., and M. Vogt. 1954. Plaque formation and isolation of pure lines with poliomyelitis viruses. J. Exp. Med. **99:**167-182.

Ehrenfeld, E., and N. L. Teterina. 2002. Initiation of translation of picornavirus RNAs: structure and function of the internal ribosome entry site. In: B. L. Semler and E. Wimmer (Eds), Molecular Biology of Picornaviruses, ASM Press, Washington DC, pp. 159-169.

Enders, J. F., T. H. Weller, and F. C. Robbins. 1949. Cultivation of the Lansing strain of poliomyelitis virus in culture of various human embryonic tissues. Science **109:**85-87.

Evans, D. M., G. Dunn, P. D. Minor, G. C. Schild, A. J. Cann, G. Stanway, J. W. Almond, K. Currey, and J. V. Jr. Maizel. 1985. Increased neurovirulence associated with a single nucleotide change in a noncoding region of the Sabin type 3 poliovaccine genome. Nature **314(6011):**548-550.

Fernández-Miragall, O., S. L. de Quinto, and E. Martínez-Salas. 2009. Relevance of RNA structure for the activity of picornavirus IRES elements. Virus Research **139(2):**172-182.

Fitzgerald, K. D., and B. L. Semler. 2009. Bridging IRES elements in mRNAs to the eukaryotic translation apparatus. Biochim Biophys Acta. Article in press.

Flanegan, J. B., R. F. Petterson, V. Ambros, N. J. Hewlett, and D. Baltimore. 1977. Covalent linkage of a protein to a defined nucleotide sequence at the 5'-terminus of virion and replicative intermediate RNAs of poliovirus. Proc. Natl. Acad. Sci. USA **74(3):**961-965.

Freistadt, M. S., G. Kaplan, and V. R. Racaniello. 1990. Heterogeneous expression of poliovirus receptor-related proteins in human cells and tissues. Mol. Cell. Biol. **10(11):**5700-5706.

Freistadt, M. S., and K. E. Eberle. 1997. CD155 (poliovirus receptor). Worshop Panel Report.VI. International Worshop and Conference on Human Leukocyte Differentiation Antigens. Garland, Cambridge, pp. 1075-1077.

Garcia-Sastre, A., and C. A. Biron. 2006. Type 1 interferons and the virus-host relationship: a lesson in détente. Science **312(5775):**879-882.

Gamarnik, A.V., and R. Andino. 1997. Two functional complexes formed by KH domain containing proteins with the 5' noncoding region of poliovirus RNA. RNA. 3(8):882-892.

Gmyl, A. P., E. V. Pilipenko, S. V. Maslova, G. A. Belov, and V.I. Agol. 1993. Functional and genetic plasticities of the poliovirus genome: quasi-infectious RNAs modified in the 5'-untranslated region yield a variety of pseudorevertants. J. Virol. **67:**6309-6316.

Gosert, R., K. H. Chang, R. Rijnbrand, M. Yi, D. V. Sangar, and S. M. Lemon. 2000. Transient Expression of Cellular Polypyrimidine-Tract Binding Protein

Stimulates Cap-Independent Translation Directed by Both Picornaviral and Flaviviral Internal Ribosome Entry Sites In Vivo. Mol. Cell. Biol. **20(5):**1583-1595.

Gromeier, M., H. H. Lu, and E. Wimmer. 1995. Mouse neuropathogenic poliovirus strains cause damage in the central nervous system distinct from poliomyelitis. Microb. Pathog. **18:**253-67.

Gromeier, M., L. Alexander, and E. Wimmer. 1996. Internal ribosomal entry site substitution eliminates neurovirulence in intergeneric poliovirus recombinants. Proc. Natl. Acad. Sci. USA **93:**2370–2375.

Gromeier, M., S. Mueller, D. Solecki, B. Bossert, G. Bernhardt, and E. Wimmer. 1997. Determinants of poliovirus neurovirulence. J. Neurovirol. **3(Suppl 1):**S35-S38.

Gromeier, M., B. Bossert, M. Arita, A. Nomoto, and E. Wimmer. 1999. Dual stem loops within the poliovirus internal ribosomal entry site control neurovirulence. J. Virol. **73(2):**958-964.

Gromeier, M., S. Lachmann, M. R. Rosenfeld, P. H. Gutin, and E. Wimmer. 2000. Intergeneric poliovirus recombinants for the treatment of malignant glioma, Proc. Natl. Acad. Sci. USA **97:**6803-6808.

Gromeier, M., and A. Nomoto. 2002. Determinants of poliovirus pathogenesis. In: Semler BL, Wimmer E, (eds). Molecular Biology of Picornaviruses, ASM Press, Washington DC, pp. 367–379.

Grossman, J. S., M. I. Meyer , Y. C. Wang , G. J. Mulligan, R. Kobayashi, and D. M. Helfman. 1998. The use of antibodies to the polypyrimidine tract binding protein (PTB) to analyze the protein components that assemble on alternatively spliced pre-mRNAs that use distant branch points. RNA **4(6):**613-625.

Guest, S., E. Pilipenko, K. Sharma, K. Chumakov, and R. P. Roos. 2004. Molecular mechanisms of attenuation of the Sabin strain of poliovirus type 3. J. Virol. **78(20):**11097-11107.

Haller, A. A., S. R. Stewart, and B. L. Semler. 1996. Attenuation stem-loop lesions in the 5' noncoding region of poliovirus RNA: neuronal cell-specific translation defects. J. Virol. **70(3):**467-474.

Haller, O., G. Kochs, and F. Weber. 2007. Interferon, Mx, and viral countermeasures. Cytokine Growth Factor Rev. **18(5-6):**425-433.

Harris, J. R., and V. R. Racaniello. 2003. Changes in rhinovirus protein 2C allow efficient replication in mouse cells. J. Virol. **77(8):**4773-4780.

Harris J. R., and V. R. Racaniello. 2005. Amino acid changes in proteins 2B and 3A mediate rhinovirus type 39 growth in mouse cells. J. Virol. **79(9):**5363-5373.

Hellen, C. U., G. W. Witherell, M. Schmid, S. H. Shin, T. V. Pestova, A. Gil, and E. Wimmer. 1993. A cytoplasmic 57-kDa protein that is required for translation of picornavirus RNA by internal ribosomal entry is identical to the nuclear pyrimidine tract-binding protein. Proc. Natl. Acad. Sci. USA **90(16):**7642-7646.

Hellen, C. U., T. V. Pestova, M. Litterst, and E. Wimmer. 1994. The cellular polypeptide p57 (pyrimidine tract-binding protein) binds to multiple sites in the poliovirus 5' nontranslated region. J. Virol. **68(2):**941-950.

Hogle, J. M., R. Syed, C. E. Fricks, J. P. Icenogle, O. flore, and D. J. Filman. 1990. Role of conformational transitions in poliovirus assembly and cell entry. *In* New aspects of positive strand RNA viruses, (M.A. Brinton and F.X. Heinz, ed), American Society for Microbiology, Washington D.C.

Hogle, J. M. 2002. Poliovirus cell entry: common structural themes in viral cell entry pathways. Annu. Rev. Microbiol. **56:**677-702.

Hunt, S. L., and R. J. Jackson. 1999a. Polypyrimidine-tract binding protein (PTB) is necessary, but not sufficient, for efficient internal initiation of translation of human rhinovirus-2 RNA. RNA **5(3):**344-359.

Hunt, S. L., J. J. Hsuan, N. Totty, and R. J. Jackson. 1999b. unr, a cellular cytoplasmic RNA-binding protein with five cold-shock domains, is required for internal initiation of translation of human rhinovirus RNA. Genes Dev. **13(4):**437-448.

Holland, J. J., L. C. McLaren, and J. T. Syverton. 1959. The mammalian cell-virus relationship. IV. Infection of naturally insusceptible cells with enterovirus ribonucleic acid. J. Exp. Med. **110:**65-80.

Ida-Hosonuma, M., T. Iwasaki, T. Yoshikawa, N. Nagata, Y. Sato, T. Sata, M. Yoneyama, T. Fujita, C. Taya, H. Yonekawa, and S. Koike. 2005. The alpha/beta interferon response controls tissue tropism and pathogenicity of poliovirus. J. Virol. **79:**4460-4469.

Iwasaki, A., R. Welker, S. Mueller, M. Linehan, A. Nomoto, and E. Wimmer. 2002. Immunofluorescence analysis of poliovirus receptor expression in Peyer's patches of humans, primates, and CD155 transgenic mice: implications for poliovirus infection. J. Infect. Dis. **186(5):**585-592.

Jacobson, M. F., and D. Baltimore. 1968. Morphogenesis of poliovirus. I. Association of the viral RNA with coat protein. J. Mol. Biol. **33(2)**:369-378.

Jang, S. K., H. G. Kräusslich, M. J. Nicklin, G. M. Duke, A. C. Palmenberg, and E. Wimmer. 1988. A segment of the 5' nontranslated region of encephalomyocarditis virus RNA directs internal entry of ribosomes during in vitro translation. J. Virol. **62(8):**2636-2643.

Jang, S. K., and E. Wimmer. 1990a. Cap-independent translation of encephalomyocarditis virus RNA: structural elements of the internal ribosomal entry site and involvement of a cellular 57-kd RNA-binding protein. Genes Dev. **4:**1560-1572.

Jang, S. K., T. V. Pestova, C. U. Hellen, G. W. Witherell, and E. Wimmer. 1990b. Cap-independent translation of picornavirus RNAs: structure and function of the internal ribosomal entry site. Enzyme **44:**292-309.

Jang, S. K. 2006. Internal initiation: IRES elements of picornaviruses and hepatitis c virus. Virus Res. **119(1):**2-15.

Johnson V. H., and B. L. Semler. 1988. Defined recombinants of poliovirus and coxsackievirus: sequence-specific deletions and functional substitutions in the 5'-noncoding regions of viral RNAs. Virology **162:**47-57.

Johnston, J. B., S. H. Nazarian, R. Natale, and G. McFadden. 2005. Myxoma virus infection of primary human fibroblasts varies with cellular age and is regulated by host interferon responses. Virology **332(1):**235-248.

Kaminski, A., M. T. Howell, and R. J. Jackson. 1990. Initiation of encephalomyocarditis virus RNA translation: the authentic initiation site is not selected by a scanning mechanism. EMBO J. **9(11):**3753-3759.

Katze, M. G., Y. He and M. G. Jr. 2002. Viruses and interferon: A fight for supremacy. Nature rev. **2:**675-687.

Kauder, S. E., and V. R. Racaniello. 2004. Poliovirus tropism and attenuation are determined after internal ribosome entry. J. Clin. Invest. **113(12):**1743-1753.

Kauder, S., S. Kan, and V. R. Racaniello. 2006. Age-dependent poliovirus replication in the mouse central nervous system is determined by internal ribosome entry site-mediated translation. J. Virol. **80(6):**2589-2595.

Kawamura, N, M. Kohara, S. Abe, T. Komatsu, K. Tago, M. Arita, and A. Nomoto. 1989. Determinants in the 5' noncoding region of poliovirus Sabin 1 RNA that influence the attenuation phenotype. J. Virol. **63(3):**1302-1309.

Kew, O. M., R. W. Sutter, E. M. de Gourville, W. R. Dowdle, and M. A. Pallansch. 2005. Vaccine-derived polioviruses and the endgame strategy for global polio eradication. Annu. Rev. Microbiol. **59:**587-635.

Khan, S., X. Peng, J. Yin, P. Zhang, and E. Wimmer. 2008. Characterization of the New World monkey homologues of human poliovirus receptor CD155. J. Virol. **82(14):**7167-7179.

Kikuchi, T., M. Ichikawa, J. Arai, H. Tateiwa, L. Fu , K. Higuchi, N. Yoshimura. 2000. Molecular cloning and characterization of a new neuron-specific homologue of rat polypyrimidine tract binding protein. J. Biochem. **128(5):**811-821.

Kitamura, N., B. L. Semler, P. G. Rothberg, G. R. Larsen, C. J. Adler, A. J. Dorner, E. A. Emini, R. Hanecak, J. J. Lee, S. van der Werf, C. W. Anderson, and E. Wimmer. 1981. Primary structure, gene organization and polypeptide expression of poliovirus RNA. Nature **291:**547-553.

Koike, S., H. Horie, I. Ise, A. Okitsu, M. Yoshida, N. Iizuka, K. Takeuchi, T. Takegami, and A. Nomoto. 1990. The poliovirus receptor protein is produced both as membrane-bound and secreted forms. EMBO J. **9:**3217-3224.

Koike, S., C. Taya, T. Kurata, S. Abe, I. Ise, H. Yonekawa, and A. Nomoto. 1991. Transgenic mice susceptible to poliovirus. Proc. Natl. Acad. Sci. USA **88:**951-955.

La Monica, N., C. Meriam, and V. R. Racaniello. 1986. Mapping of sequences required for mouse neurovirulence of poliovirus type 2 Lansing. J. Virol. **57:**515-525.

La Monica, N., and V. R. Racaniello. 1989. Differences in replication of attenuated and neurovirulent polioviruses in human neuroblastoma cell line SH-SY5Y. J. Virol. **63(5):**2357-2360.

Landsteiner, K., and E. Popper. 1909. Ubertragung der Poliomyelitis acuta auf Affen. Z. Immunnitats Forsch Orig. **2:**377-390.

Lange, R., X. Peng , E. Wimmer , M. Lipp , G. Bernhardt. 2001. The poliovirus receptor CD155 mediates cell-to-matrix contacts by specifically binding to vitronectin. Virology **285(2):**218-227.

Lee, Y. F., A. Nomoto, B. M. Detjen, and E. Wimmer. 1977. A protein covalently linked to poliovirus genome RNA. Proc. Natl. Acad. Sci. USA **74(1):**59-63.

Li, C. P., and M. Schaefer. 1953. Adaptation of type 1 poliovirus to mice. Proc. Soc. Exp. Biol. Med. **82:** 477-481.

Li, X., H. H. Lu, S. Mueller, and E. Wimmer. 2001. The C-terminal residues of poliovirus proteinase 2A(pro) are critical for viral RNA replication but not for cis- or trans-proteolytic cleavage. J. Gen. Virol. **82(Pt 2):**397-408.

Lilleväli, K., A. Kulla , and T. Ord. 2001. Comparative expression analysis of the genes encoding polypyrimidine tract binding protein (PTB) and its neural homologue (brPTB) in prenatal and postnatal mouse brain. Mech. Dev. **101(1-2):**217-220.

Loddo, B., W. Ferrari, G. Brotzu, and A. Spanedda. 1962. In vitro inhibition of infectivity of polio viruses by guanidine. Nature **193:**97-98.

Lomax, N. B., and F. H. Yin. 1989. Evidence for the role of the P2 protein of human rhinovirus in its host range change. J. Virol. **63(5):**2396-2399.

Lopez-Guerrero, J. A., M. Alonso, F. Martin-Belmonte, and L. Carrasco. 2000. Poliovirus induces apoptosis in the human U937 promonocytic cell line. Virology **272(2):**250-256.

Lu, H. H., and E. Wimmer. 1996. Poliovirus chimeras replicating under the translational control of genetic elements of hepatitis C virus reveal unusual properties of the internal ribosomal entry site of hepatitis C virus. Proc. Natl. Acad. Sci. USA **93:**1412-1417.

Macadam, A. J., S. R. Pollard, G. Ferguson, G. Dunn, R. Skuce, J.W. Almond, and P.D. Minor. 1991. The 5' noncoding region of the type 2 poliovirus vaccine strain contains determinants of attenuation and temperature sensitivity. Virology **181(2):**451-458.

Macadam, A. J., G. Ferguson, J. Burlison, D. Stone, R. Skuce, J.W. Almond, and P.D. Minor. 1992. Correlation of RNA secondary structure and attenuation of Sabin vaccine strains of poliovirus in tissue culture. Virology **189(2):**415-422.

Martin, A., C. Wychowski, T. Couderc, R. Crainic, J. Hogle, and M. Girard. 1988. Engineering a poliovirus type 2 antigenic site on a type 1 capsid results in a chimaeric virus which is neurovirulent for mice. EMBO J. **7(9):**2839-2847.

Markovtsov, V., J. M. Nikolic, J. A. Goldman, C. W. Turck, M. Y. Chou, and D. L. Black. 2000. Cooperative assembly of an hnRNP complex induced by a tissue-specific homolog of polypyrimidine tract binding protein. Mol. Cell Biol. **20(20):**7463-7479.

Meerovitch, K., J. Pelletier, and N. Sonenberg. 1989. A cellular protein that binds to the 5'-noncoding region of poliovirus RNA: implications for internal translation initiation. Genes Dev. **3(7):**1026-1034.

Meerovitch, K., Y. V. Svitkin, H. S. Lee, F. Lejbkowicz, D. J. Kenan, E. K. Chan, V. I. Agol , J. D. Keene, and N. Sonenberg. 1993. La autoantigen enhances and corrects aberrant translation of poliovirus RNA in reticulocyte lysate. J. Virol. **67(7):**3798-3807.

Mendelsohn, C., B. Johnson, K. A. Lionetti, P. Nobis, E. Wimmer and V. R. Racaniello. 1986. Transformation of a human poliovirus receptor gene into mouse cells. Proc. Natl. Acad. Sci. **83:**7845–7849.

Mendelsohn, C. L., E. Wimmer, and V. R. Racaniello. 1989. Cellular receptor for poliovirus: molecular cloning, nucleotide sequence, and expression of a new member of the immunoglobulin superfamily. Cell **56:**855-865.

Merrill, M. K., E. Y. Dobrikova, and M. Gromeier. 2006a. Cell-type-specific repression of internal ribosome entry site activity by double-stranded RNA-binding protein 76. J. Virol. **80(7):**3147-3156.

Merrill, M. K., and M. Gromeier. 2006b. The double-stranded RNA binding protein 76:NF45 heterodimer inhibits translation initiation at the rhinovirus type 2 internal ribosome entry site. J. Virol. **80(14):**6936-6942.

Minor, P. D., M. Ferguson, K. Katrak, D. Wood, A. John, J. Howlett, G. Dunn, K. Burke, and J. W. Almond. 1991. Antigenic structure of chimeras of type 1 and type 3 polioviruses involving antigenic sites 2, 3 and 4. J. Gen. Virol. **72(Pt 10):**2475-2481.

Minor, P. D., and J. W. Almond. 2002. Poliovirus vaccines: molecular biology and immune response. In: Semler BL, Wimmer E, (eds). Molecular Biology of Picornaviruses, ASM Press, Washington DC, pp. 381–390.

Molla, A., A. V. Paul, and E. Wimmer. 1991. Cell-free, de novo synthesis of poliovirus. Science **254(5038):**1647-1651.

Mueller, S., and E. Wimmer. 2003. Recruitment of nectin-3 to cell-cell junctions through trans-heterophilic interaction with CD155, a vitronectin and poliovirus receptor that localizes to alpha(v)beta3 integrin-containing membrane microdomains. J. Biol. Chem. **278(33):**31251-31260.

Mueller, S., D. Papamichail, J. R. Coleman, S. Skiena, and E. Wimmer. 2006. Reduction of the rate of poliovirus protein synthesis through large-scale codon deoptimization causes attenuation of viral virulence by lowering specific infectivity. J. Virol. **80(19):**9687-9696.

Murray, M.G., J. Bradley, X. F. Yang, E. Wimmer, E. G. Moss, and V. R. Racaniello. 1988. Poliovirus host range is determined a short amino acid sequence in neutralization antigenic site I. Science **241:**213-215.

Mora, R., E. Rodriguez-Boulan, P. Palese, and A. Garcia-Sastre. 2002. Apical budding of a recombinant influenza A virus expressing a hemagglutinin protein with a basolateral localization signal. J. Virol. **76:**3544-3553.

Nakamura, T., A. Asano, S. Okano, J. H. Ko, Y. Kon, T. Watanabe, and T. Agui. 2005. Intracellular localization and antiviral property of canine Mx proteins. J. Interferon Cytokine Res. **25(3):**169-173.

Nathanson, N. 2008. The pathogenesis of poliomyelitis: what we don't know. Adv. Virus Res. **71:**1-50.

Nomoto, A., B. Detjen, R. Pozzati, and E. Wimmer. 1977. The location of the polio genome protein in viral RNAs and its implication for RNA synthesis. Nature **268:**208-213.

Nomoto, A., T. Omata, H. Toyoda, S. Kuge, H. Horie, Y. Kataoka, Y. Genba, Y. Nakano, and N. Imura. 1982. Complete nucleotide sequence of the attenuated poliovirus Sabin 1 strain genome. Proc. Natl. Acad. Sci. USA **79(19):**5793-5797.

Omata, T., M. Kohara, S. Kuge, T. Komatsu, S. Abe, B. L. Semler, A. Kameda, H. Itoh, M. Arita, E. Wimmer, and A. Nomoto. 1986. Genetic analysis of the attenuation phenotype of poliovirus type 1. J. Virol. **58(2):**348–358.

Parsley, T. B., J. S. Towner, L. B. Blyn, E. Ehrenfeld, and B. L. Semler. 1997. Poly (rC) binding protein 2 forms a ternary complex with the 5'-terminal

sequences of poliovirus RNA and the viral 3CD proteinase. RNA **3(10):**1124-1134.

Paul, A. V., J. Mugavero, J. Yin, S. Hobson, S. Schultz, J. H. van Boom, and E. Wimmer. 2000. Studies on the attenuation phenotype of polio vaccines: poliovirus RNA polymerase derived from Sabin type 1 sequence is temperature sensitive in the uridylylation of VPg. Virology **272(1):**72-84.

Paul, A. V. 2002. Possible unifying mechanism of picornavirus genome replication. In: B. L. Semler and E. Wimmer (Eds), Molecular Biology of Picornaviruses, ASM Press, Washington DC, pp. 227-246.

Pelletier, J., and N. Sonenberg. 1988. Internal initiation of translation of eukaryotic mRNA directed by a sequence derived from poliovirus RNA. Nature **334(6180):**320-325.

Pestova, T.V., C. U. Hellen, and E. Wimmer. 1991. Translation of poliovirus RNA: role of an essential cis-acting oligopyrimidine element within the 5' nontranslated region and involvement of a cellular 57-kilodalton protein. J. Virol. **65:**6194-6204.

Pilipenko, E. V., A. P. Gmyl, S. V. Maslova, Y. V. Svitkin, A. N. Sinyakov, and V. I. Agol. 1992. Prokaryotic-like cis elements in the cap-independent internal initiation of translation on picornavirus RNA. Cell **68:**119-131.

Pilipenko, E. V., T. V. Pestova, V. G. Kolupaeva, E.V. Khitrina, A. N. Poperechnaya, V. I. Agol, and C. U. Hellen. 2000. A cell cycle-dependent protein serves as a template-specific translation initiation factor. Genes Dev. **14(16):**2028-2045.

Pilipenko, E. V., E. G. Viktorova, S. T. Guest, V. I. Agol, and R. P. Roos. 2001. Cell-specific proteins regulate viral RNA translation and virus-induced disease. EMBO J. **20(23):**6899-6908.

Pipkin, P. A., D. J. Wood, V. R. Racaniello, and P. D. Minor. 1993. Characterization of L cells expressing the human poliovirus receptor for the specific detection of polioviruses in vitro. J. Virol. Methods **41(3):**333-340.

Pisarev, A.V., L.S. Chard, Y. Kaku, H. L. Johns, I. N. Shatsky, and G. J. Belsham. 2004. Functional and structural similarities between the internal ribosome entry sites of hepatitis C virus and porcine teschovirus, a picornavirus. J. Virol. **78:**4487-4497.

Pollard, S. R., G. Dunn , N. Cammack , P. D. Minor, J. W. Almond . 1989. Nucleotide sequence of a neurovirulent variant of the type 2 oral poliovirus vaccine. J. Virol. **63(11):**4949-4951.

Polydorides, A. D., H. J. Okano , Y. Y. Yang, G. Stefani , R. B. Darnell. 2000. A brain-enriched polypyrimidine tract-binding protein antagonizes the ability of Nova to regulate neuron-specific alternative splicing. Proc. Natl. Acad. Sci. USA. **97(12):**6350-6355.

Racaniello, V.R., and D. Baltimore. 1981a. Cloned poliovirus complementary DNA is infectious in mammalian cells. Science **214:**916-919.

Racaniello, V.R., and D. Baltimore. 1981b. Molecular cloning of poliovirus cDNA and determination of the complete nucleotide sequence of the viral genome. Proc. Natl. Acad. Sci. USA. **78:**4887-4891.

Racaniello, V.R. 1988. Poliovirus neurovirulence. *In* Advances in Virus Research. (K. Maramorosch, F.A. Murphy and A.J. Shatkin, ed), Academic Press, San Diego, pp. 217-246.

Reed, L. J., and M. Muench. 1938. A simple method for estimating fifty percent endpoints. Am. J. Hyg. **27:**493-497.

Reich, N. C., and L. Liu. 2006. Tracking STAT nuclear traffic. Nat. Rev. Immunol. **6(8):**602-612.

Reich, N. C. 2007. STAT dynamics. Cytokine Growth Factor Rev. **18(5-6):**511-518.

Ren, R., F. Costantini, E. J. Gorgacz, J. J. Lee, and V. R. Racaniello. 1990. Transgenic mice expressing a human poliovirus receptor: a new model for poliomyelitis. Cell **63:**353-362.

Ren, R., and V. R. Racaniello. 1992. Poliovirus spreads from muscle to the central nervous system by neural pathways. J. Infect. Dis. **166:**747-752.

Reuter, G., A. Boldizsar, and P. Pankovics. 2009. Complete nucleotide and amino acid sequences and genetic organization of porcine kobuvirus, a member of a new species in the genus Kobuvirus, family Picornaviridae. Arch. Virol. **154:**101-108.

Sabin, A.B., W. A. Hennessen, and J. Winsser. 1954. Studies on variants of poliomyelitis virus: I. Experimental segregation and properties of avirulent variants of three immunologic types. J. Exp. Med. **9:** 551-576.

Sabin, A. B. 1956. Pathogenesis of poliomyelitis; reappraisal in the light of new data. Science **123:**1151-1157.

Sabin, A.B. and L. R. Boulger. 1973. History of Sabin attenuated poliovirus oral live vaccine strains. J. Biol. Stand. **1:** 115-118.

Semler, B. L., V. H. Johnson, and S. Tracy. 1986. A chimeric plasmid from cDNA clones of poliovirus and coxsackievirus produces a recombinant virus that is temperature-sensitive. Proc. Natl. Acad. Sci. USA **83(6):**1777-1781.

Shiroki, K., T. Ishii, T. Aoki, M. Kobashi, S. Ohka, and A. Nomoto. 1995. A new cis-acting element for RNA replication within the 5' noncoding region of poliovirus type 1 RNA. J. Virol. **69(11):**6825-6832.

Skinner, M.A., V. R. Racaniello, G. Dunn, J. Cooper, P. D. Minor, and J. W. Almond. 1989. A new model for the secondary structure of the 5' noncoding RNA of poliovirus is supported by biochemical and genetic data which also show that RNA secondary structure is important to neurovirulence. J. Mol. Biol. **207:** 379-392.

Smura, T. P., N. Junttila , S. Blomqvist , H. Norder , S. Kaijalainen , A. Paananen , L. O. Magnius , T. Hovi , and M. Roivainen. 2007. Enterovirus 94, a proposed new serotype in human enterovirus species D. J. Gen. Virol. **88(Pt3):**849-858.

Sonenberg, N. 1990. Poliovirus Translation. *In* V.R. Racaniello, (Eds), Picornaviruses, Springer-Verlag, New York, pp. 23-48.

Sonenberg, N. 1991. Picornavirus RNA translation continues to surprise. TIG. **7:**105-106.

Stanway, T. H. G., N. J. Knowles, and T. Hovi. 2002. Molecular and biological basis of picornavirus taxonomy. *In:* B.L. Semler and E. Wimmer (Eds.), Molecular Biology of Picornaviruses, ASM Press, Washington DC, pp. 17-24.

Svitkin, Y. V., and V. I. Agol. 1978. Complete translation of encephalomyocarditis virus RNA and faithful cleavage of virus-specific proteins in a cell-free system from Krebs-2 cells. FEBS Lett. B7-11.

Svitkin, Y. V., S. V. Maslova, and V. I. Agol. 1985. The genomes of attenuated and virulent strains differ in their in vitro translation efficiencies. Virology. **147(2):**243-252.

Svitkin, Y. V., T. V. Pestova , S. V. Maslova , and V. I. Agol. 1988. Point mutations modify the response of poliovirus RNA to a translation initiation factor: a comparison of neurovirulent and attenuated strains. Virology **166(2):**394-404.

Svitkin, Y. V., N. Cammack, P. D. Minor, and J. W. Almond. 1990. Translation deficiency of the Sabin type 3 poliovirus genome: association with an attenuating mutation C472----U. Virology **175(1):**103-109.

Tardy-Panit M., Blondel B., Martin A., Tekaia F., Horaud F., and Delpeyroux, F. 1993. A mutation in the RNA polymerase of poliovirus type 1 contributes to attenuation in mice. J. Virol. 67:4630-4638.

Tolskaya, E. A. , L. I. Romanova, M. S. Kolesnikova, T. A. Ivannikova, E. A. Smirnova, N. T. Raikhlin, and V. I. Agol. 1995. Apoptosis-inducing and apoptosis-preventing functions of poliovirus. J. Virol. **69(2):**1181-1189.

Toyoda, H., M. Kohara, Y. Kataoka, T. Suganuma, T. Omata, N. Imura, and A. Nomoto. 1984. Complete nucleotide sequences of all three poliovirus serotype genomes. Implication for genetic relationship, gene function and atigenic determinants. J. Mol. Biol. **174:**561-585.

Toyoda, H., D. Franco , K. Fujita , A. V. Paul, and E. Wimmer. 2007a. Replication of poliovirus requires binding of the poly(rC) binding protein to the cloverleaf as well as to the adjacent C-rich spacer sequence between the cloverleaf and the internal ribosomal entry site. J. Virol. **81(18):**10017-10028.

Toyoda, H., J. Yin, S. Mueller, E. Wimmer, and J. Cello. 2007b. Oncolytic treatment and cure of neuroblastoma by a novel attenuated poliovirus in a novel poliovirus-susceptible animal model. Canc. Res. **67:**2857-2864.

Trono, D., R. Andino, and D. Baltimore. 1988. An RNA sequence of hundreds of nucleotides at the 5' end of poliovirus RNA is involved in allowing viral protein synthesis. J. Virol. **62(7):**2291-2299.

van der Werf, S., J. Bradley, E. Wimmer, F. W. Studier, and J. J. Dunn. 1986. Synthesis of infectious poliovirus RNA by purified T7 RNA polymerase. Proc. Natl. Acad. Sci. USA **78:**2330-2334.

Walter, B. L., J. H. Nguyen, E. Ehrenfeld , and B. L. Semler. 1999. Differential utilization of poly(rC) binding protein 2 in translation directed by picornavirus IRES elements. RNA **5(12):**1570-1585.

Walter, B. L., T. B. Parsley, E. Ehrenfeld, and B. L. Semler. 2002. Distinct poly(rC) binding protein KH domain determinants for poliovirus translation initiation and viral RNA replication. J. Virol. **76(23):**12008-12022.

Westrop, G.D., K. A. Wareham, D. M. A. Evans, G. Dunn, P. D. Minor, D. I. Magrath, F. Taffs, S. Marsden, M. A. Skinner, G. C. Schild, and J. W. Almond. 1989. Genetic basis of attenuation of the Sabin type 3 oral poliovirus vaccine. J. Virol. **63:**1338-1344.

Whitton, J. L., C. T. Cornell, and R. Feuer. 2005. Host and virus determinants of picornavirus pathogenesis and tropism. Nat. Rev. Microbiol. **3(10):**765-776.

Wimmer, E. 1982. Genome-linked proteins of viruses. Cell. **28(2):**199-201.

Wimmer, E., R. Kuhn, S. Pincus, C. -F. Yang, H. Toyoda, M. Nicklin, and N. Takeda. 1987. Molecular events leading to picornavirus genome replication. *In* Virus Replication and genome Interaction: Seventh John Innes Symposium. (J. Davies, ed). The Company of Biologists LTD, Cambridge, England. pp. 251-276.

Wimmer, E., C. U. T. Hellen, and X. M. Cao. 1993. Genetics of poliovirus. Ann. Rev. Genet. **27:**353-436.

Wimmer, E., J. J. Harber, J. A. Bibb, M. Gromeier, H.-H. Lu, and G. Bernhardt. 1994. Poliovirus Receptors. *In:* E. Wimmer (ed.), Cellular receptors for animal viruses, Cold Spring Harbor Laboratory, Cold Spring Harbor. pp. 101-127.

Yanagiya, A., S. Ohka, N. Hashida, M. Okamura, C. Taya, N. Kamoshita, K. Iwasaki, Y. Sasaki, H. Yonekawa, and A. Nomoto. 2003. Tissue-specific replicating capacity of a chimeric poliovirus that carries the internal ribosome entry site of hepatitis C virus in a new mouse model transgenic for the human poliovirus receptor. J. Virol. **77:**10479-10487.

Yanagiya, A, Q. Jia, S. Ohka, H. Horie, and A. Nomoto. 2005. Blockade of the poliovirus-induced cytopathic effect in neural cells by monoclonal antibody against poliovirus or the human poliovirus receptor. J. Virol. **79(3):**1523-1532.

Yin, F. H., and N. B. Lomax. 1983. Host range mutants of human rhinovirus in which nonstructural proteins are altered. J. Virol. **48(2):**410-418.

Yin, J., A. V. Paul, E. Wimmer, and E. Rieder. 2003. Functional dissection of a poliovirus *cis*-acting replication element [PV-cre(2C)]: analysis of single- and dual-cre viral genomes and proteins that bind specifically to PV-cre RNA. J. Virol. **77:**5152–5166.

Yoshikawa, T., T. Iwasaki, M. Ida-Hosonuma, M. Yoneyama, T. Fujita, H. Horie, M. Miyazawa, S. Abe, B. Simizu, and S. Koike. 2006. Role of the alpha/beta interferon response in the acquisition of susceptibility to poliovirus by kidney cells in culture. J. Virol. **80(9):**4313-4325.

Appendix

A Host-specific, temperature sensitive translation defect determines the attenuation phenotype of a human rhinovirus/poliovirus chimera PV1(RIPO)

Nusrat Jahan, Eckard Wimmer, and Steffen Mueller

(Paper submitted to Journal of Virology)

A Host-specific, temperature sensitive translation defect determines the attenuation phenotype of a human rhinovirus/poliovirus chimera PV1(RIPO)

Nusrat Jahan, Eckard Wimmer, and Steffen Mueller*

Department of Molecular Genetics and Microbiology, Stony Brook University,

Stony Brook, NY 11794, USA

Running title: Host restriction of poliovirus/rhinovirus chimeras

Word count (abstract): 263

Word count (main text): 6,305

*corresponding author:

Department of Molecular Genetics and Microbiology, Life Sciences Building

Stony Brook University

Stony Brook, NY 11794-5222

Tel. 631-632-8804

Fax. 631-632-8891

email. smueller@ms.cc.sunysb.edu

ABSTRACT

There is little insight into the role of internal ribosome entry sites (IRES) as a post-entry determinant of picornavirus tissue and host tropism. Using PV1(RIPO), a chimeric poliovirus, utilizing the cognate IRES of Human Rhinovirus type 2 (HRV2), we set out to shed light on the mechanism by which this variant expresses its remarkably attenuated phenotype in poliovirus-sensitive, CD155 transgenic (tg) mice.

Here we describe that, in addition to the growth restriction in human neuronal cells previously observed, PV1(RIPO) also exhibits a strong species-specific defect at physiological temperature in cells of murine origin. The block in replication was enhanced at 39.5^{o}C but, remarkably, it was absent at 33^{o}C. PV1(RIPO) revertants, overcoming the block in either mouse cells or human neuronal cells, were derived by serial passage under restrictive conditions. Virus adaptation in mouse cells, but not in human neuronal cells, resulted in increased mouse neurovirulence *in vivo*.

A translation defect associated with the HRV2 IRES was observed in mouse cells that correlated with the attenuation phenotypes of PV1(RIPO) in different mouse cell lines and in CD155tg mice.

This work demonstrates that changes in the 5'NTR of PV1(RIPO) alone, particularly the mutations in the HRV2 IRES, are sufficient to rescue the defective IRES-mediated translation and, consequently, RNA replication in mouse cells and neurovirulence in CD155tg transgenic mice.

Our results serve to caution that the assessment of the neurovirulent potential of poliovirus variants in CD155tg mice, the approved method for releasing live attenuated oral poliovirus vaccine lots, may be masked by mouse specific defects, which may not allow to accurately predict human neurovirulence.

INTRODUCTION

It is generally assumed that the primary determinant of the host range of picornaviruses, a large family of plus strand RNA viruses, is the tissue specific expression of a virus' cellular receptor. In the case of poliovirus, CD155 (also known as Pvr) (31, 22) narrowly restricts the virus to humans and nonhuman primates. The isolation and characterization of the PV receptor CD155 made possible the construction of CD155 transgenic (tg) mice (23, 41). These tg animals, when injected with PV, show symptoms of paralysis similar to those of human poliomyelitis. Although CD155 could be detected in various human and tg mouse tissues, many of those tissues are not necessarily sites of PV replication (31, 10, 16). This indicated that receptor expression is necessary but not sufficient for PV replication.

Picornavirus genomic RNA and mRNA are of identical sequence. However, the virion RNA is linked at its 5'-end to the small protein VPg that is cleaved off when the genome engages in translation (49). Thus, in contrast to eukaryotic host cellular mRNAs, picornavirus genomic RNAs, that serve as mRNA lack the 5' cap structure. Instead picornaviruses control their translation with an internal ribosomal entry site (IRES) within the 5' nontranslated regions (5' NTRs) of their genome (18, 38, 9).

Picornavirus IRES elements are large, extensively structured segments of RNA (~450 nt). Although these elements are quite distinct in structure, they are interchangeable between viruses of different genera and even of different

families, yielding novel chimeric infectious viruses (1, 11, 12, 28, 8). Some of these studies with IRES-chimeric viruses illustrated the potential contribution of the IRES element toward cell tropism of the virus (11, 8, 20).

The IRES dependent tissue tropism as a determinant of picornaviral pathogenesis was studied previously using PV1(RIPO), a chimeric virus containing the IRES of human rhinovirus type 2 in the background of the genome of poliovirus, type 1 (Mahoney) [PV1(M)] (11). PV1(RIPO) was found to replicate well in human cervical carcinoma cells (HeLa) but replication was significantly reduced in human neuroblastoma cells (SK-N-MC) at 37^{o}C. Subsequently it was observed that PV1(RIPO) exhibited a temperature-sensitive (*ts*) growth phenotype (5), characterized by severely impaired viral replication on SK-N-MC cells at 39.5^{o}C. A *ts* phenotype has also been documented for all three Sabin vaccine strains and it is considered an important factor in neuroattenuation (29, 30). Furthermore, PV1(RIPO) had lost the neurovirulent phenotype of PV1(M) in CD155tg mice, and in non-human primates (11, 13). It is at least 1,000,000 times less pathogenic in CD155tg mice than wild-type PV. Similar results were obtained when an IRES recombinant between HRV2 and the neurovirulent *wt* Leon/37 poliovirus of type 3 was tested in the CD155tg mouse model (6).

The question whether the IRES is an important determinant of PV pathogenesis, led to a nearly two decades long study of attenuated and neurovirulent polioviruses by different groups. Early studies showed that the reduced efficiency of *in vitro* translation of Sabin type 3 PV RNA compared to that of the neurovirulent strains of type 3 PV is the result of the known

attenuating mutation (C472→U) in the IRES of Sabin type 3 PV (43, 44). Supporting evidence for this observation came from the work of La Monica and Racaniello (24). Using cell culture models they showed the C472→U mutation in Sabin type 3 PV results in low titer growth and reduced translation efficiency in neuroblastoma cells but not in HeLa cells. Later on they performed experiments to test the role of IRES-mediated translation initiation as a determinant of PV tissue tropism and pathogenesis (19, 20). Replacing the IRES of PV1(M) with that of coxsackie virus B or hepatitis C virus and using the Sabin type 3 PV IRES, Kauder and colleagues (19) originally reported that the tropism of wild type and vaccine strains of poliovirus is determined in a step after IRES-mediated translation. In a subsequent study, however, using a different experimental strategy, they suggested that IRES-derived translation plays an important role in replication of a chimeric virus (P1/HRV2) in an age-dependent manner in CD155tg mice (20).

The neuroattenuation of PV1(RIPO) in CD155tg mice correlated with it's inability to replicate in human SK-N-MC neuroblastoma cells and in non-human primates (11, 13). It is not yet known whether a host species specific block, may contribute to the attenuation phenotype. In this study we examined the IRES dependent tissue tropism of PV1(RIPO) with the aim of distinguishing between a tissue specific block (neuronal vs non-neuronal) and a host species specific block (mouse vs human) by comparing the growth phenotypes of PV1(RIPO) in different human and mouse cell lines of neuronal and non-neuronal origin. Our results indicate that PV1(RIPO) possesses a strong temperature dependent

119 growth defect in all the mouse cell lines tested (both neuronal and non-neuronal
120 expressing the human PV receptor CD155), an observation suggesting that
121 mouse tissues are generally unable to support HRV2 IRES-dependent initiation
122 at temperatures higher than 33^{o}C. All CD155-expressing mouse cell lines, on the
123 other hand, are perfectly susceptible to infection by wild type PV. These results
124 correlate with high attenuation of this chimeric virus in CD155tg mice. This
125 attenuation phenotype might be related to a mouse species specific block of
126 PV1(RIPO) growth at higher temperatures. The CD155tg mice models therefore
127 have their limitations to assess the neurovirulence of chimeric virus PV1(RIPO)
128 and perhaps other similar chimeras.
129

MATERIALS AND METHODS

Viruses and cells. The neurovirulent poliovirus type 1 [Mahoney; PV1(M)] is the strain being used routinely in the laboratory (4). PV1(RIPO) was constructed as described previously (11). The construction of PN6 mutant virus has been described elsewhere (47). The mouse neuroblastoma cell line stably expressing CD155α (Neuro-2a^{CD155}) (35, 46), mouse fibroblast cell lines (L cells) expressing either CD155α (H20A) (31), or CD155δ (L20B) (31, 39) and mouse fibroblast cell line stably expressing CD155α (NIH3T3^{CD155}, Mueller and Wimmer unpublished), all of which are susceptible to poliovirus infection, were maintained in DMEM containing 1% penicillin/streptomycin and 10% fetal bovine serum. HEK293 (Ad transformed neuroepithelial) cells (A gift from M. Gromeier; 3) were maintained in Dulbecco's minimal essential medium (DMEM) containing 1% penicillin/streptomycin and 10% fetal bovine serum. HeLa (human cervical cancer) cells, and human neuroblastoma cell lines SK-N-MC and SK-N-SH were obtained from the American Type Culture Collection (Manassas, VA) and were maintained according to the suppliers's specification.

Serial passages of PV1(RIPO) in SK-N-MC and L20B cells. The selection of PV1(RIPO) isolates capable of efficient replication in mouse cells and human neuroblastoma cells was carried out according to the following procedure: H20A and SK-N-MC cells were infected at an MOI (multiplicity of infection) of 10 with PV1(RIPO) and incubated at 37°C for 4 days, or until the appearance of CPE. After 7 blind passages complete CPE was observed and RNA extracted from the

152 viral cell lysate served as template for reverse transcription-PCR (RT-PCR) and
153 the purified PCR amplicons were used for sequencing reactions.
154 **RNA extraction, RT-PCR, and DNA sequencing.** Viral RNA was extracted
155 from infected cells using TRIzol solution (Invitrogen) and used as template for
156 RT-PCR. Titan One-Tube RT-PCR system was used to perform RT-PCRs
157 following the manufacturer's instructions (Roche, Mannheim), and the PCR
158 amplicons were purified with the QIAquick gel extraction kit (QIAGEN). The
159 sequence of the purified PCR products was determined with oligonucleotide
160 primers in cycle sequencing (ABI Prism Big Dye terminator cycle sequencing
161 ready reaction kit; Applied Biosystems) in an automated sequencer (model 310;
162 Applied Biosystems).
163 **Construction of plasmids.** Several recombinant variants with phenotypes
164 quite distinct from the parent PV1(RIPO) were constructed using different
165 combination of mutations in the 5'NTR, that had been identified in the adapted
166 isolates. For instance, the plasmid for one of the recombinant variants, R-1235,
167 (see below), was constructed as follows and was named R-1235r: cDNA
168 prepared from R-1235 viral RNA was cut with *BbrpI* and *SacI* and ligated to a
169 similarly restricted PV1(RIPO) fragment. To construct R-2r, which has a single
170 C133G mutation in the 5'-NTR of PV1(RIPO), site-directed mutagenesis was
171 carried out in a two step PCR reaction. For the first-step PCR, two PCR
172 fragments F1 and F2 were amplified by using pT7PV1(RIPO) as template and
173 the primer pair 5'TTAAAACAGCTCTGGGGTTGTACCCACCCC 3' and 5'
174 TCAGTAATCTGGCTGATTACCGCCTATTGGTCTTTGTGAAAAAC 3'for F1

175 fragment and the primer pair 5' GTCCTGTTTCGAAGCCGCGTTACTAGC 3' and
176 5' AGTTTTTCACAAAGACCAATAGGCGGTAATCAGCCAGATTACTG 3' for F2
177 fragment. The two PCR fragments, F1 and F2 carrying overlapping ends were
178 then used as templates for the second-step PCR. R-123r, R-12r, R-35r, R-3r, R-
179 5r were constructed by choosing appropriate restriction endonuclease sites
180 within R-1235r and PV1(RIPO) plasmids and exchanging fragments between
181 these plasmids. Mutations in the final constructs were verified by sequencing
182 using the ABI Prism DNA Sequencing kit.

183 ***In vitro* transcription, transfection and virus isolation.** All plasmids were
184 linearized with *Dra*I. RNAs were synthesized with phage T7 RNA polymerase,
185 and the RNA transcripts were transfected into HeLa R19 cell monolayers by the
186 DEAE-dextran method as described previously (48). The incubation time was 2
187 to 3 days for full-length viral constructs. Virus titer was determined by a plaque
188 assay, as described before (34).

189 **One-step growth curves at 33 ^{o}C, 37 ^{o}C, and 39 ^{o}C.** One-step growth
190 experiments in different human and mouse cell lines were carried out as follows.
191 Cell monolayers in 35 mm plastic culture dishes were washed with DMEM and
192 inoculated at an MOI of 10 with the virus to be tested. The dishes were rocked for
193 30 min at room temperature, the cells were thoroughly washed to remove
194 unbound virus and placed at 33^{o}C or 37^{o}C or 39.5^{o}C. At 0, 2, 4, 6, 8, 12, 24 and
195 48 hr post infection (p.i.), the dishes were subjected to three consecutive freeze-
196 thaw cycles, and the viral titers of the supernatants were determined by plaque
197 assay on HeLa cells, as describe before (34).

198 **Poliovirus luciferase replicons and luciferase assays.** We previously
199 described a wt replicon PV1(M)-luc, in which the PV capsid coding sequence
200 was replaced by that of firefly luciferase gene (25). In addition we constructed
201 two new chimeric replicons that, in analogy to their full length infectious
202 counterparts, carrying either the wt HRV2 IRES [PV1(RIPO)-luc] or a mouse-
203 adapted HRV2 IRES (R-1235r-luc). *In vitro* transcribed replicon RNA was
204 transfected into monolayers (35-mm-diameter dishes) of HeLa, SK-N-MC and
205 L20B cells using a modified DEAE-Dextran transfection method (36) and
206 incubated at 33°C, 37°C or 39.5°C in DMEM, 2% BCS. At different time points
207 post-transfection the growth medium was removed from the dishes, and the cells
208 were washed gently with 2 ml of phosphate-buffered saline. The cells were lysed
209 in passive lysis buffer (Promega) and the firefly luciferase activity was measured
210 by methods described previously (51) using a firefly luciferase substrate kit
211 (Promega). The rate of viral translation was assayed by incubating transfected
212 cells in the presence of 2mM guanidine hydrochloride (GuHCl), a potent inhibitor
213 of PV replication. RNA replication of a construct, on the other hand, can be
214 assessed by considering the ratio of luficerase signals obtained in the absence
215 and presence of the guanidine.
216 **Neurovirulence assays in mice.** Groups of four CD155tg mice (23) were
217 inoculated with any given amount of virus ranging from 10^2 to 10^8 plaque-forming
218 units (pfu; 30 µL/mouse) i.c. with different viruses. Mice were examined daily for
219 21 days after inoculation for paralysis and/or death. The virus titer that induced
220 paralysis or death in 50% of the mice (PLD_{50}) was calculated by the method of

221 Reed and Muench (40). All experiments involving mice were conducted in
222 compliance with institutional IACUC regulations and federal guidelines.
223

RESULTS

Previously a picornavirus genomic hybrid, PV1(RIPO), was constructed in which the IRES element of PV1(M) was replaced with that of human rhinovirus type 2 (11) (Fig. 1A). PV1(RIPO) was cloned by using an upstream *EcoRI* restriction site in the spacer region between the clover leaf and the IRES of the PV1(M) genome. This *EcoRI* site was originally generated through linker insertion scanning in the 5'NTR of PV1(M) resulting in poliovirus variant PN6, which displayed wt growth characteristics in HeLa cells (47) (Fig. 1A). We have previously described that modifications within this spacer region by mutation of two nearby clusters of C residues (45), or of the dinucleotide UA(101/102)GG (4, 7), or by insertion of a stem-loop (51, 46) significantly changed the phenotypes of the parental virus. PV1(RIPO) exhibited a replication phenotype and *ts* growth restriction in SK-N-MC neuroblastoma cells (5) but the effect, if any, of the linker insertion in strain PN6 on the replication in cells of neuronal origin remained unknown.

The growth phenotype of PV1(RIPO) and PN6 in human cell lines at different temperature. Upon further analysis of the spacer region of entero and rhinoviruses we identified a previously not recognized highly conserved sequence in the spacer region corresponding to nt position 103-112 of the PV genome (Fig. 9). The question thus arose, whether the longer spacer region artificially extended by the *EcoRI* linker was the cause for PV1(RIPO) attenuation phenotype. The growth phenotypes of PV1(RIPO) and PN6 in HeLa R19 was

246 first analyzed at 33^{o}C, 37^{o}C and 39.5^{o}C and found to be similar to that of
247 PV1(M) (Fig. 1B). When tested in three different human cell lines of neuronal
248 origin (Fig. 2) PN6 replicated with similar growth kinetics as PV1(M) at all three
249 temperatures (closed triangles) whereas the growth of PV1(RIPO) was inhibited
250 in SK-N-MC cells (11), and in HEK293 cells (3). A *ts* phenotype of PV1(RIPO)
251 observed at 39.5^{o}C was particularly pronounced in SK-N-MC and HEK293 cells.
252 For reasons that remain unknown, the growth defect at 33°C is reduced in all
253 three human neuronal cell lines tested, and even absent in SK-N-SH (Fig. 2). In
254 any event, the phenotypes of PV1(RIPO) observed in Fig. 2 could be the result
255 solely of the presence of the HRV2 IRES in the PV1(M) background, or of the
256 presence of the HRV2 IRES plus the insertion preceding the HRV2 IRES (Fig.
257 1A). It should be noted that the *EcoRI* linker insertion increases the length of the
258 spacer region, and thus the distance between cloverleaf and IRES by 12
259 nucleotides. The corresponding sequence changes in the spacer between clover
260 leaf and IRES in PN6, however, exerted little, if any effect in cells of human
261 origin.

262 **PV1(RIPO) has a mouse cell-specific propagation defect which can be**
263 **rescued by growth at lower temperature.** We then tested whether the growth
264 phenotypes of PV1(RIPO) in mouse cells of neuronal and non-neuronal origin
265 reflects that in human cells. For the experiments we used N2a^{CD155}, a mouse
266 neuroblastoma cell line stably expressing the human PV receptor CD155 (35) as
267 well as the two CD155- expressing mouse fibroblast cell lines L20B (31, 39) and
268 NIH3T3$^{CD155\alpha}$ (see the Materials and Methods). Infections were carried out at

269 33°C, 37°C and 39.5°C. Whereas PV1(M) and PN6 replicated well in all cell lines
270 at 33°C and 37°C, PN6 expressed a *ts* phenotype at 39.5°C that was pronounced
271 in NIH3T3$^{CD155\alpha}$ cells (Fig. 3C). Surprisingly, PV1(RIPO) did not replicate in any
272 mouse cell at either 37°C or 39.5°C (Fig. 3A-C). In stark contrast, all three cells
273 supported replication at 33°C. At 33°C, therefore, even cells of neuronal origin
274 (N2a^{CD155} cells) are an adequate substrate for PV1(RIPO) replication (Fig. 3A).
275 **PV1(RIPO) is defective in IRES mediated translational initiation at the**
276 **restricted temperature.** After CD155 mediated internalization, the PV particle
277 uncoats and the viral genome RNA serves as mRNA for the translation of a
278 single polyprotein by a cap-independent mechanism, followed by replication of
279 the incoming genome (49, 37). In order to understand at which stage of
280 replication the attenuation of PV1(RIPO) occurs in some human cell lines the
281 functionality of PV-specific replicons expressing the Luciferase gene was
282 analyzed. Specifically, we used PV1(M)-Luc and PV1(RIPO)-Luc, containing the
283 firefly luciferase reporter gene in place of the PV capsid proteins, to assess their
284 ability to be translated and replicated in SK-N-MC and L20B cells. To differentiate
285 between the luciferase signals due to translation from the incoming viral RNA
286 from signals due to translation from mRNA synthesized during replication the
287 cells were grown in the presence and in the absence of 2mM guanidine
288 hydrochloride (GuHCl). At this concentration, GuHCl inhibits viral RNA replication
289 without any toxic effect on cellular processes or viral translation (2, 17, 26).
290 HRV2 IRES-mediated translation and RNA replication were measured in HeLa
291 R19 cells, mouse L20B cells and SK-N-MC cells by transfecting the cells with *in*

292 *vitro* transcribed RNA of poliovirus luciferase replicons and incubation of the cells
293 at 33^{o}C, 37^{o}C and 39.5^{o}C in the presence (for translation) or in the absence (for
294 replication) of 2 mM GuHCl (Fig. 4). Translation and replication mediated by the
295 HRV2 IRES in case of the PV1(RIPO)-luc replicon were similar to that of the
296 PV1(M)-luc replicon in HeLa R19 cells (Fig.4A). In contrast, in SK-N-MC cells
297 HRV2 IRES-mediated translation, and consequently replication, was low and it
298 decreased with increasing temperature (Fig. 4B). Most strikingly, in mouse L20B
299 cells the PV1(RIPO)-luc replicon failed to show any replication activity at 37^{o}C
300 and 39.5^{o}C, likely as a result the greatly reduced translation activity (Fig. 4C),
301 This finding is consistent with the growth characteristics of the corresponding
302 chimeric virus, PV1(RIPO), in different mouse cell lines (Fig. 3B). Therefore, we
303 conclude that in mouse cell lines the HRV2 IRES-mediated translation is
304 defective in a *ts* manner, which is ultimately affecting viral RNA replication.
305 **Genetic variants in the 5'NTR of PV1(RIPO) are adapted to growth in**
306 **mouse cells and human neuronal cells.** Serial passage of an attenuated strain
307 of PV1(M) facing a replication block may results in the evolution of modified
308 variants with increased replication properties. With the aim of isolating such
309 adapted variants, PV1(RIPO) was serially passaged in SK-N-MC cells and in
310 mouse H20A cells at 37^{o}C, respectively. Two variants (R-1 and R-7) were
311 isolated from SK-N-MC passages and seven (R-1235, R-123, R-124, R-234, R-
312 136, R-12, and R-23) from H20A passages (Fig. 5) (see Materials and Methods).
313 These variants showed increased replication in the cell types in which their
314 progenitor was highly restricted in growth. The 5' NTRs of the adapted isolates

were sequenced and the mutations were mapped with the aim of understanding the molecular determinants of the high-titer growth phenotype (Fig. 5). The three most common changes that were observed were: i) either a 12 or a 13 nucleotide deletion in the spacer between cloverleaf and IRES (mutation 1); ii) point mutation 2; and iii) point mutation 3. Among these, mutation 1 was observed for both human SK-N-MC cells and mouse H20A cells and was either a 12 or a 13 nucleotide deletion in the spacer between the CL and the IRES (Fig. 5). Interestingly, this deletion sequence corresponds to the *EcoRI* linker insertion (originally derived from the parental PN6 virus) which was used for cloning of this virus. On the other hand point mutations 2 and 3 are most likely important for mouse-specific adaptation because they are only present in the mouse cell-adapted isolates. The isolates containing different combination of these changes (R-1235, R-123, R-12 and R-23) were then tested for their growth in different mouse cell lines at various temperatures (Fig. 6). Although they all grew very well at 33^{o}C and 37^{o}C, at 39.5^{o}C they showed growth defects similar to PV1(RIPO).

To distinguish between a tissue specific (neuronal vs non-neuronal) and/or host species specific (mouse vs human) block, the SK-N-MC-and L20B-adapted isolates were evaluated in a crosswise comparison of their growth restriction in L20B and SK-N-MC cells, respectively. The mouse cell-adapted PV1(RIPO) isolate, R-1235, with a replication phenotype nearly identical to wt PV1(M) in mouse cells, also replicated with kinetics similar to wt PV1(M) in SK-N-MC cells (Fig. 7A), whereas human neuron-adapted PV1(RIPO) isolate (R-1) still showed an attenuated phenotype in L20B cells (Fig. 7B). This result indicates that the

deletion in the spacer region alone is not sufficient to restore a high titer growth phenotype in mouse cells, and that the additional point mutations identified in the HRV2 IRES are essential for overcoming the mouse-specific host restriction .

To identify the most effective point mutation(s) in variants of PV1(RIPO) leading to efficient replication in mouse cells (in addition to the deletion mutation), several of the mouse cell-adapted isolates were reconstructed by introducing the most commonly observed point mutation(s) into the 5'NTR of PV1(RIPO). When the deletion and three point mutations were introduced into the parental PV1(RIPO), the resulting reconstructed virus named R-1235r showed growth kinetics similar to that of the adapted isolate R-1235 in L20B cells (data not shown). This observation indicates that all important adaptive mutations are confined to the 5'NTR and that no significant second site reversions exist elsewhere in the genome. A luciferase replicon of R-1235r was then used to examine whether these mutations can restore the translation and replication activity of the replicon RNA in mouse L20B cells. As expected, the PV1(RIPO)-luc replicon failed to show translation and replication activity at higher temp (37^{o}C and 39.5^{o}C) both at early (5 hour) and late (11 hour) time points post transfection (Fig. 8). The PV1(M)-luc replicon exhibited high level of luciferase activity at all the temperatures. Convincingly, the R-1235r-luc replicon exhibited a similar luciferase activity as the PV1(M)-luc replicon, indicating that translation in mouse cells was restored by the adaptive mutations (Fig. 8). This result correlated well with the restoration of the higher growth titer of R-1235r virus in mouse L20B cells.

361 Some additional mutants were constructed *in vitro* by introducing mutations 1,
362 2, 3, and 5 either singly (R-1r, R-2r, R-3r and R-5r) or in combination (R-123r, R-
363 12r and R-35r). All these mutants were then compared with the original adapted
364 isolates for their growth phenotypes (Table 1).
365 **Co-variation between mouse-cell adaptive mutations and mouse**
366 **neurovirulence.** To further assess the relationship between the high-titer growth
367 phenotype of the mouse cell-adapted PV1(RIPO) variants, their equivalent
368 reconstructions, and the neurovirulence in CD155tg mice, groups of 4 CD155tg
369 mice were inoculated via the intracerebral route with 10^2-10^8 PFU (30 μl/mouse),
370 as previously described (11). All mice were observed and scored daily for at least
371 21 days post inoculation for symptoms of poliomyelitis and/or death. Using the
372 data obtained, the mouse paralytic/lethal dose 50 (PLD_{50}) (the virus titer that
373 induces paralysis or death in 50% of the mice) was determined using the method
374 of Reed and Muench (40) (Table 1). As was observed before, PV1(RIPO) was at
375 least 10^6 times less pathogenic in CD155tg mice than wild type PV1(M) (11,13).
376 In fact, a PLD_{50} for PV1(RIPO) could not be established (Table 1) as the virus did
377 not kill at the highest tested dose, whereas the PLD_{50} for PV1(M) was 10^2 PFU.
378 This result correlates with the inability of PV1(RIPO) to replicate in mouse L20B
379 cells (Table 1). In contrast, the mutant virus PN6 with the insertion of 11 nt
380 between the clover leaf and IRES is attenuated in CD155tg mice with a PLD_{50} of
381 $10^{4.7}$ [still by orders higher than PV1(RIPO)], presumably due to the slight
382 replication defect in mouse cells, as seen in $NH3T3^{CD155}$ cells. It should be noted
383 that the replication defect of PN6 in mouse cells is more pronounced when

384 infections are done at a low MOI (0.01), a scenario more akin to the situation a
385 virus might find upon encounter of a host cell in an infected animal.
386 PV1(RIPO) isolates, adapted to grow in mouse H20A cells, exhibited different
387 degrees of neuropathogenicity in CD155tg mice whereas, importantly, the human
388 SK-N-MC cell adapted isolate R-1 was still as neuroattenuated as PV1(RIPO)
389 (Table 1). The mouse-adapted PV1(RIPO) isolates R-1235 and R-123, on the
390 other hand, showed significantly increased neurovirulence over that of the
391 parental PV1(RIPO), which supported the fact that the mutations are not only
392 able to control the high titer replication phenotype in mouse cell tissue culture but
393 also improved neurovirulence in the CD155tg mice. When reconstructed,
394 PV1(RIPO) mutants R-1235r and R-123r show a similar trend in
395 neuropathogenicity, an observation indicating the importance of these mutations
396 (Table 1). Reconstructed mutants R-12r and R-35r, harboring combination of
397 two mutations, are still capable of inducing paralysis and/or death in CD155tg
398 mice but need a relatively higher dose of virus. Mutants R-1r, R-2r, R-3r, and R-
399 5r, which have a single mutation are incapable of improving the
400 neuropathogencity of PV1(RIPO). The conclusion from this study is that the
401 important mutations in the 5'NTR have cumulative effect in neurovirulence in
402 CD155tg mice. For example, in R-1235r they together contribute significantly to
403 render this variant a highly neurovirulent derivative of PV1(RIPO).
404 The deletion of the *EcoRI* linker in PV1(RIPO) was sufficient for the complete
405 restoration of replication in human neuronal cells. This indicates that the neuron-
406 specific defect of PV1(RIPO) is not a result of the choice of the HRV2 IRES to

407 drive translation. It is rather a result of suboptimal spacer length or disruption of
408 an unknown sequence signal or host factor binding site due to the *EcoRI* linker
409 between cloverleaf and IRES. While deletion of *EcoRI* linker alone restored
410 replication in human neuronal cells it did not suffice to restore neurovirulence in
411 CD155tg mice. This is best illustrated by the phenotype of the resulting virus (R-
412 1) retaining the mouse-specific defect, which can be overcome with additional
413 adaptive mutations within the HRV2 IRES (see above).

414 **DISCUSSION**

415 The experiments reported here were designed to further shed light on the
416 mechanism by which the PV1(M) variant PV1(RIPO), a chimera in which the
417 IRES of PV has been exchanged with that of HRV2, expresses its remarkably
418 attenuated phenotype in the spinal cord of non-human primates (13, 6) and in
419 CD155tg mice. The attenuation was discovered when it was observed that the
420 replication of PV1(RIPO) is inhibited in human cells of neuronal origin, such as
421 SK-N-MC (neuroblastoma) cells (11) or HEK293 (Ad transformed neuroepithelial)
422 cells (3) but not in non-neuronal transformed cells such as HeLa cells. It was
423 originally suggested that a specific inhibition of translation is the major cause of
424 attenuation of PV1(RIPO), a hypothesis that is supported by the data presented
425 here. It was subsequently discovered that replication of PV1(RIPO) is *ts* at
426 39.5^{o}C in neuroblastoma cells but not in HeLa or HTB-14 glioblastoma cells (5).
427 In addition to tissue-specific restriction (observed in human tissues of different
428 origin) we have now found that there is also a strong species-specific restriction
429 of the growth of PV1(RIPO) at physiological temperature: in contrast to wt

PV1(M), this chimera does not replicate in NIH 3T3^{CD155}, L20B^{CD155} or N2a^{CD155} cells, three mouse cell lines stably transformed with the poliovirus receptor CD155 (see Materials and Methods). The block in replication is enhanced at 39.5^{o}C but, remarkably, it is absent at 33^{o}C (Fig. 3). These data, which have been obtained by two different investigators with the different cell lines at different times, are highly reproducible. They are, nevertheless, at variance with a report by Kauder *et. al.* (20) in which a construct very similar to PV1(RIPO) was found to replicate in L20B cells, albeit with much delayed kinetics. The exquisite temperature sensitivity observed here, and in particular the rescue of the *ts* phenotype at temperatures below 37^{o}C, may be the reason why this phenomenon has eluded us in an earlier study (11), during which incubation temperatures may not have been tightly controlled at perhaps less than 37^{o}C.

The replication of human rhinoviruses is broadly restricted in mouse cells. However, host range variants of HRV2 (50) and HRV 39 (27) that bypassed the block in mouse L cells have been reported to produce 2C protein with altered electrophoretic mobility. Harris *et. al.* (14, 15) have shown more recently that these host cell restrictions can be overcome by specific mutations in proteins mapping to the P2/P3 non-structural region of the genome. However, in the background of a full length rhinovirus genome, no mouse-adaptive mutations were ever reported to localize to the IRES. The mouse specific mutations in the HRV2 IRES, observed here, suggests to us that the poliovirus replication machinery may interact poorly with the PV1(RIPO) 5'NTR at some stage during the viral life cycle. This may also explain why the remarkable host restriction is

453 only seen in the context of a PV genome (full length or replicon), but apparently
454 not IRES driven reporter constructs (19, 3).
455 This conclusion is supported by our translation experiments using Luciferase
456 expressing PV replicons (Fig. 4) which indicate that the lack of translational
457 activity in mouse cells is the most likely reason for the observed phenotype of
458 PV1(RIPO). In hindsight it is perhaps not surprising that the HRV2 IRES in a PV
459 background brings about a *ts* phenotype (at least in some cell types), as IRES
460 function is likely to be optimized at the natural replication temperature of
461 rhinoviruses of approximately 33^{o}C.
462 Assays with reporter genes, however, call for cautious interpretation of the
463 data. Campbell *et. al.* (3) have reported that assays with IRES-driven Luciferase
464 reporter constructs that consisted only of the HRV-2 IRES and the reporter gene,
465 did express Luc well (or even better) in HEK293 or SK-N-MC cells than the
466 equivalent PV IRES driven reporter constructs. The authors comment that the
467 “results indicate that translation in a reporter context does not recapitulate the
468 neuron-specific functional deficit of the HRV2 IRES in the context of the PV
469 genome” (3). If so, the results of the interesting IRES studies of Kauder *et. al.*
470 (19, 20) using dicistronic reporter mRNA produced by an adenovirus might not
471 have yielded results that can be interpreted to reflect IRES tropism or
472 attenuation. On the other hand, it is intriguing to speculate that the non-structural
473 proteins have to cooperate with the IRES to facilitate maximal expression of the
474 polyprotein, and that this expression is dependent also on “IRES translation
475 activating factors” (ITAFs) (N. Jahan and S. Mueller, unpublished results).

476 Our work demonstrates that changes in the 5'NTR alone, particularly the
477 mutations in the HRV2 IRES, are sufficient to rescue HRV2 IRES-mediated
478 translation in mouse cells and, consequently, RNA replication in mouse L cells.
479 Most importantly, these mutations were not only able to rescue the defective
480 growth of PV1(RIPO) in mouse cells but also to produce a highly neurovirulent
481 virus in CD155tg mice.
482 Previous studies (11, 13) showed that the PV1(RIPO) IRES containing
483 domains V and VI of the PV1(M) IRES exhibited the same neurovirulence as
484 PV1(M) in CD155tg mice. This observation suggested that both of these domains
485 of the PV1(M) IRES are required for mouse neurovirulence. Subsequently, they
486 have extended these studies using chimeric IRES constructs and using human
487 HEK293 cells as indicator cells for neurovirulence. In these studies, domain VI of
488 the IRES was dispensable for the expression of attenuation but the entire domain
489 V was required for a growth phenotype of PV1(RIPO) in HEK293 cells (3). In the
490 study presented here, the focus was on the genetics of the expression of
491 conditional phenotypes (*ts*) and of the host range of PV1(RIPO). We have
492 confirmed that PV1(RIPO) is restricted in human neuroblastoma and HEK293
493 cells at 37^{o}C and we describe that the replication of the chimera at 39.5^{o}C is
494 severely inhibited. In mouse cells, however, regardless of whether they originate
495 from neuronal (N2a^{CD155}) or non-neuronal (L20B and NIH 3T3^{CD155}) precursors,
496 PV1(RIPO) is unable to replicate to any measurable level at 37^{o}C or 39.5^{o}C.
497 Interestingly, PV1(RIPO) can grow in any of the mouse cells analyzed with wt PV

498 kinetics at 33^{o}C, an observation suggesting that there is “nothing wrong” with the
499 basic design of a replicating poliovirus in mouse cells.
500 In this regard, it did not matter whether the mouse cells were of neuronal
501 origin (N2a^{CD155}) or non-neuronal origin (L20B, NIH 3T3^{CD155}). Thus, besides the
502 previously described defect in human neuronal cells (11, 5) PV1(RIPO) displays
503 an exquisite mouse specific block in propagation. In fact, the mouse specific
504 defect may contribute significantly to the tremendous attenuation of PV1(RIPO)
505 seen in CD155tg mice. Our results serve to caution investigators as to the
506 interpretation of pathogenicity data obtained with PV variants in the transgenic
507 mouse models. Attenuation of PV variants in CD155tg mice should be
508 corroborated by the absence of a replication block in tissue culture of CD155
509 expressing mouse cells, such as the widely available L20B.
510 In spite of the low apparent proliferation of PV1(RIPO) in mouse cells or
511 neuroblastoma cells at 37^{o}C, serial blind passages produced novel genotypes
512 adapted to replication in these restrictive cells to varying degrees. Sequence
513 analyses of the 5'NTR of the new variants identified mutations responsible not
514 only for efficient growths in mouse cells but also for inducing paralysis and/or
515 death in CD155tg mice.
516 Interestingly, 6 out of 9 isolates from separate passage in human SK-N-MC
517 cells and mouse H20A cells possess a common mutation (mutation 1), which is
518 either a 12 or a 13 nucleotide deletion (AGGAATTCAACT or
519 AGGAATTCAACTT) in the spacer I between the cloverleaf and IRES (Fig. 5).
520 This deletion contains the *EcoRI* restriction site (GAATTC), which was introduced

521 into the linker sequence between the clover leaf and the IRES (47) (strain PN6),
522 a construct used as parent virus of PV1(RIPO) (Fig. 1). While the striking
523 neuroattenuation of PV1(RIPO) in CD155tg mice correlates with it's inability to
524 replicate in SK-N-MC neuroblastoma cell line (Fig. 7) variant R-1 grew well in SK-
525 N-MC cells but still replicated only poorly in mouse L20B cells (Fig. 7). In
526 keeping with this trend, R-1 still showed high degree of neuroattenuation in
527 CD155tg mice (Table 1). Replication in a human neuronal cell (SK-N-MC) and
528 neurovirulence in CD155tg mice, therefore, do not co-vary. As has been pointed
529 out before by Campbell *et. al.* (3), assays in neuronal tissue culture cells alone
530 may not be a reliable indicator of neurovirulence.
531 The selection of R-1 variants indicates that the inserted linker sequence is not
532 neutral in SK-N-MC or in mouse cells. In the context of poliovirus propagated in
533 HeLa cells, however, the insertion appears to be stable presumably because the
534 advantage of deleting it is very small under these conditions. The deletion
535 restores both the sequence and the length of a highly conserved region
536 (GTAACTTAGAAG) in PV and HRV genomes between the clover leaf and IRES
537 (Fig. 9 and supplementary Fig. 1). Similar observations by De Jesus *et. al.* (7)
538 have indicated an abundance of conserved nucleotides amongst different PV
539 serotypes and human C-cluster coxsackie A viruses in this region although the
540 significance of these conserved regions is not known. It should be noted that we
541 have previously found hotspots in the short spacer that are important for RNA
542 synthesis (45) or essential for neurovirulence in mice (4, 7, 46).

543 Mutation 2 (R-2), a C133G transversion, was observed in 5 out of 7 H20A
544 adapted isolates (Fig. 5). It maps downstream of a highly conserved sequence of
545 six nt (CAATAG) in domain II of the IRES that is found in different PV serotypes
546 and different HRV serotypes (Fig. 9 and supplementary Fig. 1). Interestingly, a
547 transition A133G was observed at the same position by Shiroki *et. al.* (42), when
548 a heat-resistant mutant was isolated by serial passage at 40^{o} C of wild type PV in
549 L cells expressing the PV receptor CD155. Remarkably, Toyoda *et. al.* (46) also
550 reported an A133G transition when a poliovirus carrying the cis acting element
551 *cre* in the spacer region (mono-*cre*PV) was either passaged in mouse N2a^{CD155}
552 cells or isolated from a mouse tumor (neuroblastoma). Again, the 133 mutation
553 was responsible for the increased replication of this A_{133}Gmono-crePV1 variant,
554 as compared to mono-*cre*PV in mouse N2a$^{CD155\alpha}$ cells. These observations,
555 together with the R-2 mutation reported here, indicate that a G residue in position
556 133 favors replication in mouse cells and is, thus, a host range mutation.
557 The mechanism by which certain poliovirus derivatives express an attenuated
558 phenotype is poorly understood. In our view, the IRES does play an important
559 role in this process. In the three Sabin vaccine strains, a point mutation in each of
560 the domain V has been implicated in contributing to attenuation and there are
561 numerous experiments in support of this assertion (49, 21). Gromeier and his
562 colleagues have dissected the HRV2 IRES in the context of the poliovirus
563 background (11, 13) and have recently come to the conclusion that the V
564 domain alone is the structure that confers the low replication phenotype to
565 PV1(RIPO) if “attenuation” assayed in HEK293 cells (3). Merrill *et. al.* (32) and

566 Merrill and Gromeier (33) have presented evidence that a double-stranded RNA
567 binding protein (DRBP76) is responsible for *trans*-dominant repression of
568 PV1(RIPO) in neuronal cells but the locus of binding of this protein to the HRV2
569 IRES has not yet been determined.

570 Is domain V of the IRES in PV1(RIPO) involved in regulating viral proliferation
571 in mouse cells? As seen in Fig. 5 only three mutations (R-4, -5, -6) were found to
572 map to domain V in variants isolated after blind passages. Genetic analyses of
573 mutant combinations showed that these mutations were not required for other
574 variants to regain replication in mouse cells (see constructs R-12 and R-123; Fig.
575 6) although variant R-1235 has regained the highest replication ability.
576 Neurovirulence tests in CD155tg mice co-varied with replication capabilities in
577 tissue culture cells of the mutant combinations (Table 1). Because of this co-
578 variation, neurovirulence tests of the chimeric virus in CD155tg mice do not allow
579 us to draw conclusions about the attenuation phenotype of PV1(RIPO) in these
580 transgenic animals. One striking point remains to be made. All the variants,
581 isolated after serial passages and after reconstructing into cDNA, resulting
582 viruses retain their *ts* phenotype at 39.5^{o}C. This phenotype is similar to the *ts*
583 phenotype of PV1(RIPO) in SK-N-MC cells. Surprisingly, under the conditions of
584 the experiments, the *ts* phenotypes of the various variants do not prevent their
585 killing of the animals at low PLD_{50}.

586 **ACKNOWLEDGEMENTS**

587 We are deeply indebted to Aniko Paul for help and suggestions during the
588 preparation of this manuscript. The authors would like to thank Reinhold Welker,

589 Yixin Fu, and Sean Connolly for their contribution to aspects of this project over
590 the years. This work was supported by NIH Grants 5R01AI03948508,
591 5R37AI01512233 to Eckard Wimmer.

592 **REFERENCES**

593 1. **Alexander L., H. H. Lu, and E. Wimmer.** 1994. Polioviruses containing
594 picornavirus type 1 and/or type 2 IRES elements: genetic hybrids and the
595 expression of a foreign gene. Proc. Natl. Acad. Sci. USA **91:**1406-1410.
596 2. **Caliguiri, L. A., and I. Tamm.** 1968. Action of guanidine on the replication of
597 poliovirus RNA. Virology **35(3):**408-417.
598 3. **Campbell, S. A., J. Lin, E. Y. Dobrikova, and M. Gromeier.** 2005. Genetic
599 determinants of cell type-specific poliovirus propagation in HEK 293 cells. J.
600 Virol. **79(10):**6281-6290.
601 4. **Cello, J., A. Paul, and E. Wimmer.** 2002. Chemical synthesis of poliovirus
602 cDNA: generation of infectious virus in the absence of natural template.
603 Science **297:**1016-1018.
604 5. **Cello, J., H. Toyoda, N. De Jesus, E. Y. Dobrikova, M. Gromeier, and E.**
605 **Wimmer.** 2008. Growth phenotypes and biosafety profiles in poliovirus-
606 receptor transgenic mice of recombinant oncolytic polio/human rhinoviruses.
607 J. Med. Virol. **80:**352-359.
608 6. **Chumakov, K., E. Dragunsky, A. Ivshina, J. Enterline, V. Wells, T.**
609 **Nomura, M. Gromeier, and E. Wimmer.** 2001. Inactivated vaccines based
610 on alternatives to wild-type seed virus. Dev. Biol. (Basel) **105:**171-177.

7. **De Jesus, N., D. Franco, A. Paul, E. Wimmer, and J. Cello.** 2005. Mutation of a single conserved nucleotide between the cloverleaf and internal ribosome entry site attenuates poliovirus neurovirulence. J. Virol. **79(22):**14235-14243.
8. **Dobrikova, E., P. Florez, S. Bradrick, and M. Gromeier.** 2003. Activity of a type 1 picornavirus internal ribosomal entry site is determined by sequences within the 3' nontranslated region. Proc. Natl. Acad. Sci. USA **100(25):**15125-15130.
9. **Ehrenfeld, E., and N. L. Teterina.** 2002. Initiation of translation of picornavirus RNAs: structure and function of the internal ribosome entry site, p. 159-169. *In* B. L. Semler and E. Wimmer (ed), Molecular Biology of Picornaviruses. ASM Press, Washington, DC.
10. **Freistadt, M. S., G. Kaplan, and V. R. Racaniello.** 1990. Heterogeneous expression of poliovirus receptor-related proteins in human cells and tissues. Mol. Cell. Biol. **10(11):**5700-5706.
11. **Gromeier, M., L. Alexander, and E. Wimmer.** 1996. Internal ribosomal entry site substitution eliminates neurovirulence in intergeneric poliovirus recombinants. Proc. Natl. Acad. Sci. USA **93:**2370–2375.
12. **Gromeier M, S. Mueller, D. Solecki, B. Bossert, G. Bernhardt, and E. Wimmer.** 1997. Determinants of poliovirus neurovirulence. J. Neurovirol. **3 Suppl 1:**S35-S38.
13. **Gromeier, M., B. Bossert, M. Arita, A. Nomoto, and E. Wimmer.** 1999. Dual stem loops within the poliovirus internal ribosomal entry site control neurovirulence. J. Virol. **73(2):**958-964.

14. **Harris, J. R., and V. R. Racaniello.** 2003. Changes in rhinovirus protein 2C allow efficient replication in mouse cells. J. Virol. **77(8):**4773-4780.
15. **Harris, J. R., and V. R. Racaniello.** 2005. Amino acid changes in proteins 2B and 3A mediate rhinovirus type 39 growth in mouse cells. J. Virol. **79(9):**5363-5373.
16. **Ida-Hosonuma, M., T. Iwasaki, T. Yoshikawa, N. Nagata, Y. Sato, T. Sata, M. Yoneyama, T. Fujita, C. Taya, H. Yonekawa, and S. Koike.** 2005. The alpha/beta interferon response controls tissue tropism and pathogenicity of poliovirus. J. Virol. **79:**4460–4469.
17. **Jacobson, M. F., and D. Baltimore.** 1968. Morphogenesis of poliovirus. I. Association of the viral RNA with coat protein. J. Mol. Biol. **33(2)**:369-378.
18. **Jang, S. K., H. G. Kräusslich, M. J. Nicklin, G. M. Duke, A. C. Palmenberg, and E. Wimmer.** 1988. A segment of the 5' nontranslated region of encephalomyocarditis virus RNA directs internal entry of ribosomes during in vitro translation. J. Virol. **62(8):**2636-2643.
19. **Kauder, S. E., and V. R. Racaniello.** 2004. Poliovirus tropism and attenuation are determined after internal ribosome entry. J. Clin. Invest. **113(12):**1743-1753.
20. **Kauder, S., S. Kan, and V. R. Racaniello.** 2006. Age-dependent poliovirus replication in the mouse central nervous system is determined by internal ribosome entry site-mediated translation. J. Virol. **80(6):**2589-2595.

21. **Kew, O. M., R. W. Sutter, E. M. de Gourville, W. R. Dowdle, and M. A. Pallansch.** 2005. Vaccine-derived polioviruses and the endgame strategy for global polio eradication. Annu. Rev. Microbiol. **59:**587-635.
22. **Koike, S., H. Horie, I. Ise, A. Okitsu, M. Yoshida, N. Iizuka, K. Takeuchi, T. Takegami, and A. Nomoto.** 1990. The poliovirus receptor protein is produced both as membrane-bound and secreted forms. EMBO J. **9(10):**3217-3224.
23. **Koike, S., C. Taya, T. Kurata, S. Abe, I. Ise, H. Yonekawa, and A. Nomoto.** 1991. Transgenic mice susceptible to poliovirus. Proc. Natl. Acad. Sci. USA **88(3):**951-955.
24. **La Monica, N., and V. R. Racaniello.** 1989. Differences in replication of attenuated and neurovirulent polioviruses in human neuroblastoma cell line SH-SY5Y. J. Virol. **63(5):**2357-2360.
25. **Li, X., H. H. Lu, S. Mueller, and E. Wimmer.** 2001. The C-terminal residues of poliovirus proteinase 2A(pro) are critical for viral RNA replication but not for cis- or trans-proteolytic cleavage. J. Gen. Virol. **82(Pt 2):**397-408.
26. **Loddo, B., W. Ferrari, G. Brotzu, and A. Spanedda.** 1962. In vitro inhibition of infectivity of polio viruses by guanidine. Nature **193:**97-98.
27. **Lomax, N. B., and F. H. Yin.** 1989. Evidence for the role of the P2 protein of human rhinovirus in its host range change. J. Virol. **63(5):**2396-2399.
28. **Lu, H. H., and E. Wimmer.** 1996. Poliovirus chimeras replicating under the translational control of genetic elements of hepatitis C virus reveal unusual

properties of the internal ribosomal entry site of hepatitis C virus. Proc. Natl. Acad. Sci. USA **93:**1412-1417.

29. **Macadam, A. J., S. R. Pollard, G. Ferguson, G. Dunn, R. Skuce, J.W. Almond, and P.D. Minor.** 1991. The 5' noncoding region of the type 2 poliovirus vaccine strain contains determinants of attenuation and temperature sensitivity. Virology **181(2):**451-458.

30. **Macadam, A. J., G. Ferguson, J. Burlison, D. Stone, R. Skuce, J.W. Almond, and P.D. Minor.** 1992. Correlation of RNA secondary structure and attenuation of Sabin vaccine strains of poliovirus in tissue culture. Virology **189(2):**415-422.

31. **Mendelsohn, C. L., E. Wimmer, and V. R. Racaniello.** 1989. Cellular receptor for poliovirus: molecular cloning, nucleotide sequence, and expression of a new member of the immunoglobulin superfamily. Cell **56:**855-865.

32. **Merrill, M. K., E. Y. Dobrikova, and M. Gromeier.** 2006. Cell-type-specific repression of internal ribosome entry site activity by double-stranded RNA-binding protein 76. J. Virol. **80(7):**3147-3156.

33. **Merrill, M. K., and M. Gromeier.** 2006. The double-stranded RNA binding protein 76:NF45 heterodimer inhibits translation initiation at the rhinovirus type 2 internal ribosome entry site. J. Virol. **80(14):**6936-6942.

34. **Molla, A., A. V. Paul, and E. Wimmer.** 1991. Cell-free, de novo synthesis of poliovirus. Science **254(5038):**1647-1651.

699 35. **Mueller, S., and E. Wimmer.** 2003. Recruitment of nectin-3 to cell-cell
700 junctions through trans-heterophilic interaction with CD155, a vitronectin and
701 poliovirus receptor that localizes to alpha(v)beta3 integrin-containing
702 membrane microdomains. J. Biol. Chem. **278(33):**31251-31260.
703 36. **Mueller, S., D. Papamichail, J. R. Coleman, S. Skiena, and E. Wimmer.**
704 2006. Reduction of the rate of poliovirus protein synthesis through large-scale
705 codon deoptimization causes attenuation of viral virulence by lowering
706 specific infectivity. J. Virol. **80(19):**9687-9696.
707 37. **Paul, A. V.** 2002. Possible unifying mechanism of picornavirus genome
708 replication, p. 227-246. *In* B. L. Semler and E. Wimmer (ed.), Molecular
709 Biology of Picornaviruses. ASM Press, Washington, DC.
710 38. **Pelletier, J., and N. Sonenberg.** 1988. Internal initiation of translation of
711 eukaryotic mRNA directed by a sequence derived from poliovirus RNA.
712 Nature **334(6180):**320-325.
713 39. **Pipkin, P. A., D. J. Wood, V. R. Racaniello, and P. D. Minor.** 1993.
714 Characterisation of L cells expressing the human poliovirus receptor for the
715 specific detection of polioviruses in vitro. J. Virol. Methods **41(3):**333-340.
716 40. **Reed, L. J., and M. Muench.** 1938. A simple method for estimating fifty
717 percent endpoints. Am. J. Hyg. **27:**493-497.
718 41. **Ren, R., F. Costantini, E. J. Gorgacz, J. J. Lee, and V. R. Racaniello.**
719 1990. Transgenic mice expressing a human poliovirus receptor: a new model
720 for poliomyelitis. Cell **63:**353-362.

721 42. **Shiroki, K., T. Ishii, T. Aoki, M. Kobashi, S. Ohka, and A. Nomoto.** 1995. A
722 new cis-acting element for RNA replication within the 5' noncoding region of
723 poliovirus type 1 RNA. J. Virol. **69(11):**6825-6832.
724 43. **Svitkin, Y. V., S. V. Maslova, and V. I. Agol.** 1985. The genomes of
725 attenuated and virulent strains differ in their in vitro translation efficiencies.
726 Virology **147(2):** 243-252.
727 44. **Svitkin, Y. V., N. Cammack, P. D. Minor, and J. W. Almond.** 1990.
728 Translation deficiency of the Sabin type 3 poliovirus genome: association with
729 an attenuating mutation C472----U. Virology **175(1):**103-109.
730 45. **Toyoda, H., D. Franco, K. Fujita, A. V. Paul, and E. Wimmer.** 2007.
731 Replication of poliovirus requires binding of the poly(rC) binding protein to the
732 cloverleaf as well as to the adjacent C-rich spacer sequence between the
733 cloverleaf and the internal ribosomal entry site. J. Virol. **81(18):**10017-10028.
734 46. **Toyoda, H., J. Yin, S. Mueller, E. Wimmer, and J. Cello**. 2007. Oncolytic
735 treatment and cure of neuroblastoma by a novel attenuated poliovirus in a
736 novel poliovirus-susceptible animal model. Canc. Res. **67:**2857 – 2864.
737 47. **Trono, D., R. Andino, and D. Baltimore.** 1988. An RNA sequence of
738 hundreds of nucleotides at the 5' end of poliovirus RNA is involved in allowing
739 viral protein synthesis. J. Virol. **62(7):**2291-2299.
740 48. **van der Werf, S., J. Bradley, E. Wimmer, F. W. Studier, and J. J. Dunn.**
741 1986. Synthesis of infectious poliovirus RNA by purified T7 RNA polymerase.
742 Proc. Natl. Acad. Sci. USA **78:**2330-2334.

743 49. **Wimmer, E., C. U. T. Hellen, and X. M. Cao.** 1993. Genetics of poliovirus.
744 Ann. Rev. Genet. **27:**353-436.
745 50. **Yin, F. H., and N. B. Lomax.** 1983. Host range mutants of human rhinovirus
746 in which nonstructural proteins are altered. J. Virol. **48(2):**410-418.
747 51. **Yin, J., A. V. Paul, E. Wimmer, and E. Rieder.** 2003. Functional dissection
748 of a poliovirus *cis*-acting replication element [PV-cre(2C)]: analysis of single-
749 and dual-cre viral genomes and proteins that bind specifically to PV-cre RNA.
750 J. Virol. **77:**5152–5166.
751

751 **FIGURE LEGENDS**

752

753 **FIG. 1:** A. Genetic structure of the 5'NTRs of PV1(M), PN6, and PV1(RIPO).
754 Poliovirus open reading frame (open arrows), AUG initiation codon, the cloverleaf
755 (CL), the IRES, spacer I (S-I) and spacer-II are indicated. The linker sequence of
756 11 nt. containing the *EcoRI* restriction site shown with a black square was
757 inserted in S-I of PV1(M) between nt. 108 and 109 to construct PN6 virus. B.
758 One step growth curves of PV1(M), PN6, and PV1(RIPO) in HeLa R19 cells.
759 Cells were infected at a MOI of 10 and incubated at 33^{o}C, 37^{o}C, and 39.5^{o}C. The
760 virus titers were determined by plaque assay on monolayers of HeLa R19 cells,
761 as described in Materials and Methods.

762

763 **FIG. 2:** One step growth curves of PV1(M), PN6, and PV1(RIPO) in Human
764 neuronal cell lines, SK-N-MC (A), HEK293 (B), and SK-N-SH (C). Cells were
765 infected at a MOI of 10 and incubated at 33^{o}C, 37^{o}C, and 39.5^{o}C. The virus titers
766 were determined by plaque assay on monolayers of HeLa R19 cells, as
767 described in Materials and Methods.

768

769 **FIG. 3:** One step growth curves of PV1(M), PN6, and PV1(RIPO) in mouse cell
770 lines, N2a^{CD155} (A), L20B (B), and NIH 3T3^{CD155}(C). Cells were infected at a MOI
771 of 10 and incubated at 33^{o}C, 37^{o}C, and 39.5^{o}C. The virus titers were determined
772 by plaque assay on monolayers of HeLa R19 cells, as described in Materials and
773 Methods.

774

775 **FIG. 4:** RNA translation and replication of PV1(RIPO)-luc and PV1(M)-luc
776 replicons. Monolayers of HeLa R19 cells (A), SK-N-MC cells (B), and mouse
777 L20B cells (C) were transfected with *in vitro* transcribed RNA of poliovirus
778 luciferase replicons and incubated at 33^{o}C, 37^{o}C and 39.5^{o}C in the presence (for
779 translation) or in the absence (for replication) of 2mM guanidine hydrochloride
780 (GuHCl). RNA translation and RNA replication were assessed by measuring the
781 luciferase activity at different time point post transfection.

782

783 **FIG. 5:** Genetic analyses of the 5'NTR nucleotide sequences of the adapted
784 isolates of PV1(RIPO). (A) The isolates name and the mutation(s) they carry are
785 indicated. The mutations found are numbered according to their position in the
786 5'NTR starting from the 5'end. The number in parentheses show the number of
787 isolates out of total isolates containing any particular mutation. The sequence of
788 deletion for mutation 1 is shown. (B) List of the mutations, including their location
789 in the 5'NTR, and the nucleotide changes of the variants.

790

791 **FIG. 6:** Growth of PV1(RIPO) and selected L20B cell adapted isolates in mouse
792 cell lines, L20B (A), NIH 3T3^{CD155} (B), and N2a^{CD155} (C). Cells were infected at a
793 MOI of 10 and incubated at 33^{o}C, 37^{o}C, and 39.5^{o}C. The virus titers were
794 determined by plaque assay on monolayers of HeLa R19 cells, as described in
795 Materials and Methods.

796

FIG. 7: Evaluation of species-specific growth restriction of mouse cell-adapted and human neuronal cell-adapted isolates of PV1(RIPO). Human neuronal cell-adapted (R-1) and mouse fibroblast-adapted (R-1235) variants of PV1(RIPO) were used to infect human SK-N-MC cells (A) or mouse L20B cell at a MOI of 10 and incubated at 37^{o}C. The virus titers at various time points were determined by plaque assay on monolayers of HeLa R19 cells, as described in Materials and Methods. Mouse-adapted variant R-1235 completely restores replication competency on human neuronal cells, while neuron-adapted variant R-1 does not.

FIG. 8: RNA translation and replication of R-1235r-luc replicon in L20B cells. Monolayers mouse L20B cells were transfected with *in vitro* transcribed RNA of luciferase replicons and incubated at 33^{o}C, 37^{o}C and 39.5^{o}C in the presence (for translation) or in the absence (for replication) of 2 mM guanidine hydrochloride (GuHCl). RNA translation and RNA replication were assessed by measuring the luciferase activity at 5 and 11 hr post transfection.

FIG. 9: Sequence alignments of spacer I and part of stem-loop-II in the 5' NTR of human enteroviruses and human rhinoviruses, reveals a highly conserved sequence motif. Nucleotides in red, blue and black color represent nucleotides highly, moderately and not conserved among the viruses respectively. Dashes denote nucleotides missing in any particular virus. Part of the PV1(RIPO) sequence, representing Mutation 1 (13 nt deletion) in the adapted isolates has

been shown on the top as an extra sequence in PV1(RIPO). M, Mahoney; La, Lansing; Le, Leon. Alignments were done using Multalin (http://bioinfo.genotoul.fr/multalin/multalin.html)

**It should be noted that recently the genus Rhinovirus was incorporated into the Enterovirus genus (www.picornavirus.com)

TABLE 1: Neurovirulence study in CD155tg mice.

Virus(PFU)	PLD_{50} [a]	Relative increase in PLD_{50} [b]	Fold increase in virus titer on L20B cells [c]
PV1(RIPO)	$>10^{8}$ [d]	1	0.5
R-1	$\geq 10^{8}$ [d]	≤ 1	960
R-1r	ND	ND	400
R-2r	$>10^{8}$ [d]	1	140
R-3r	$>10^{7}$ [d]	<10	0.3
R-5r	$>10^{7}$ [d]	<10	5.7
R-35r	10^{7}	10	7,500
R-12r	10^{6}	100	8,400
R-23	$10^{5.5}$	316	12,000
R-123	10^{5}	1,000	22,000
R-123r	$10^{5.3}$	501	30,000
R-1235	10^{3}	100,000	130,000
R-1235r	$10^{3.2}$	63,096	100,000
PN6	$10^{4.7}$	1,995	16,000
PV1(M)	10^{2}	1,000,000	250,000

[a] Groups of four mice were infected intracerebrally with a given amount of virus. PLD_{50} values were calculated by the method of Reed and Muench .

[b] Relative increase in PLD_{50} was calculated by considering PLD_{50} of PV1(RIPO) as 1

[c] Fold increase virus titer in L20B cells after 24 hour infection at 10 MOI as compared with titer at 0 hour post infection

[d] LD50 could not be determined as no mice died at highest dose in oculated

837 ND: Not determined

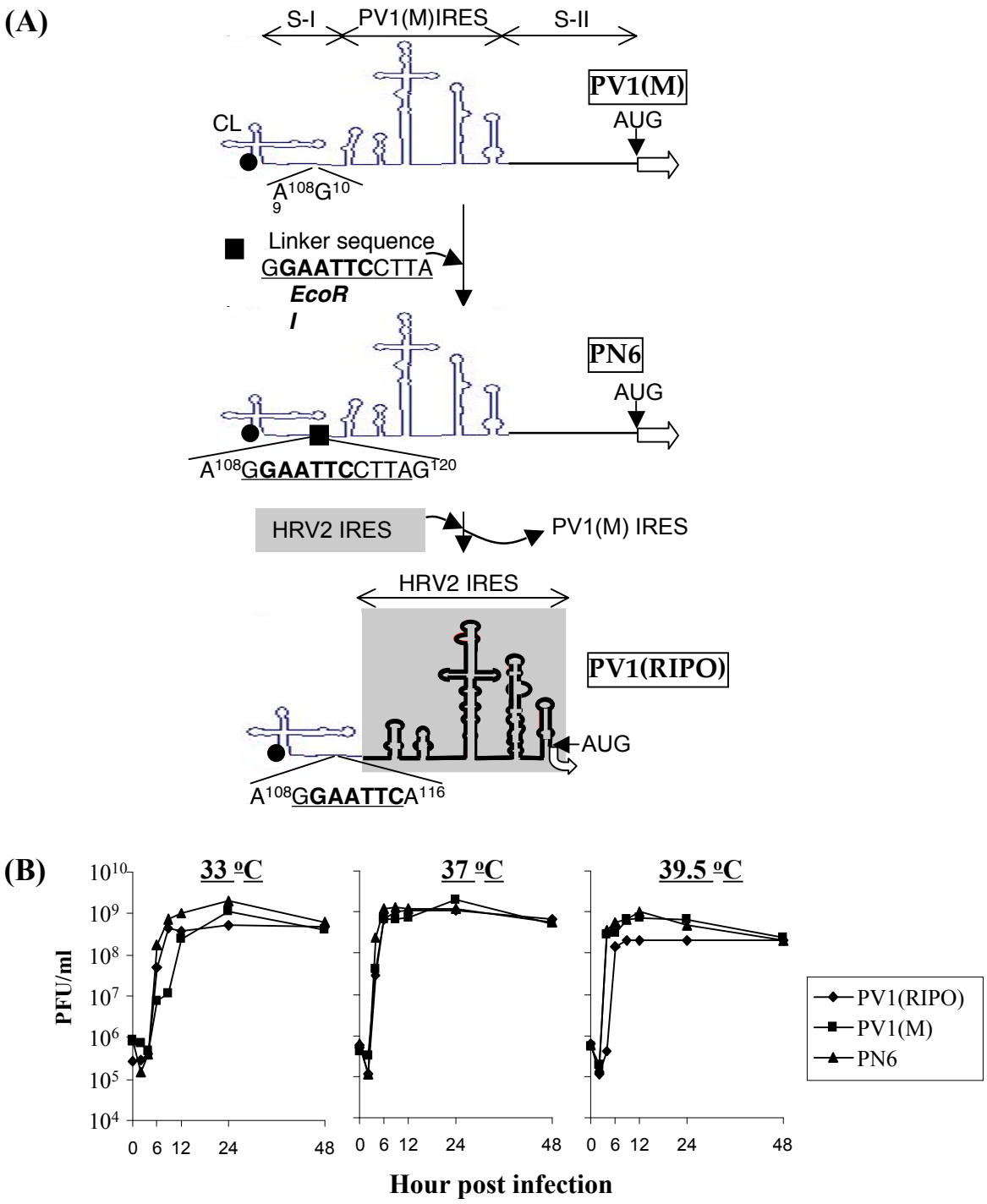

Jahan et al., FIG. 1

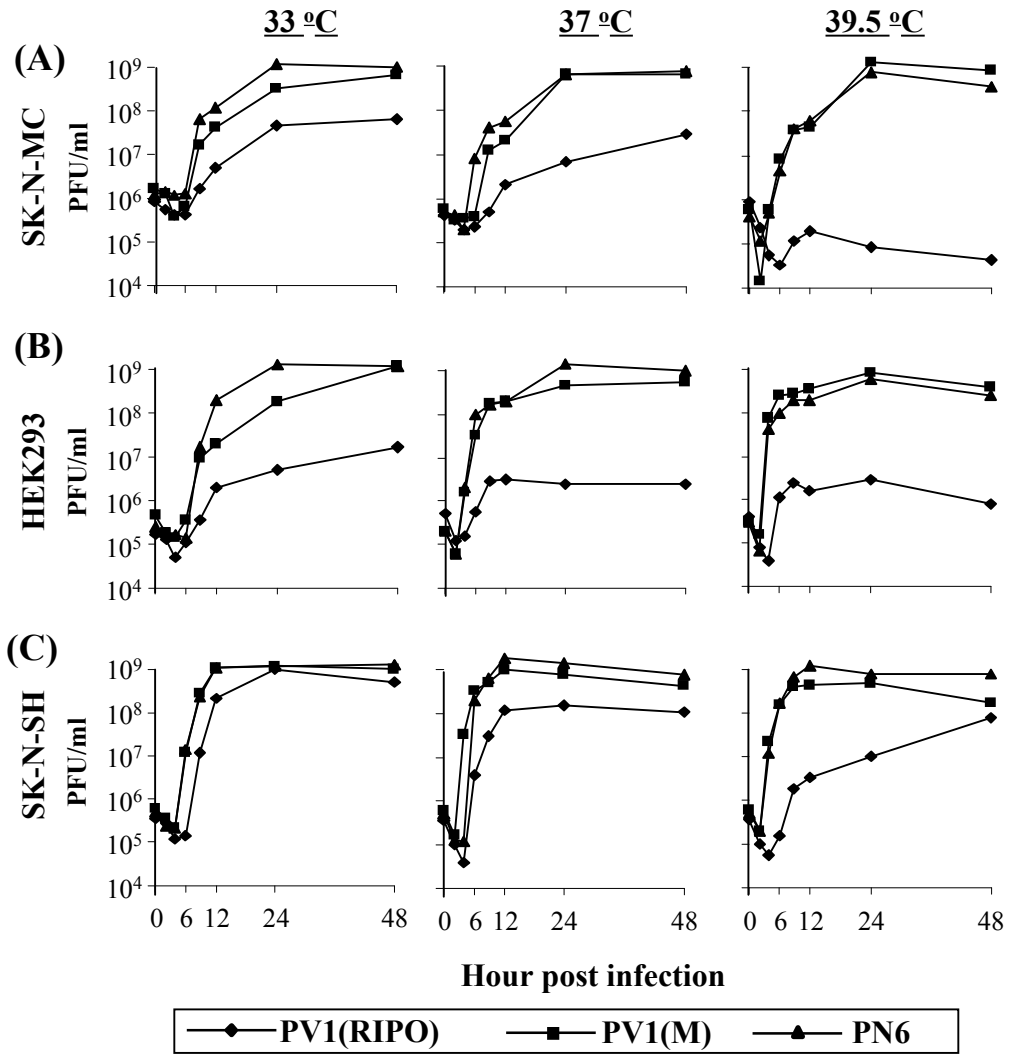

Jahan et al., FIG. 2

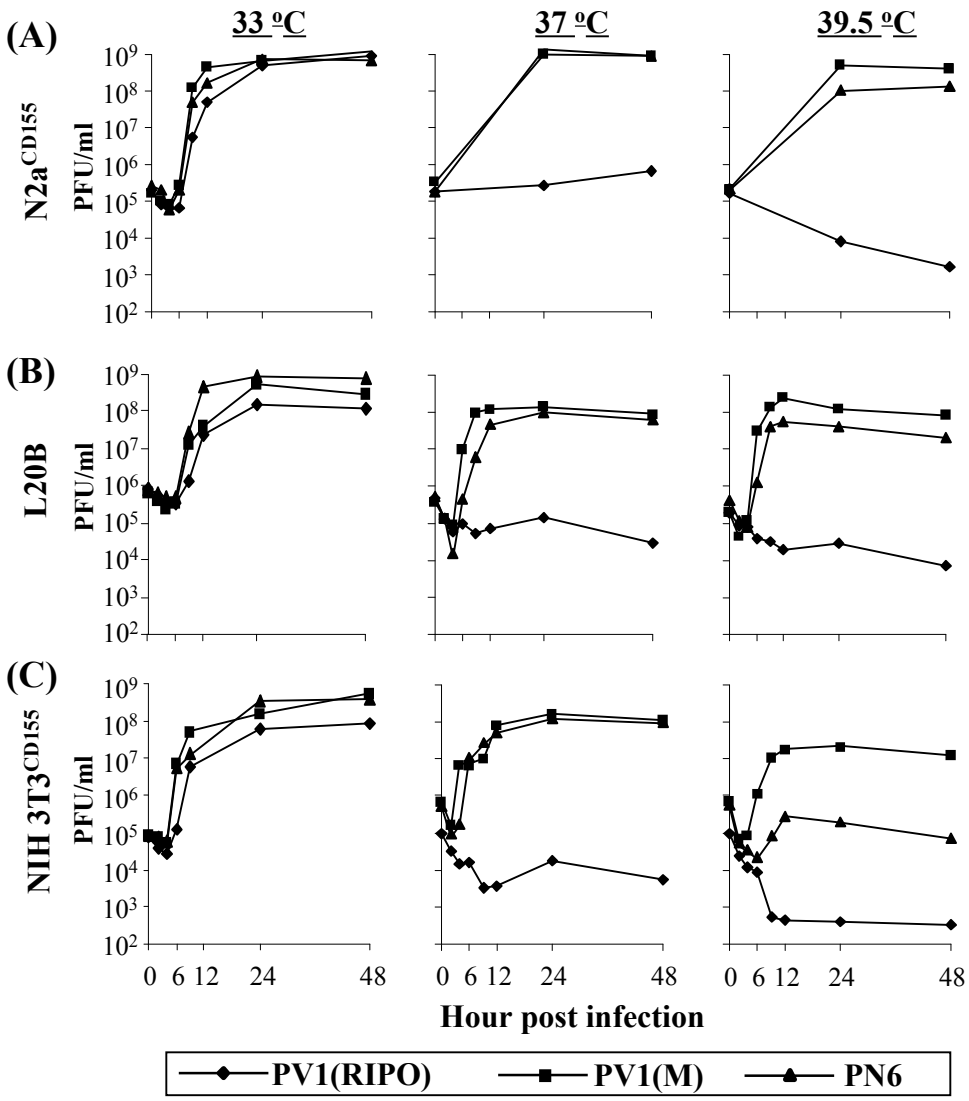

Jahan et al., FIG. 3

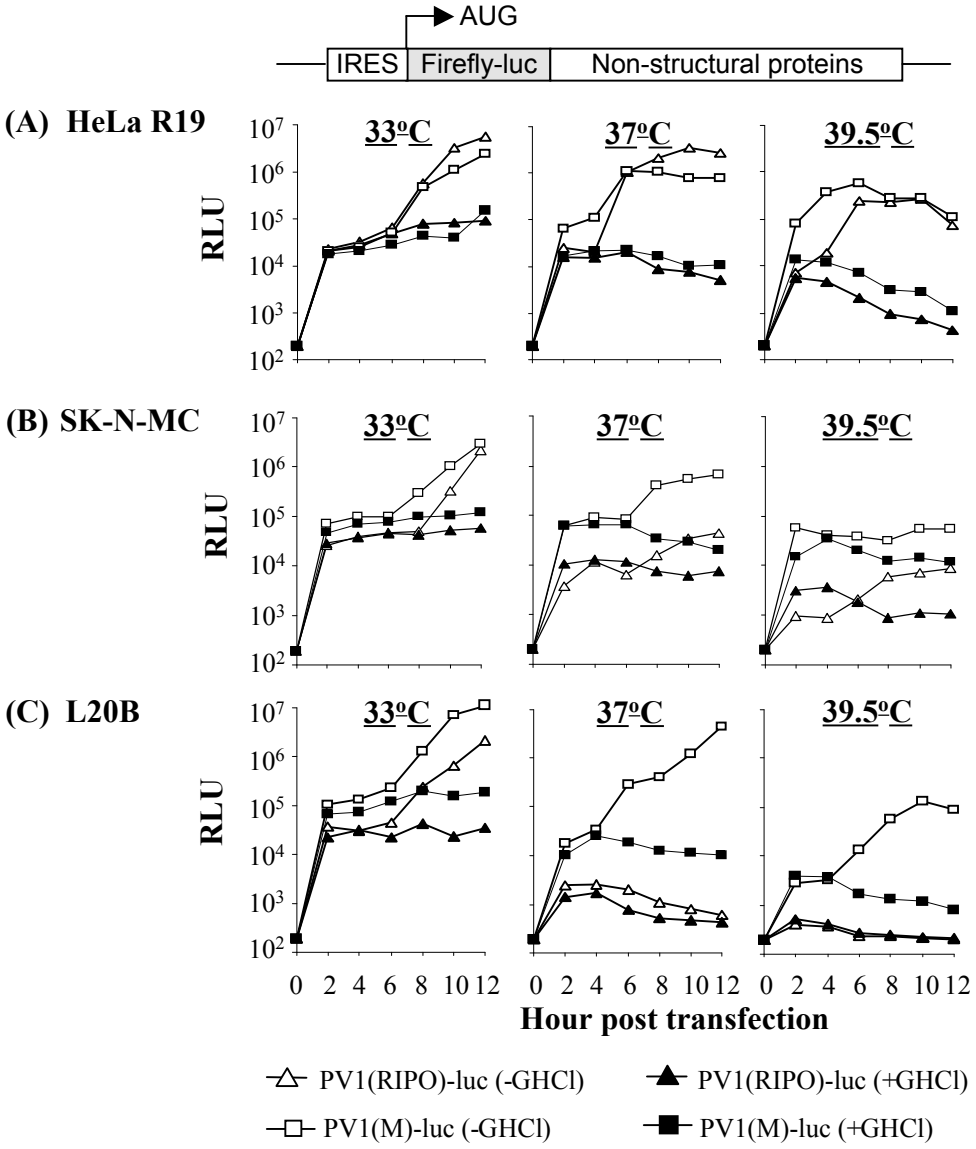

Jahan et al., FIG. 4

(A)

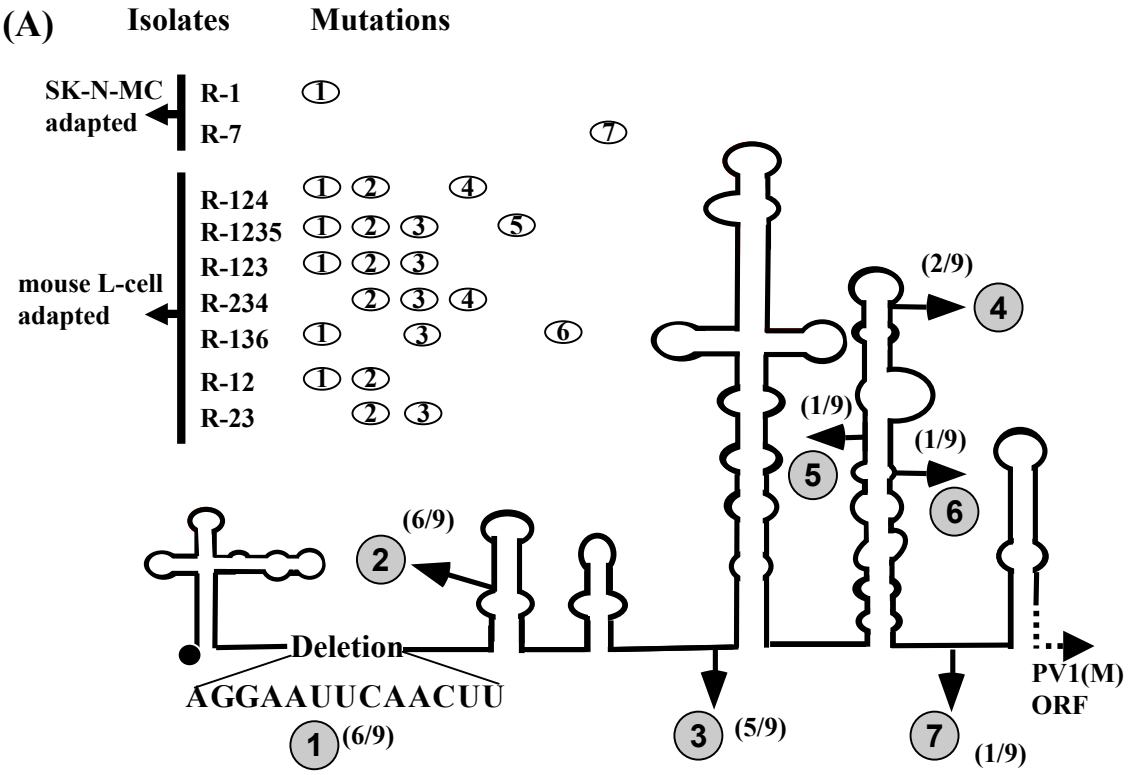

(B)

Mutation	nt. Change in PV1(RIPO)
1	Deletion of 107 to 119
2	C133G
3	A127U
4	U491C
5	U468C
6	U523C
7	C559U

Jahan et al., FIG. 5

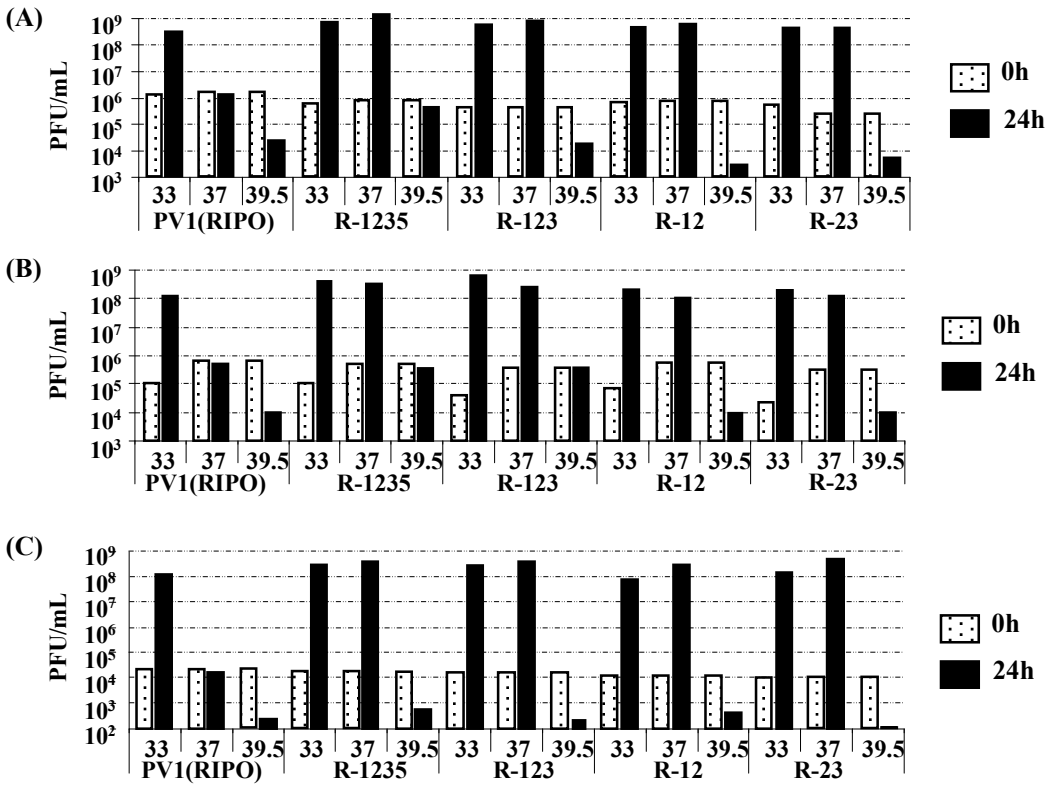

Jahan et al., FIG. 6

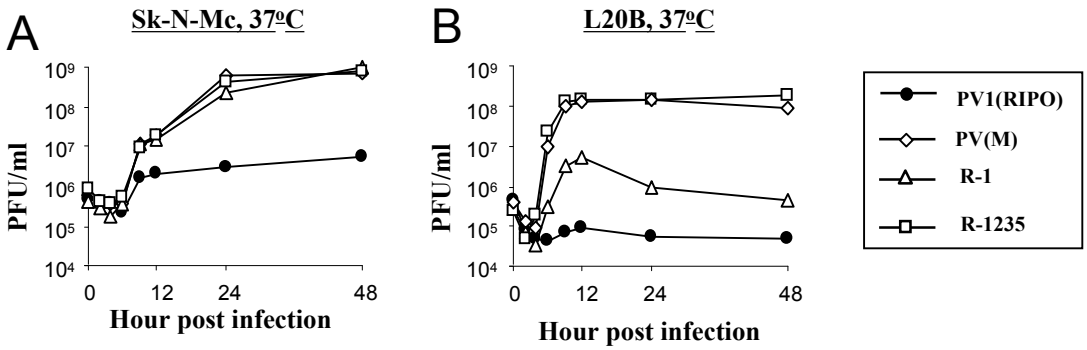

Jahan et al. FIG. 7

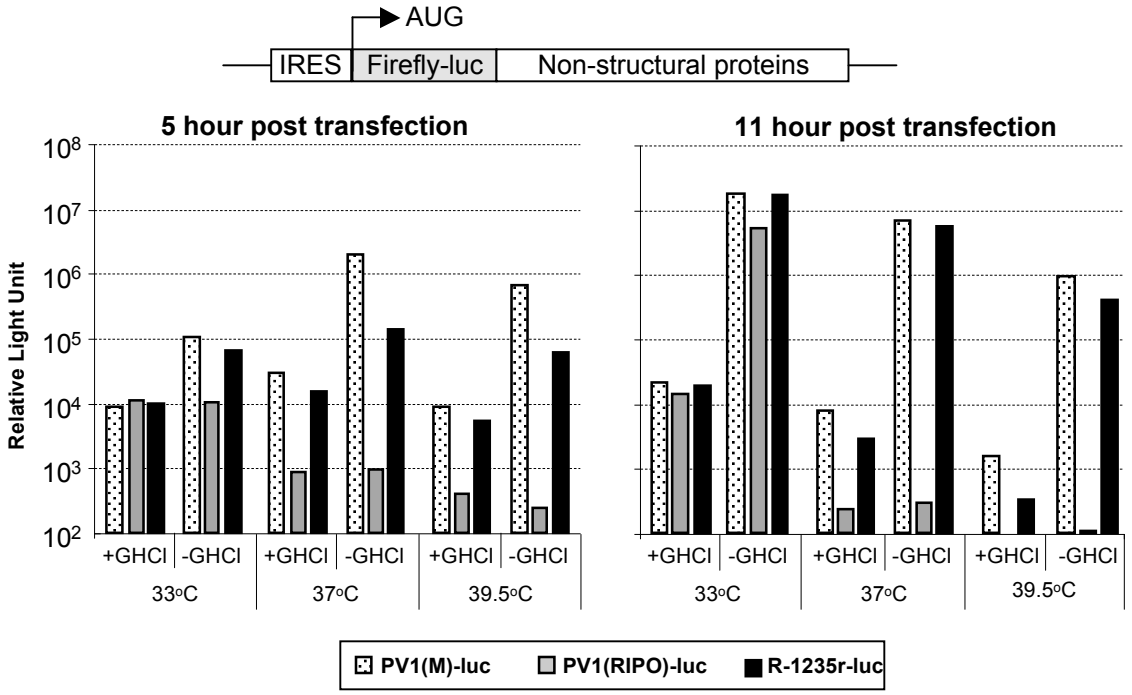

Jahan et al. FIG. 8

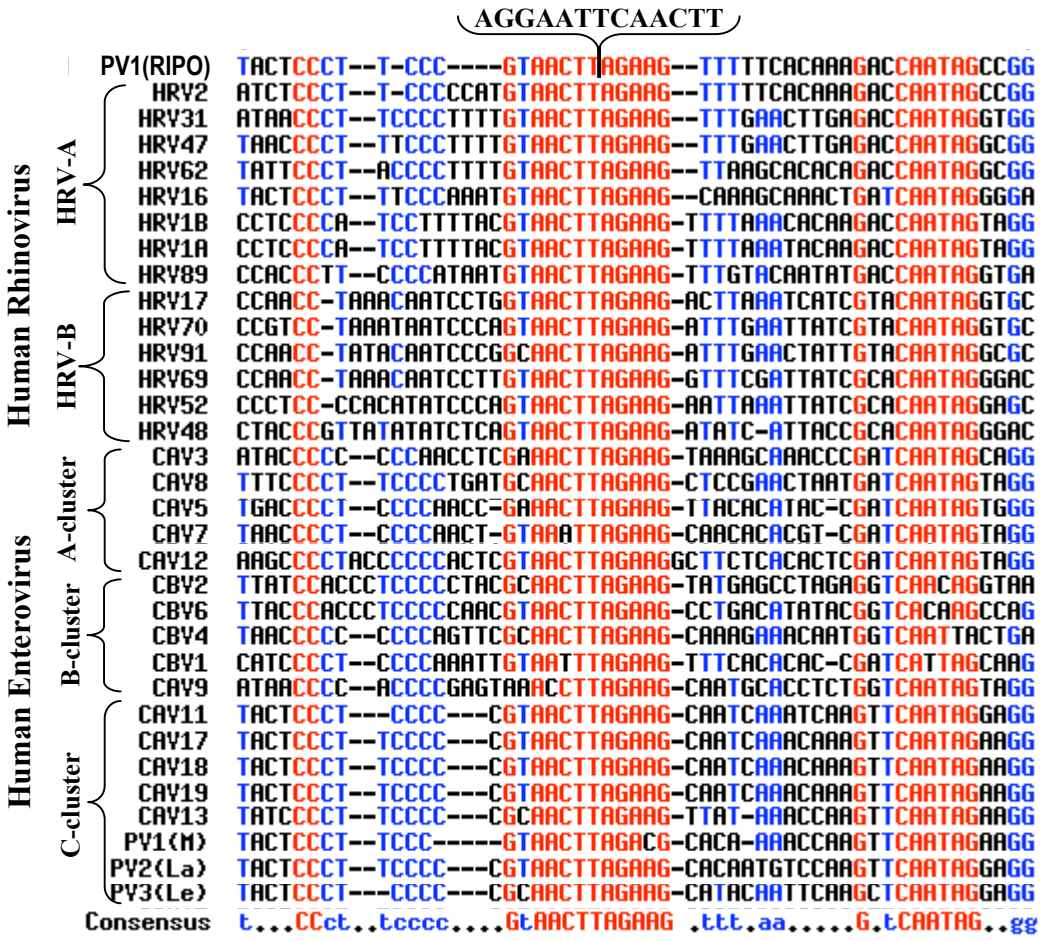

Jahan et al. FIG. 9

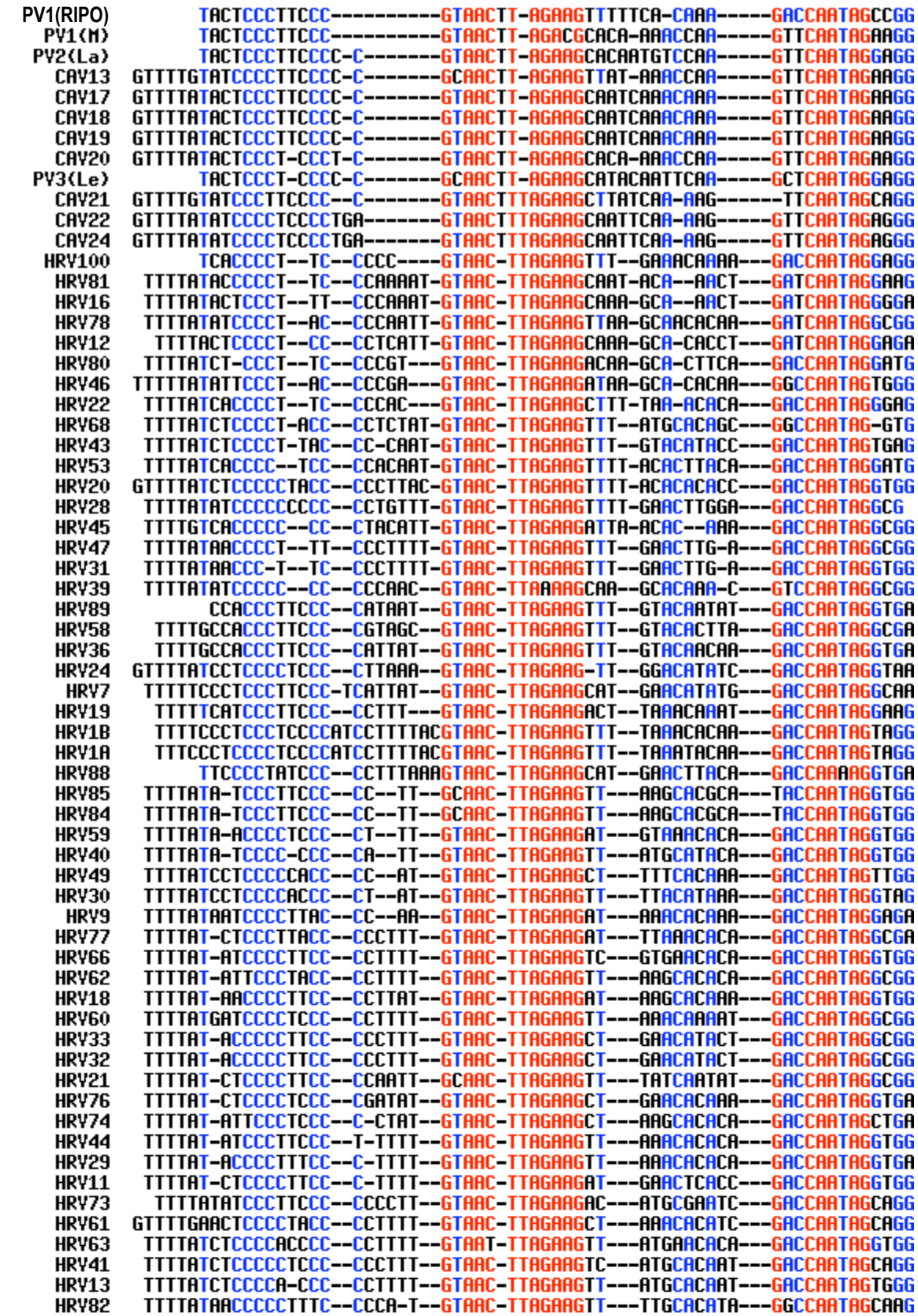
PV1(RIPO)
PV1(M)
PV2(La)
CAV13
CAV17
CAV18
CAV19
CAV20
PV3(Le)
CAV21
CAV22
CAV24
HRV100
HRV81
HRV16
HRV78
HRV12
HRV80
HRV46
HRV22
HRV68
HRV43
HRV53
HRV20
HRV28
HRV45
HRV47
HRV31
HRV39
HRV89
HRV58
HRV36
HRV24
HRV7
HRV19
HRV1B
HRV1A
HRV88
HRV85
HRV84
HRV59
HRV40
HRV49
HRV30
HRV9
HRV77
HRV66
HRV62
HRV18
HRV60
HRV33
HRV32
HRV21
HRV76
HRV74
HRV44
HRV29
HRV11
HRV73
HRV61
HRV63
HRV41
HRV13
HRV82

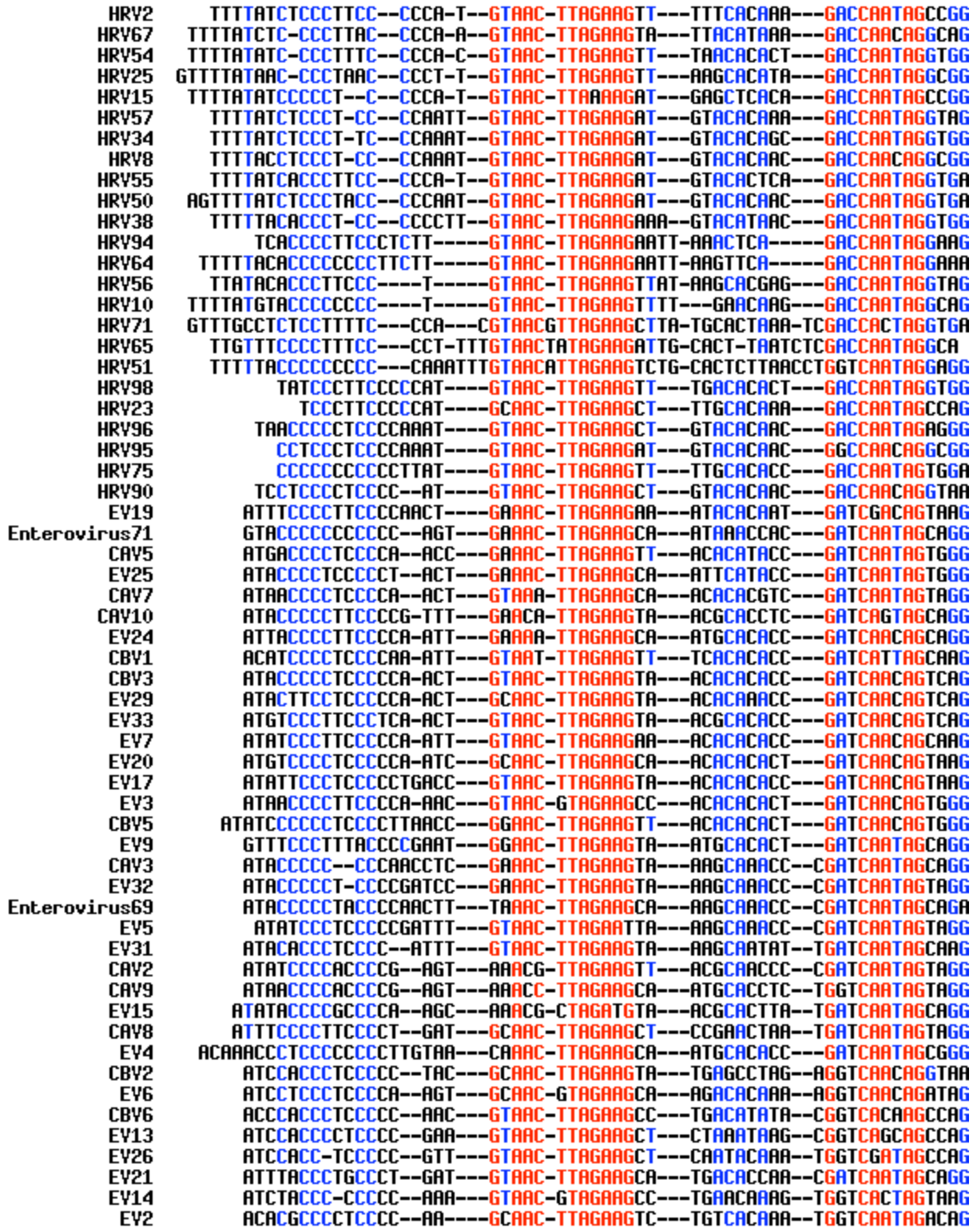
HRV2
HRV67
HRV54
HRV25
HRV15
HRV57
HRV34
HRV8
HRV55
HRV50
HRV38
HRV94
HRV64
HRV56
HRV10
HRV71
HRV65
HRV51
HRV98
HRV23
HRV96
HRV95
HRV75
HRV90
EV19
Enterovirus71
CAV5
EV25
CAV7
CAV10
EV24
CBV1
CBV3
EV29
EV33
EV7
EV20
EV17
EV3
CBV5
EV9
CAV3
EV32
Enterovirus69
EV5
EV31
CAV2
CAV9
EV15
CAV8
EV4
CBV2
EV6
CBV6
EV13
EV26
EV21
EV14
EV2

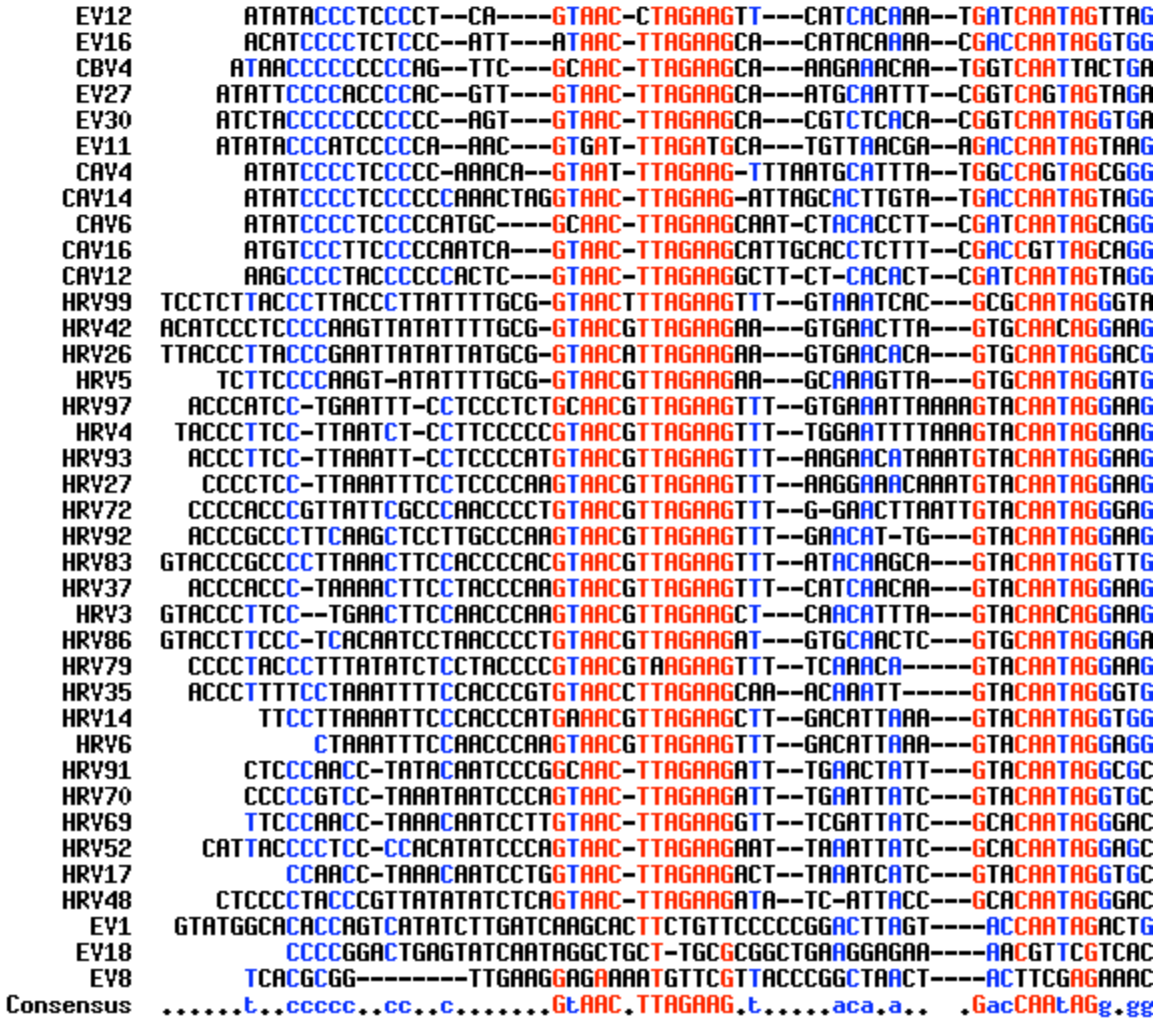

Supplementary FIG. 1: Nucleotide sequence alignments of spacer I and part of stem-loop II in the 5'NTR of human enteroviruses, human rhinoviruses (HRV) and PV1(RIPO). Nucleotides in red, blue and black color represent nucleotides highly, moderately and not conserved among the viruses respectively. Dashes denote nucleotides missing in any particular virus but that are otherwise present in other polioviruses or human rhino viruses. Mutation 1 (13 nt deletion) in the adapted isolates, restoring the highly conserved sequence, has been underlined in the PV1(RIPO) sequence and shown as looped out sequence. M, Mahoney; S, Sabin; La, Lansing; Le, Leon. Alignments were done using Multalin (http://bioinfo.genotoul.fr/multalin/multalin.html)